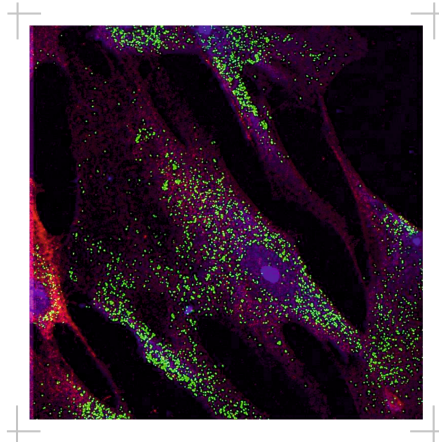# Reactive oxygen species (ROS) and lipid metabolism in idiopathic pulmonary fibrosis - role of peroxisomes in the pathogenesis of this devastating disease

GANI ORUQAJ

INAUGURAL DISSERTATION
submitted to the Faculty of Medicine
in partial fulfillment of the requirements
for the PhD-Degree
of the Faculties of Veterinary Medicine and Medicine
of the Justus Liebig University Giessen

Reactive oxygen species (ROS) and lipid metabolism in idiopathic pulmonary fibrosis - role of peroxisomes in the pathogenesis of this devastating disease

Inaugural Dissertation submitted to the
Faculty of Medicine in partial fulfillment
of the requirements for the PhD-Degree
of the Faculties of Veterinary Medicine and Medicine
of the Justus Liebig University Giessen

by

Gani Oruqaj

of

Prizren, Kosovo

Giessen 2016

From the Institute for Anatomy and Cell Biology- Medical Cell Biology

of the Faculty of Medicine of the Justus Liebig University of Giessen

Director / Chairperson: Prof. Dr. Eveline Baumgart-Vogt

First Supervisor and Committee Member: Prof. Dr. Eveline Baumgart-Vogt

Second Supervisor and Committee Member: Prof. Dr. Manfred Reinacher

Examination Chair and Committee Member: Prof. Dr. Jürgen Lohmeyer

Thesis Reviewer and Committee Member: Prof. Dr. Martin Kolb

Third Supervisor-Mentor: Prof. Dr. Wei Shi

Date of Doctoral Defense: 21.04.2016

Dedicated to:

My parents

Emrlla and Nadije Oruqaj

My beloved wife and little sweet daughter

Learta Pervizaj Oruqaj and Aulona Oruqaj

And

My family

Table of Contents

List of Figures and Tables

List of Abbreviations

ABCD3	ABC transporter D3 = PMP70 = 70 kDa peroxisomal membrane protein
ACOX1	acyl-coenzyme A oxidase 1
AECII	alveolar epithelial cells type II
AP-1	activator protein 1
ARE	antioxidant response element
ARD	adult Refsum´s disease
ASM	airway smooth muscle
α−SMA	alpha-smooth muscle actin
BLM	bleomycin lung model
BAL	bronchoalveolar lavage
COL1	collagen I protein
Ctrl	control
DHE	dihydroethidium
Dlco	diffusing capacity of the lung for carbon monoxide
DMEM	Dulbecco's Modified Eagle's Medium
DMSO	dimethylsulfoxide
DNA	deoxyribonucleic acids
dNTP	deoxy-NTP
DPBS	Dulbecco´s phosphate-buffered saline
EDTA	ethylene diamine tetraacetic acid
ECM	extra cellular matrix
EMT	epithelial mesenchymal transition
Fn	fibronectin
FBS	fetal bovine serum
FVC	forced vital capacity
GAPDH	glyceraldehyde-3-phosphate dehydrogenase
GR	glutathione reductase
H_2O_2	hydrogen peroxide
HO-1	heme oxygenase 1
HRP	horseradish peroxidase
IF	immunofluorescence
IPF	idiopathic pulmonary fibrosis
KO	knockout

KD	knockdown
LAP	latency-associated peptide
LTBP	latent TGF-β binding protein
Mg^{2+}	magnesium ion
mmHg	millimeters of mercury
mRNA	messenger RNA
MMP2	matrix metalloproteinase 2
NO_2	nitrogen dioxide
Nrf2	nuclear factor erythroid 2–related factor 2
N-terminal	amino-terminal
NTP	nucleotide triphosphate
O_2	oxygen molecule
PBS	phosphate-buffered saline
PDI	protein disulfide isomerases, prolyl 4-hydroxylase beta polypeptide
PEX11α	peroxisomal biogenesis protein 11 alpha = Peroxin 11 alpha protein
PEX11β	peroxisomal biogenesis protein 11 beta = Peroxin 11 beta protein
PEX13p	peroxisomal biogenesis protein 13 = Peroxin 13 protein
PEX14p	peroxisomal biogenesis protein 14 = Peroxin 14 protein
PFA	paraformaldehyde
PFS	progressive free survival
PPAR	peroxisome proliferator-activated receptor
PPRE	PPAR response element
PCR	polymerase chain reaction
PTEN	phosphatase and tensin homologue
PVDF	polyvinylidene difluoride membranes
RNA	ribonucleic acid
RNS	reactive nitrogen species
ROS	reactive oxygen species
RT	room temperature
SBE	Smad binding element
SDS-PAGE	sodium dodecyl sulfate-polyacrylamide gel electrophoresis
siRNA	small interfering RNA
Smad3 WT	*Smad3*-wild-type
Smad3 KO	*Smad3*-knockout

SOD1	CuZnSOD or CuZn⁻ superoxide dismutase
SOD2	MnSOD or Mn superoxide dismutase
SOD3	ECSOD or extracellular superoxide dismutase
SSc	systemic sclerosis
SV40	simian virus 40
TAE	Tris/acetic acid/EDTA buffer
TβRII	TGF-beta receptor II
TβRI-WT	TGF-β receptor I wildtype
TβR-I^{CA}	TGF-β receptor I constitutively active
TGF-β	transforming growth factor-beta
TIMP	tissue inhibitors of metalloproteinases
TNF-α	tumor necrosis factor-alpha
TNFR	TNF receptor
T-TBS	Tween 20-tris-buffered saline
UIP	usual interstitial pneumonia
VC	vital capacity
VLCFA	very long chain fatty acid(s)
WB	Western blot
WNT	wingless integrated 1
WISP1	WNT1 inducible signalling pathway protein 1
WT	wild-type
Zn^{2+}	zinc ion

1. Introduction

1.1. Overview on idiopathic pulmonary fibrosis

Idiopathic pulmonary fibrosis (IPF) is a chronic, devastating, and lethal fibrotic disorder in human lung, known also as cryptogenic fibrosing alveolitis, with a reported median survival of 3 to 6 yr, its incidence continues to rise and the prognosis is even worse than in many cancers [1-4]. IPF lung specimens show different histological patterns and the usual interstitial pneumonia (UIP) is seen in the majority of patients, where this terminology was also used as synonym [1] (Fig.3). IPF is characterized by a worsening of pulmonary function, and persistent alterations of the lung parenchyma because of fibrotic foci formation by activated fibroblasts and myofibroblasts and excessive production and deposition of extracellular matrix components (ECM) [5-8] (Fig.1). In the lung of IPF patients, an increase in relative number of myofibroblasts to fibroblasts is present along with the formation of fibroblastic foci with progressive deposition of abundant extracellular matrix in the interstitial tissue of the alveolar region [2, 8]. Several factors were thought to influence and initiate this lung disease, such as free radicals generated in the microenvironment of the alveolar region, smoking, pollution, general infections and to some extent also unknown genetic factors, leading to the ultimate death of patients (Fig.1). To date not a single factor could be identified solely causing this devastating disease [8]. IPF differs from other usual interstitial pneumonias in containing low antioxidant levels and having a poor prognosis. The correct diagnosis of IPF is difficult, since it exhibits similarities in physiology, clinical and pathological conditions with other interstitial lung diseases [9]. However, the histology of IPF in lung samples is characterized by the typical interstitial fibrosis and the honey comb like structure in end stage IPF samples, distinguishing IPF from other diseases with interstitial pneumonia [9].
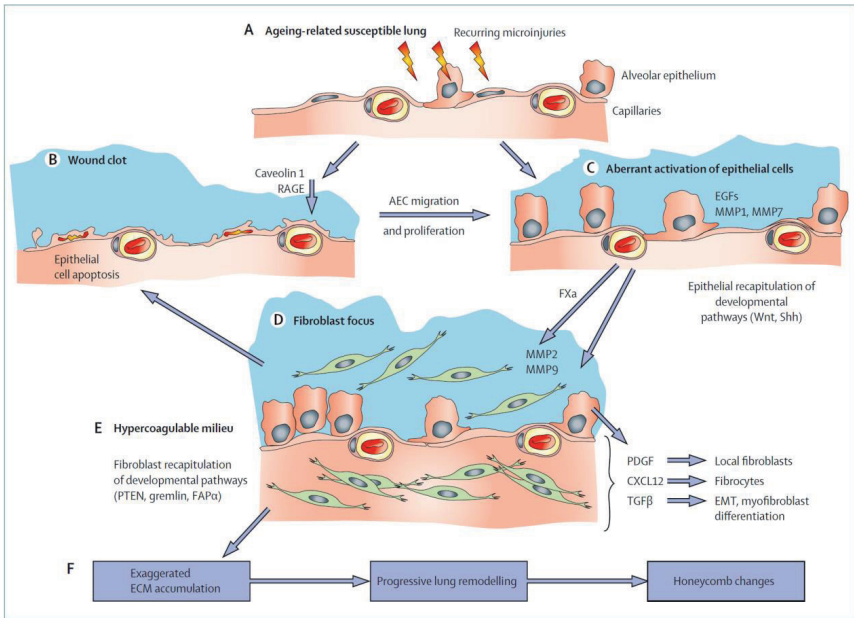
Fig 1. Mechanism involved in idiopathic pulmonary fibrosis [2].

Lung fibrosis in IPF begins in subpleural areas with fibroblast proliferation, alveolar epithelial atypia and spreads centrally later with time forming honeycombing structures as a marker of advanced lung fibrosis in fibrotic regions of the IPF lung [10](Fig.2). Inflammation in IPF is relatively low if compared to other interstitial lung diseases with high abundance of neutrophils and lymphocytes. Moreover, immature fibrotic regions with active myofibroblastic foci are more prone to extracellular matrix production in IPF [10] (Fig. 1, 2).
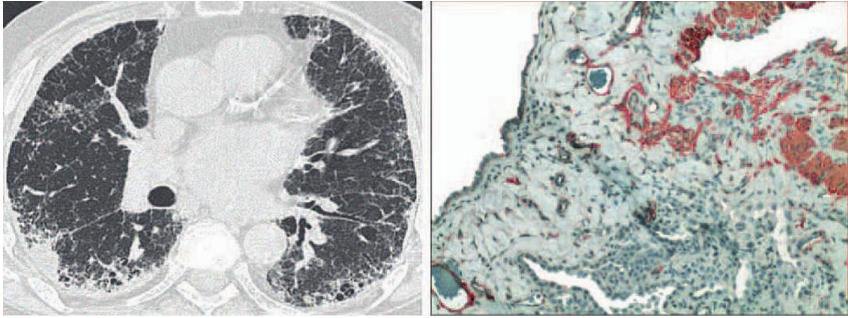
Fig 2. High resolution computerized tomography (HRCT), subpleural honeycombing (left), subpleural fibroblast proliferation and epithelial atypia *right*). Alpha-actin positive cells show *red staining* in photomicrographs (200× magnification) [10].

Furthermore, chronic inflammation is assumed to be the key factor in IPF with inflammatory mediators such as chemokines, cytokines, growth factors, and reactive oxygen species being discussed as key players in the progression of this disease [3]. In addition, it is shown in this thesis that TNF-α seems to play an important role in initiation and perpetuation of the fibrotic processes via AP-1 signaling pathway [11]. It is well accepted that TGF-β signaling plays a critical role in IPF development. Inhibition of TGF-β signaling by blocking its downstream *Smad3* gene expression protects against bleomycin induced fibrosis in animal models [12, 13]. However, the mechanisms by which TGF-β and TNF-α promote the fibrotic response in IPF are incompletely understood.
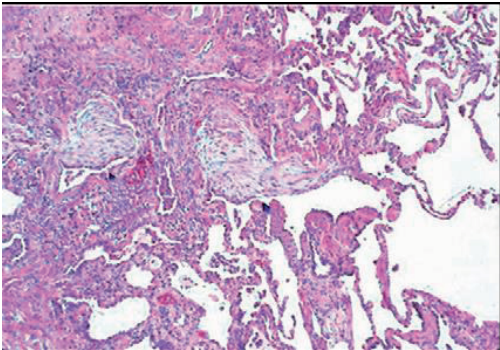
Fig. 3. Histopathological appearance: fibrotic foci in idiopathic pulmonary fibrosis [2].

3

1.2. The pathogenesis of idiopathic pulmonary fibrosis

The pathogenesis of idiopathic pulmonary fibrosis is a very complex process, there is no unifying mechanism that explains the complete lung fibrogenesis and most likely it is a multifactorial process [14]. The current hypotheses suggest that two different cellular mechanisms exist, 1) the inflammatory pathway and 2) the epithelial pathway, which could lead to development of lung fibrosis [2, 15, 16]. As a key process are suggested the multiple subclinical injuries to the lung with epithelial damage and subsequent alveolar basement membrane destruction [17]. This damage exerts a deteriorating process with fibrogenic cell infiltration, generation of myofibroblasts from fibroblasts exhibiting the expression of alpha smooth muscle actin (α−SMA), and subsequent ECM production [17, 18]. An essential role in the pathogenesis of IPF plays the TGF-β signal transduction pathway resulting in increased ECM and collagen production [19]. The *Smad3* knockout mice, deficient in a downstream mediator of TGF-β signaling, were shown to be protected from bleomycin-induced pulmonary fibrosis [13]. According to one theory, the increase of oxidants or a toxic event might lead to the destruction of the alveolar epithelium and its basement membrane, inducing hyperplasia of fibroblasts and a reactive synthesis of extracellular matrix in the underlying region of the connective tissue [20]. Several inflammatory mediators such as cytokines, chemokines, growth factors and reactive oxygen species (ROS) are implicated in the pathogenesis of IPF [20]. Furthermore, the WISP1 protein localized in alveolar type II cells (AECII), a downstream molecule of WNT signaling is involved in pulmonary fibrosis. Its depletion attenuates the bleomycin induced lung fibrosis in vivo, while WISP1 treatment increased ECM production and epithelial mesenchymal transition (EMT) [21, 22]. Moreover, the phosphotase and tensin homologue (PTEN) seems to be a crucial protective factor in the pathogenesis of many non-malignant diseases such as rheumathoid arthritis, asthma and pulmonary fibrosis. The expression of PTEN in patients with IPF was found to be downregulated in myofibroblasts with fibroblastic foci [23, 24]. The exact contribution of each process in the pathogenesis of IPF is incompletely understood. In the bleomycin lung fibrosis mouse model, one third of lung fibroblasts derive from the lung epithelium two weeks after bleomycin treatment, and bone marrow accounts for one fifth of fibroblasts, but only a minority of cells are α−SMA$^+$ myofibroblasts and just a few of these cells seem to derive from EMT [25]. Possibly, bleomycin accelerates the conversion of the AECII into AECI cells, and different cell types proliferate in the fibrotic lesions and exclude the epithelial cell populations and pericytes as the origin of lung myofibroblasts [26].

1.3. Overview on treatment approaches for IPF

As mentioned above, IPF is characterized by a continuous decline in pulmonary function that mainly leads to respiratory failure and death, and to date its therapeutic approaches are very limited [2]. The treatment approach for acute exacerbations of IPF used to consist of high doses of corticosteroids, even though there are no data from controlled trials to prove their efficacy in IPF patients [27, 28]. However, a beneficial effect of anticoagulant therapy on the overall survival, but not on clinical condition improvement of IPF patients was demonstrated [27]. In addition, there is also no convincing evidence shown to prove cyclosporine A as beneficial in treatment of acute exacerbations [28, 29]. Data from randomized clinical trials suggest a possible role and benefit of patients with IPF from sildenafil, as secondary outcome including relieve of dyspnoea and improving the quality of life, by optimizing the ventilation-perfusion matching in patients with pulmonary fibrosis [30]. Also, treatment of IPF patients with bosentan, an endothelin receptor antagonist, was not superior to placebo and no changes from baseline were observed within one year, by measuring the quality of life or dyspnoea [2]. Importantly, a study from a randomized phase III clinical trial demonstrated pirfenidone, an inhibitor of both production and activity of TGF-β, as a promising agent, with a therapeutic potential for treatment of IPF [31]. This drug possesses combined anti-inflammatory, anti-oxidant and anti-fibrotic properties, which preserves vital capacity (VC) and improves progressive free survival (PFS) better than placebo in patients with IPF in Japan [31]. Moreover, Nintedanib an intracellular inhibitor that targets multiple tyrosine kinases was shown to slow the disease progression and FVC decline in patients with idiopathic pulmonary fibrosis [32]. In addition, in a mouse model of bleomycin-induced pulmonary fibrosis in mice, TNF-alpha antagonists inhibit inflammation and fibrosis development [33], indicating a possible beneficial function in diminishing the fibrotic response in patients with IPF. However, etanercept, a TNF-alpha antagonist, used as treatment for IPF in a clinical study revealed no differences in the predefined endpoints among patients with IPF who received the drug or placebo [34]. A clinical trial from Demedts and colleagues demonstrated that the acetylcysteine added to prednisone and azathioprine therapy in patients with IPF maintains the vital capacity and Dlco (diffusing capacity of the lung for carbon monoxide) better than solely standard therapy [35]. Transplantation of prominin-1/CD133 positive epithelial progenitor cells (PEPs) in bleomycin-induced lung fibrosis mice suppressed proinflammatory and profibrotic response and protected mice from bleomycin-induced pulmonary fibrosis [36, 37]. Lung transplantation is considered as final treatment approach in patients with end-stage

of IPF. Mostly, a bilateral rather than a single lung transplantation is taken into consideration [38].

1.4. TGF-β signaling in the promotion of fibrosis

TGF-β1 is a growth factor produced by several cell types, and the most studied cytokine critical in pathogenesis and development of IPF with variable functions in cell differentiation, proliferation, apoptosis and cancerogenesis [39, 40]. Initial microinjuries and cell damage to the alveolar epithelium trigger the production of the fibrogenic mediator TGF-β1 by inflammatory and epithelial cells, which in turn induces the synthesis of extracellular matrix proteins and inhibits collagen degradation by activation of protease inhibitors and MMPs [40, 41]. In mammals, three variant isoforms of the TGF-β family exist: TGF-β1, -2, and -3 [42], from which TGF-β1 is most related to the development of IPF [39]. This cytokine is first secreted in an inactivated form, in a complex of latent TGF-β bound to the latency associated protein (LAP) and latent TGF-β-binding protein (LTBP) (Fig. 4).
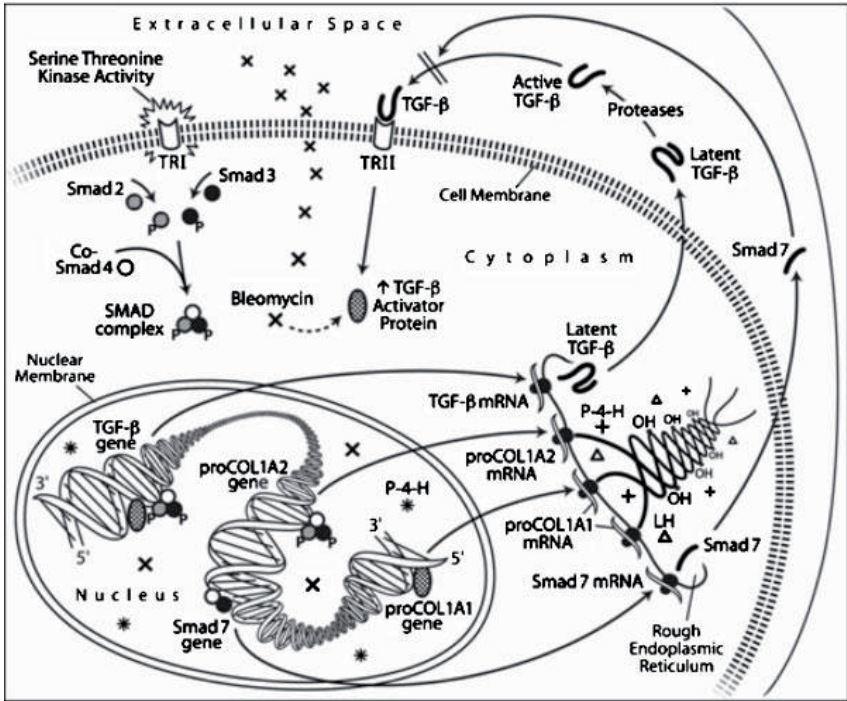
Fig.4. The mechanisms of extracellular activation and intracellular signaling of TGF-β1 on the expression of the TGF-β1, proCOL1A1, proCOL1A2, and Smad 7 genes. Synthesis and post translation hydroxylation modification of proCOL1A1, proCOL1A2 polypeptides, collagen triple helix formation, and propeptide globular extension formation [43].

The active TGF-β release from the LAP/LTBP complex can be mediated by matrix metalloproteinases (e.g. MMP2 and MMP9), tissue stiffness, by reactive oxygen species, acidic pH changes, thrombospondin-1 and integrins αVβ3, αVβ5, αVβ8, αVβ6, which have been demonstrated to play a critical role in TGF-β1 activation and the fibrotic response [40, 44-48]. Active TGF-β1 binds to two types of receptor serine/threonine kinases, type I and type II [49]. Activation of TGF-β1 leads to phosphorylation and activation of the TGF-β receptor type I by the type II receptor, inducing the activation of the Smad signaling pathway by phosphorylating Smad transcription factors such as Smad2 and 3, which shuttle to the nucleus and form a complex with Smad4 [49, 50] (Fig. 4).

7

1.5. Extracellular matrix (ECM) components in fibrosis

1.5.1. Collagen and fibronectin

Abnormal collagen production/deposition is a major feature of pulmonary fibrosis. In the late 1980s, it has been suggested that all types of collagen are produced after the TGF-β stimulation, and that fibroblasts from both normal and fibrotic human lungs would synthesize the same amounts of collagens [51]. Distribution of collagens is variable, type I collagen is localized to the interstitium of alveolar septa, type III is more prominent and has irregular perivascular and septal localization, while type IV is present in alveolar and capillary basement membranes [52]. Superoxide anions are inducing collagen type I degradation via activation of neutrophiles and release of collagenases [53]. Furthermore, as mentioned before epithelial injury and deterioration of the alveolar basement membrane (comprised of type IV collagen) are known to contribute to the pathogenesis of lung fibrosis [10, 54]. Fibronectin is a glycoprotein and an abundant compound of the ECM. It is comprised of N-terminal 70 kDa domain, the central binding domain 120 kDa, and the heparin-binding domain HepII4 [55]. These domains interact with cell-surface receptors and bind to integrin- and heparin sulphate proteoglycan (HSPG) cell-surface receptors, which trigger the reorganization of actin cytoskeleton [55]. TGF-β1 activity induces the alternative splicing and the increase of the fibronectin gene expression [55, 56]. Moreover, fibronectin (Fn) participates in the activation of latent TGF-β by αVβ6 integrins on epithelial cells,, upon binding to the latent TGF-β binding protein (LTBP-1), and deletion of fibronectin fails to activate TGF-β1 [55]. TGF-β1 as key mediator in ECM regulation stimulates the expression and secretion of different ECM proteins, such as fibronectin, thrombospondin, tenascin and vitronectin [55, 57]. Fibronectin receptors are critical for the induction of TGF-β1 and thereby myofibroblast differentiation [58].

1.5.2. Fibroblasts and myofibroblasts in IPF

Fibroblasts are mesenchymal cells, very abundant in the loose connective tissue. They play a critical role in ECM production, remodeling and wound repair [59, 60]. Various studies have proposed circulating fibrocytes, epithelial derived fibroblasts, resident fibroblasts and pericytes as main source of lung myofibroblasts [26, 61]. Proliferation rate is higher in human lung fibroblasts derived from fibrotic lung tissue compared with the normal lung, and the highest proliferation rate was found in fibroblasts obtained from areas with early fibrosis

compared with normal lung areas, whereas proliferation rate is obviously reduced in cells obtained from dense fibrotic tissue [51, 62]. Furthermore, fibroblasts are a very heterogeneous population, with phenotypic diversity, difference in surface markers, cytoskeletal structure and cytokine release [62, 63]. Myofibroblasts as unique subpopulation of fibroblasts are the main source of ECM production, express smooth muscle features, and are responsible for collagen accumulation [62, 64, 65]. TGF-β1 is the key cytokine of fibroblast-myofibroblast differentiation provoking such effects via the Smad-dependent signal transduction pathway, including proliferation, migration, chemoattraction of inflammatory cells and tissue repair [66, 67]. A characteristic difference between the two cell types "fibroblasts versus myofibroblasts" is the resistance of myofibroblasts to apoptosis, a property similar to malignant cells, which may lead to abnormal wound healing or contractive tissue repair processes, leading to fibrogenesis [68]. In addition, myofibroblasts release ROS and are under oxidative stress, a major factor contributing to apoptosis [47]. In IPF, the apoptotic process seems to be impaired, resulting in over production of ROS, cytokine release and epithelial cell injury [19, 47].

1.6. TGF-β role in myofibroblast differentiation and ECM regulation

Differentiation of fibroblasts into myofibroblasts is another proinvasive feature of TGF−β1. These myofibroblasts secrete excessive TGF-β1, which provokes ATII cell apoptosis, hereby deteriorating the wound healing process [40, 43] (Fig. 5). Lung fibroblasts are key cells for synthesizing collagen and generation of ECM, and TGF-β1 is the "master switch" for the pulmonary fibrosis [19, 69]. The collagen type I was the major type synthesized by both normal and fibrotic cell types, whereas TGF-beta induces the synthesis of different collagen types such as I, III, and V in fibroblasts and myofibroblasts [51, 70]. TGF-β/Smad signaling enhances the transcriptional activation of collagens, as consequence myofibroblasts express high levels of ECM especially collagens and fibronectin, contributing to the deposition of collagens and fibrosis [40, 43].
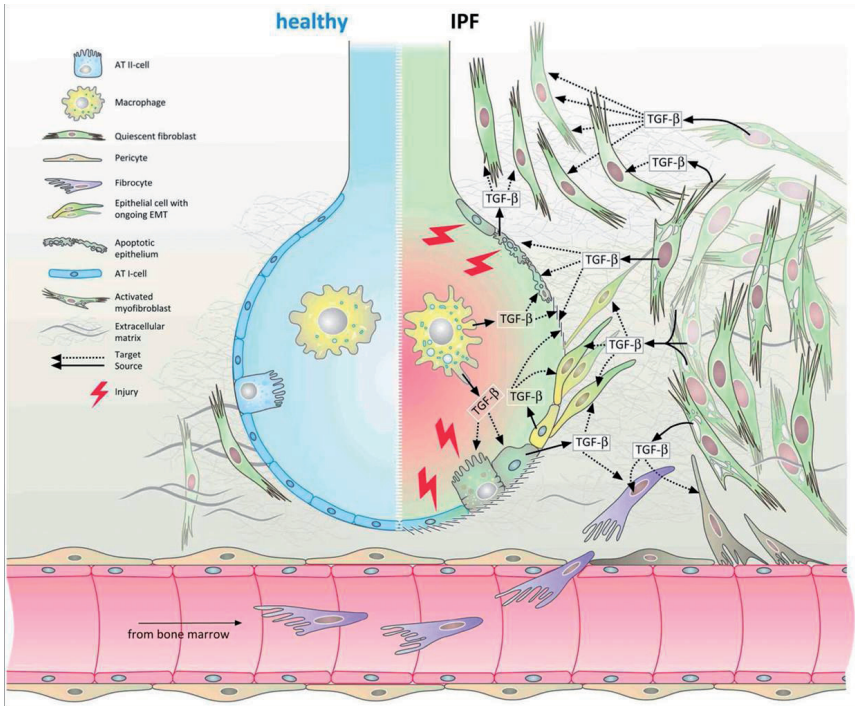
Fig. 5. Role of TGF–β in idiopathic pulmonary fibrosis (IPF) pathogenesis. Multiple presumed microinjuries to the alveolar epithelium induce the apoptosis of alveolar type I (ATI) and alveolar type II (ATII) cells, basal membrane disruption, and TGF–β production in macrophages, epithelial cells, or activated myofibroblasts. This condition perpetuates the aberrant wound healing process by inducing extracellular matrix production, promoting myofibroblast recruitment and activation from resident lung fibroblasts, epithelial mesenchymal transition (EMT) or endothelial mesenchymal transition (EndoMT), bone-marrow derived fibrocytes, or pericytes from the surrounding vessels and interstitium [40].

1.7. TGF-β1 in induction of epithelial-mesenchymal transition (EMT)

Fibroblast heterogeneity isolated from IPF lungs suggests that fibroblasts are derived from multiple cell types [71]. Kim and colleagues found that IPF lungs have acquired mesenchymal features from epithelial cells, and that this process is triggered by activation of the integrin αVβ6 and subsequently TGF-β1 activation, suggesting the implication of the EMT process during fibrogenesis [71]. The complete mechanism of EMT remains to be explained. TGF-β1

10

signaling through Smad specific proteins, as well as various other downstream kinases, including mitogen-activated protein kinase (MAPK), Rho kinase, Rac1, integrin linked kinase, etc. Which are Smad-independent pathways [72-74].

1.8. Matrix metalloproteinases in abnormal lung remodelling in IPF

MMPs are critical in would repair and in tissue remodelling [75]. They can activate growth factors such as TGF-β1 and other cytokines and play an important role in various diseases as arthritis and fibrosis [75, 76]. Various metalloproteinases such as MMP-1, MMP-2 and MMP-9 were found to be upregulated in human pulmonary fibrosis and animal models of pulmonary fibrosis [22, 77, 78]. In addition, an increased MMP-7 was also reported in usual interstitial pneumonia (UIP), a histological description for fibroblastic foci [79]. Consistently, MMP-7 knockout mice were protected from bleomycin-induced pulmonary fibrosis [79], suggesting that inhibition of MMP-7 may be used as therapeutic tool in this chronic deteriorating disease [79]. Furthermore, MMP-3 is found to be directly involved in the epithelial-mesenchymal transition, a pivotal process in pathogenesis of fibrosis and neoplasia [76], and genetic abrogation of MMP-3 protects the mice from bleomycin-induced lung fibrosis [75].

1.9. TGF-β1 and reactive oxygen species in the pathogenesis of IPF
1.9.1. Role of TGF-β1 and ROS generation

Human lungs are permanently exposed to higher concentrations of oxygen compared to other organs. Therefore, alveolar epithelial cells are more prone to oxidative injury [5, 80]. Reactive oxygen species (ROS), such as superoxide anions (O_2^{-}), hydrogen peroxide (H_2O_2), and hydroxyl radical ($OH^{\cdot}$) regulate cell signaling in physiological conditions, but an excess of reactive oxygen species leads to organ injury [81]. ROS can damage alveolar epithelias cells, such as DNA, proteins and lipids. Many studies suggest that the imbalance between oxidants and antioxidants could play a major role in development of lung fibrosis [45, 58]. For example, TGF-β1 triggers extracellular secretion of H_2O_2 in lung fibroblasts in humans, by activating NADH:flavin:O2 oxidoreductase [82], while ROS play an important role in induction of TGF-β1 signaling, leading in consequence to collagen-I synthesis and fibrogenesis in pulmonary fibrosis [45, 83, 84]. ROS are critical components involved in fibrotic process, shown in IPF patients and bleomycin-induced pulmonary fibrosis in animal. Absence of ROS in mice with deficiency for the p47[phox] subunit of NADPH-oxidase (Nox)

protects the mice against bleomycin induced lung fibrosis [83, 85]. NOX4-dependent generation of H_2O_2 is also crucial for TGF-β1-induced myofibroblast differentiation and ECM production [86]. Upregulation of NOX-4 is found in human idiopathic pulmonary fibrosis and in the mouse lungs subjected to non-infectious injury [86]. Moreover, superoxide dismutases (SODs), such as SOD1 (CuZnSOD), SOD2 (MnSOD), and SOD3 (ECSOD), are known to reduce oxidative stress by catalyzing the dismutation of superoxide into oxygen and hydrogen peroxide [58]. Deletion of ECSOD in mice aggravates the pulmonary damage after exposure to bleomycin or asbestos [87].

1.9.2. Fibrogenesis induced by oxidative stress

In the literature, it was speculated that direct injury to the alveolar epithelium and the inflammation in the alveolar and bronchiolar regions could induce the activation of signaling pathways, that lead to the elevated expression of proinflammatory genes in fibroblasts, and to the release of profibrotic cytokines (TGF-β1, TNF-alpha, IL-1, IL-6, IL-8), growth factors such as PDGF and chemokines [58, 88]. Besides proliferation of myofibroblasts in IPF lungs, cytokine-mediated ROS release can lead to apoptosis of type I alveolar epithelial cells, with subsequent exposure of the basement membrane and the ECM production leading to the activation of alveolar macrophages [45]. Elevation of ROS production via activation of immune cells such as macrophages, neutrophils through NADPH oxidase activation is also noted in IPF patients [88]. Furthermore, also imbalance of MMPs and TIMPs (tissue inhibitor of matrix metalloproteinases) might trigger ROS or RNS alterations, generating the overdeposition of secreted extracellular matrix material [88, 89] (Fig.6). TGF-β activation by ROS is specific for the TGF-β1 isoform and the methionine residue 253 in the TGF-β1/LAP complex is important and functions as redox switch center [90]. In addition, the oxidation of LAP was always paralleled by increased levels of HO-1, this was implicated later in releasing the mature TGF-β1 [91] (Fig.6). Induced activation of TGF-β1 by increased ROS and apoptosis was also demonstrated in peroxiredoxin 6 knockout mice (Prdx6) [92].
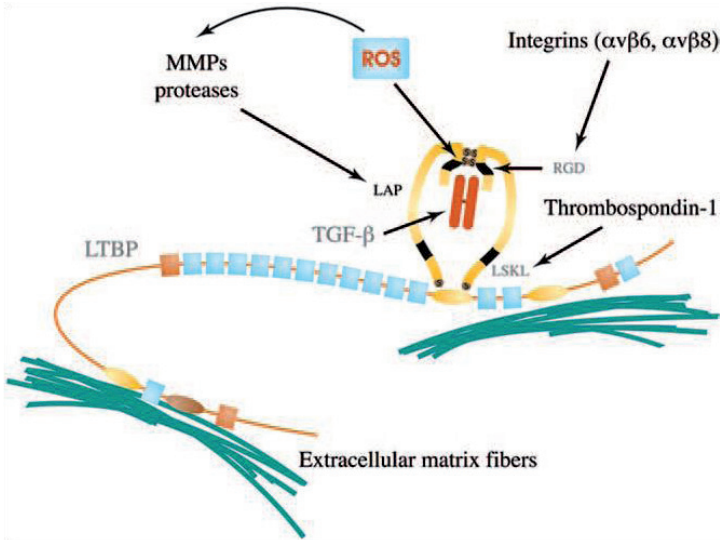
Fig. 6. Activation of latent TGF-β complexes by ROS- MMPs and integrins [90].

1.10. AP-1 signaling in idiopathic pulmonary fibrosis

The transcription factor activator protein 1 (AP-1) is a dimeric molecule composed of members of the Jun (c-Jun, JunB, and JunD), Fos (c-Fos, FosB, Fra-1, and Fra-2) and ATF families of proteins [93, 94]. C-Jun is involved in regulation of cell proliferation and fibroblasts deficient in c-Jun exhibit reduced proliferation due to a cell cycle defect as well as an increase of the tumour suppressor genes p53 and p21 [95, 96]. AP-1 family members are implicated in different stress signals and control subsequent processes including proliferation, apoptosis, wound healing, inflammation, tumourigenesis [97, 98]. In particular, Fra-2 and JunD are involved in regulation of ECM synthesis and aberrant activation of fibroblasts [98]. These effects have made AP-1 a potential candidate for antifibrotic therapy [97, 98]. Furthermore, inhibition of AP-1 abrogated the profibrotic effects of TGF−β signaling and in consequence prevented the development of skin fibrosis in one mouse model of SSc (systemic sclerosis), also called bleomycin-induced dermal fibrosis [97]. Therefore, this approach might become a promising therapy for treatment of fibrotic disorders [97]. Similar beneficial effects of AP-1 inhibition in preventing ECM generation and TGF-β1 signaling activation were also noted in Swiss 3T3 fibroblasts treated with TNF-alpha [99].

13

1.11. Inflammation and implication of cytokines (TNF-alpha and IL-6) in pulmonary fibrosis

Cytokine release has been one of the major critical factors leading to the fibrogenesis observed in the bleomycin-induced lung fibrosis mouse model. In particular TNF-alpha plays an essential role for the development of the BLM-induced lung injury, partially through upregulation of TGF-β1 expression [100, 101]. TNF-alpha is produced by many cell types upon injury or infection, which may participate in cell proliferation, differentiation or apoptosis [102]. The use of TNF-alpha antagonists, was effective not only in abrogating the development of lung fibrosis but also reduced an established fibrosis in bleomycin or silica instillation-induced mouse lung fibrosis models [33]. An increased expression of α-SMA and COL1 protein was also noted in recombinant human TNF-α treatment (rhTNF-α) of palmar fibroblasts in Dupuytren´s disease [101]. In addition, TNF-alpha increases TGF-β1 expression and enhances ECM synthesis in the Swiss 3T3 fibroblasts [99]. IL-6 cytokine is secreted by various cell types (including fibroblasts), and mediates inflammatory processes in the lung in a variety of disease situations including interstitial lung diseases [103]. Moreover, the role of IL-6 in the lung inflammation was further analyzed by treating wild-type and IL-6-deficient mice with bleomycin [104]. In comparison to WT-mice, the IL-6 deficient mice expressed lower numbers of macrophages, total cells and neutrophils in the bronchoalveolar lavage (BAL) [104]. Taken together, these studies indicate that inhibition of TNF-alpha or IL-6 release plays an important role in preventing and/or attenuating BLM-induced lung fibrosis, which may be a potential therapeutic approach in treating pulmonary fibrosis [103, 104].

1.12. TGF-beta receptor II kockout mice are protected from pulmonary fibrosis

Increased expression and activation of TGF-β have been demonstrated in IPF patients as well as in experimental models of pulmonary fibrosis [105, 106]. The activated TGF-β can bind to the serine/threonine kinase receptors, TGF-β receptor II and I complex (TβRII and TβRI) and lead to phosphorylation of downstream intracellular molecules such as Smad2/3 and subsequently gene expression [40, 105]. Recently, it was reported that the abrogation of the TGF-β signaling in lung resident mesenchymal cells, using a Tbx4 lung enhancer-driven Tet-On transgenic system to delete TGF-β receptor II or express dominant-negative TGF-β receptor II, has significantly inhibited the BLM-induced fibrotic response [105, 107]. In

addition, the blockade of TGF-β receptor type II in epithelium decreases epithelial permeability, preserves lung function and thus protects mice from bleomycin induced lung injury and pulmonary fibrosis [106]. Furthermore, the peroxisome is downregulated in BLM-induced wild type mouse lung fibrosis, which can be abrogated in lung mesenchyme-specific TβRII knockout mice in which significant reduction of bleomycin-induced lung fibrosis is observed [11, 105]. This suggests a critical role of peroxisomes in experimental lung fibrosis.

1.13. Smad3 deficient mice provide effective protection from BLM- induced lung fibrosis

Excessive TGF-β/Smad dependent pathway is well recognized for the fibrotic response in IPF, other fibrotic diseases such as dermal fibrosis, as well as in inflammatory processes of BLM-induced lung fibrosis [13, 97, 105]. The contribution of Smad3 in development of lung fibrosis was identified in vivo, where loss of Smad3 alleviated the bleomycin-induced tissue injury and pulmonary fibrosis in mice [13]. Furthermore, lack of Smad3 protected mice from BLM induced lung fibrosis, but presented a higher susceptibility for development of emphysema by interfering with the physiological role of TGF-β in development of alveolar structure [108]. These studies suggest that identification of specific downstream profibrotic targets of TGF-β signaling might be pivotal for using as possible therapeutical targets in treatment or attenuation of idiopathic pulmonary fibrosis.

1.14. TβR-I constitutively active mice as model to investigate the effect of TGF-β signal transduction

TβR-I is phosphorylated by TβR-II at serines and threonines in the GS domain [109], a required step to propagation of signal downstream of TGF-β. Different mutations at GS domain create constitutively active receptor forms of *TβR-I* [110]. In addition, Bartholin and colleagues generated a transgenic mouse with a Cre/loxP inducible constitutively active *TβR-I* by using a knock-in strategy into the hypoxanthine phosphoribosyl-transferase locus (Hprt) [111]. These transgenic mice are useful tool in addressing the effect of TGF-β signaling upregulation in any cell type that expresses cre-recombinase [109, 111].

1.15. Peroxisomes as ubiquitous organelles in metabolic functions

Peroxisomes are single membrane bounded ubiquitous organelles, present in all eukaryotic cells except spermatozoa and mature red blood cells (Fig.7) [112]. The lung, especially type II alveolar epithelial cells and club cells (Clara) possess a large number of peroxisomes [80]. Moreover, peroxisomes could also be identified in the apical region of ciliated bronchiolar cells as well as in type I alveolar epithelial cells, however, in the latter with less abundance and different enzyme composition [80, 112]. In general, these organelles are highly abundant in the major metabolic organs, such as hepatocytes in the liver and in epithelial cells of the proximal tubules in the kidney [112]. These organelles are highly heterogeneous and their enzyme composition and metabolic pathways vary between cell types, tissues and organs [112]. In these cell types, peroxisomes are involved in many metabolic functions, including degradation of reactive oxygen species (ROS) and bioactive lipid mediators (prostaglandins and leukotriens) and synthesis of antioxidant lipids (polyunsaturated fatty acids, plasmalogens, etc.) [112]. Peroxisomes might proliferate in number due to metabolic needs or impact of different environmental factors [112]. It is well known that, reactive oxygen species and nitrogen species induce lung injury due to direct exposure of the lung epithelia to this reagents or secondary due to higher oxygen and different environmental oxidants in the inspired air, causing oxidation of cellular DNA, proteins and lipids [113]. In this respect, it is of interest that deficiency or dysfunction of peroxisomes results in increased cellular oxidative stress, accumulation of lipid derivatives normally metabolized in these organelles, leading to severe pathological consequences in many organ systems [114, 115]. Different studies have shown that in the most severe phenotype of a peroxisome biogenesis disorder (e.g. Zellweger syndrome) also mitochondria are compromised in their respiratory function as a secondary phenomenon [115]. Moreover, children with Zellweger syndrome (cerebrohepatorenal syndrome) develop progressive liver fibrosis or cirrhosis, leading to early death of the patients during childhood [115]. Appropriate knockout mouse models exhibit a similar phenotype [116]. Most knockout mice with peroxisomal biogenesis defects die during their first day of life [116, 117]. Interestingly, in one of the mouse models (PEX11β knockout) morphological alterations of the lungs were described [117]. Whereas peroxisome deficiency leads to a profibrotic phenotype, treatment of rats with a peroxisome proliferator-activated receptor alpha (PPAR-α) specific agonist evolved a significantly attenuated tubulointerstitial renal fibrosis [118]. Many peroxisomal genes contain a PPAR-response element in their promoter region by which their transcription can be modified [119]. Independent from the fact that peroxisomal metabolism might be affected in other tissue fibrosis, the role of peroxisomes in

pulmonary fibrosis onset and progression of this devastating disease has never been described [5, 120].
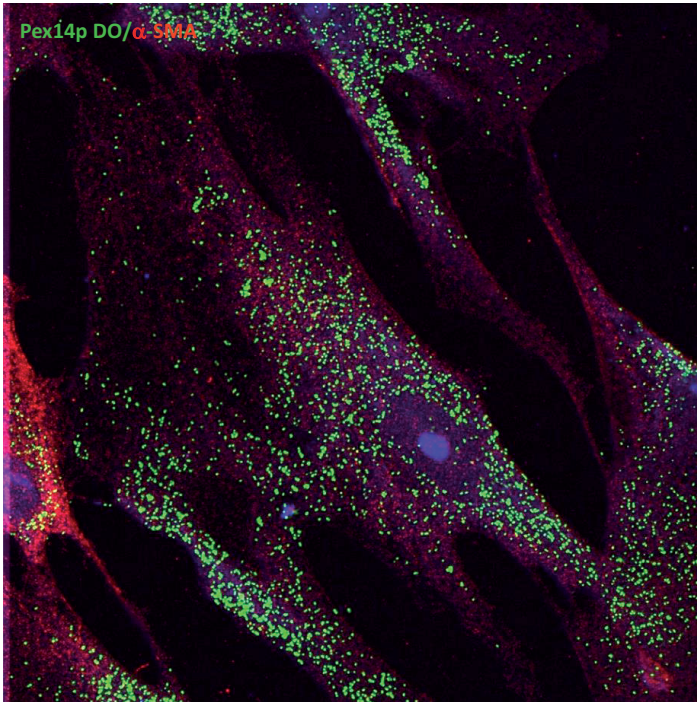
Fig.7. Example for a double immunofluorescence staining of peroxisomal biogenesis protein PEX14p (green) and alpha-smooth muscle actin (α-SMA) (red) in human lung fibroblasts of control subjects (picture is taken from results of this thesis).

1.16. Biogenesis of peroxisomes

The peroxisome biogenesis is a complex biological process, comprising three crucial steps a) formation of the peroxisomal membrane, b) import of peroxisomal matrix proteins, c) and proliferation of peroxisomes [121]. The peroxisomal proteins are first synthesized on free ribosomes and posttranslationally imported into the organelle [122, 123]. The targeting of the peroxisomal matrix proteins to the organelle is enabled via cytoplasmic shuttling receptors, Pex5p and Pex7p, binding nascent proteins with peroxisomal targeting signals (PTS1 or

PTS2) [124]. The biogenesis and the import of matrix proteins into peroxisomes is mediated by different biogenesis proteins called peroxins, which are divided into three groups: a) peroxins involved in the biogenesis of the peroxisomal membrane, Pex3p, Pex16p and Pex19p, [121] b) peroxins that are implicated in the matrix protein import, such as Pex5p, Pex7p c) and those that are involved in peroxisome proliferation Pex11p (α, β, γ) [125] (Fig.8). Moreover, Pex11α is known to play an important role in peroxisome proliferation. A PPRE is located upstream in the enhancer region of the Pex11α gene [119]. Both, PPAR-α and PPAR-γ can bind to this element and activate the transcription of *Pex11α* and *perilipin* genes [119]. Furthermore, Pex13p and Pex14p are biogenesis proteins in the docking complex of the peroxisomal membrane, which are critical for the import of peroxisomal matrix proteins with targeting signals PTS1 and PTS2 [121, 126]. Mutations in the *PEX13* gene in humans lead to Zellweger Syndrom. Accordingly, *Pex13* knockout mice exhibit a similar disease phenotype as the Zellweger Syndrom patients [114, 126].
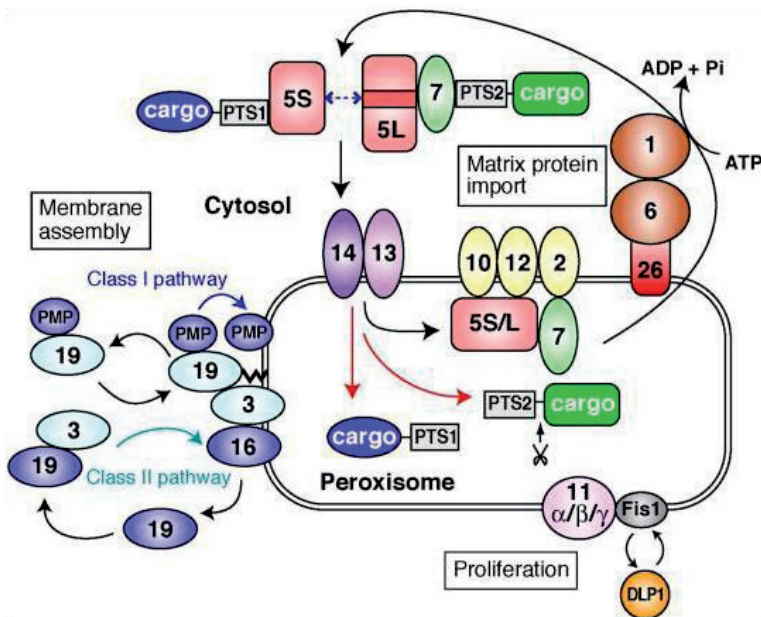
Fig. 8. A schematic illustration of peroxisome biogenesis in mammalian cells. All peroxins are illustrated with numbers only [125].

1.17. Peroxisome functions in lipid metabolism and scavenging ROS

Peroxisomal enzymes are implicated in various metabolic pathways, including scavenging of reactive oxygen species (ROS) and reactive nitrogen species (RNS), decomposition of various toxic bioactive and pro-inflammatory lipid mediators, as well as in the synthesis of cholesterol and ether lipids (plasmologens) [127-129]. The peroxisomes harbor a large variety of anti-oxidative enzymes essential in scavenging ROS, such as catalase, glutathione reductase, peroxiredoxin I and V, Cu/Zn-SOD [129]. Formerly, SOD2 was also described in this organelle, however, recently our group showed that this protein is only present in mitochondria and not in peroxisomal matrix [130]. Peroxisomes are intimately involved in lipid metabolism by catalyzing 1. Fatty acid alpha-oxidation, 2. Fatty acid beta-oxidation, 3. Biosynthesis of polyunsaturated fatty acids, 4. Ether-phospholipid synthesis and 5. Synthesis of cholesterol precursors and other isoprenoids [131]. In the peroxisomal β-oxidation pathways are oxidized lipid derivatives that are poor substrates for mitochondrial β-oxidation; e.g. very long ($\geq C_{24}$; VLCFA) chain fatty acids, branched chain fatty acids, dicarboxylic acids, eicosanoids (prostaglandins, leukotrienes), (n-3) and (n-6) polyunsaturated fatty acids and bile acid precursors [131]. Peroxisomes also oxidize a large amount of long chain fatty acids in situations in which the mitochondrial carnitine-palmitoyl transferase 1 system is overloaded or mitochondria are dysfunctional [132, 133]. The fatty acids are usually degraded in peroxisomes and thereafter transferred to the mitochondria for complete oxidation [131, 132]. Peroxisomes are involved in the oxidation of polyamines, D-amino acids, uric acid (in non-primates) via several H_2O_2 producing oxidases and in the detoxification of glyoxylate and xenobiotics [132]. An interesting feature of peroxisomes is their ability to adapt their number, form and enzyme content in response to nutritional and environmental stimuli, which is mediated in part by PPARs [134]. Interestingly, expansion of the peroxisomal compartment and upregulation of PEX genes was observed in cells exposed to oxidative stress or ultraviolet irradiation [135]. In contrast, significant reduction of catalase is observed in inflammatory processes including asthma bronchialis, infections, and allograft rejection and seems to be related to the suppressive effect of tumor necrosis factor-α on peroxisome function and peroxisome proliferator activated receptor-α [136]. It is well known, that pro and antioxidative enzymes are localized in specific subcompartments, such as the plasma membrane, the endoplasmic reticulum, peroxisomes or mitochondria and the cytoplasm [129]. Interestingly, peroxisomes contain the largest amount of prooxidative (peroxisomal oxidases and iNOS) as well as antioxidative (catalase, SOD 1, Prdx I and Prdx V, glutathione reductase) enzymes in their matrix [129, 137]. Moreover, the deficiency of peroxisomes in

knockout mice with Zellweger syndrome (PEX 5$^{-/-}$ mouse) leads to mitochondrial defects induced by generation of ROS release by the disordered mitochondrial respiratory chain in these animals [138]. In addition, lung peroxisomes express a variety of β-oxidation enzymes involved in the metabolism of fatty acid derivatives and proinflammatory eicosonaoids [80]. Unfortunately, there is scarce knowledge available on the perpetuation and chronification of inflammatory reactions in the lung [80]. The role of this cell organelle in the lung and its enzyme alterations in IPF patients are not investigated so far, and no comprehensive study has been performed on the function of different organelles in IPF. However, alterations in peroxisomal metabolism and enzyme content could exert a strong impact on the pathogenetic mechanisms in IPF.

1.18. Peroxisomal proteins in human lung

The alveolar epithelium is of particular interest, because the proliferation of alveolar type II cells with concurrent induction of antioxidant enzymes (Mn-SOD, glutathione peroxidase) makes the lung tissue resistant to high lethal oxygen concentration, normally lethal to other cell types e.g. AECI [136]. This phenomenon is apparently an adaptive response against high oxygen concentrations [136]. In the human lung, peroxisomes are highly abundant in alveolar epithelial type II cells (AEC II), club (Clara) cells, in both of which they exhibit a high catalase expression [80]. Moreover, small peroxisomes are mainly localized in high number in the apical region in ciliated cells of the respiratory and bronchiolar epithelium, directly underlying the tracheal and bronchial surface, suggesting that they might protect these epithelia against the high oxygen content and oxidative damage [112]. Peroxisomes in the cells of the alveolar and bronchial regions are also involved in the metabolism of ROS and various lipid derivatives and contain high amounts of β-oxidation enzymes as well as ether lipid and cholesterol synthesizing enzymes [112]. Peroxisomes might play a critical role in regulating the biophysical properties of surfactant through plasmalogen and cholesterol synthesis and in the breakdown and homeostasis of bioactive lipids (e.g. proinflammatory eicosanoids) and PUFAs with their β-oxidation systems as well as in the maintenance of lipid ligand levels for nuclear receptors of the PPAR family [80, 132].

1.19. Peroxisomal beta oxidation

The importance of peroxisomes in lipid metabolism and human health is crucial in maintaining the cellular functions by participating in different metabolic pathways such as enzymes involved in β-oxidation and α-oxidation of acyl-CoAs, ether-phospholipid synthesis, cholesterol and isoprenoid metabolism and bile-acid synthesis [139, 140]. Moreover, α−oxidation of phytanic acid generates pristanic acid, which undergoes three cycles of β−oxidation in peroxisomes before the chain-shortened fatty acids are exported from the peroxisome via the carnitine-dependent route (carnitine O-Octanoyltransferase) or via the free acid route through acyl-CoA thioesterases [140, 141] (Fig. 9). Patients suffering from adult Refsum´s disease (ARD) are unable to metabolize phytanic acid derived from exogenous sources (e.g. cow´s milk), phytanic acid accumulates in tissues and body fluids, due to the deficient α-oxidation process of phytanic acid to pristanic acid, whereas the subsequent β-oxidation of pristanic acid is normal [140, 142, 143]. Refsum´s disease is characterized by atypical retinitis pigmentosa, peripheral polyneuropathy, cerebellar ataxia, and high concentration of proteins in the cerebrospinal fluid, therefore phytanic acid accumulation in Refsum´s disease can be classified as a true peroxisome disorder [142]. In addition, peroxisomes contain a variety of enzymes involved in β-oxidation, such as three acyl-CoA oxidases (ACOX1, ACOX2, ACOX3), two multifunctional proteins (MFP1, MFP2), and several ketoacyl-CoA thiolase (Thiolase A and B, SCPx) [137] (Fig.9). In comparison to the peroxisomal β-oxidation pathways, mitochondria contain distinct acyl-CoA dehydrogenases [144, 145].

FATTY ACID β-OXIDATION

Peroxisomes

Fatty acid + CoA

- ATP   Acyl-CoA synthetase
- AMP + PPi Carnitine octanoyl transferase

→ Acyl-CoA

Oxidation   FAD — O_2 ACOX1
             FADH₂ ← H_2O_2 ACOX2
                                 ACOX3

Enoyl-CoA
- H_2O

Hydration   DBP
                                 LBP
3-Hydroxyacyl-CoA
- NAD⁺

Dehydrogenation   NADH + H⁺

3-Ketoacyl-CoA
- CoA   ThioA
                                 ThioB
Thiolysis   SCPx

Acyl-CoA   Acetyl-CoA
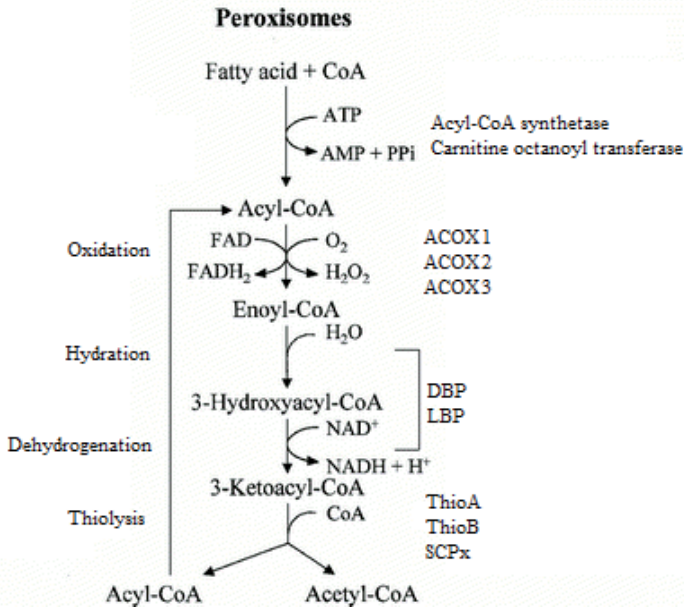
Fig. 9. The peroxisomal-inducible classical straight-chain and the non inducible branched-chain fatty acid β-oxidation systems in humans [145]. D-bifunctional protein (DBP), l-bifunctional protein (LBP), acyl-CoA oxidases 1 (ACOX1), Thiolase A, B (ThioA, ThioB), Peroxisomal Sterol Carrier Protein X (SCPx)

1.20. PPARs in the lung and idiopathic pulmonary fibrosis

Peroxisome proliferator-activated receptors (PPARs) are a family of ligand-activated transcription factors that belong to the nuclear hormone receptor family. They are important modulators of the immune system and in cell differentiation and proliferation [146, 147]. Three different subtypes of PPARs exist: PPARα, PPARβ/δ and PPARγ. PPARγ has got two isoforms, PPARγ1 which is expressed mainly in adipose tissue, while PPARγ2 is more widely expressed but is most abundant also in adipocytes [146]. Both are also expressed in different cell types in the lung, such as fibroblasts, ciliated airway epithelial cells and AEC II, alveolar macrophages, endothelial cells, airway smooth muscle cells, eosinophils, dendritic cells, T-cells and B-cells [146, 148]. Several other cell types express in addition also PPAR-α and PPAR-β/δ such as ciliated bronchial epithelial cells, alveolar macrophages, endothelial cells, T-cells and B-cells [146]. PPAR-α and PPAR-γ exhibit immunomodulatory properties and might play also a role in inflammation and wound healing processes, as well as may function as antifibrotic agents [11, 146, 149, 150]. In addition, many recent in vivo studies support the

antifibrotic properties of PPAR-γ agonists, who might promote differentiation of lung fibroblasts into fat storing lipofibroblasts and inhibit the critical differentiation of fibroblasts into myofibroblasts [147]. Furthermore, PPAR-γ ligands, like rosiglitazone and 15d-PGJ2 induce a lower mortality, reduced histological fibrosis, decreased inflammation with reduced α–SMA expression and reduced collagen content in the mouse model of bleomycin-induced lung fibrosis [147]. PPAR-γ ligands upregulate the expression of the "phosphatase and tensin homologue deleted on chromosome 10" (PTEN), whose promoter contains a peroxisome proliferator response element (PPRE). Moreover, in vitro studies have shown the inhibitory effects of PTEN on fibroblast differentiation into myofibroblasts as well as on the reduced expression of α-SMA in human and mouse fibroblasts [23, 147]. Thus PPARs might be protective therapeutic agents against the progression of IPF.

1.21. Role of PPARs in the prevention of fibrosis

PPAR-α was known to mediate the action of some drugs, mostly hypolipidemic agents that proliferate peroxisomes in rodent liver [119]. In addition, PPAR-α activates different peroxisomal and mitochondrial β-oxidation enzymes such as peroxisomal acyl-CoA oxidase and peroxisomal 3-ketoacyl-CoA thiolase [151]. In addition, PPAR-α is implicated in lipid metabolism and was shown to posses important anti-inflammantory properties especially in protection and control of airway inflammation [146, 152]. PPAR-α resulted also in boosting dexamethasone-mediated anti-inflammatory properties [153]. The combination of a PPAR-α agonist with dexamethasone had significantly increased the anti-inflammatory activity of corticoids in mice [153]. In contrast, inflammation was increased in PPAR-α knockout mice compared to wild-type controls [153]. Furthermore, fenofibrate was shown to reduce the LPS-induced inflammation in the mouse lung, demonstrated by reduced neutrophil and macrophage infiltration [154]. In accordance with the findings above, treatment of PPAR-α knockout mice with bleomycin resulted in a more severe inflammation and fibrosis development than in wild-type mice [155]. These bleomycin-treated PPAR-α knockout mice exhibited higher levels of cytokines such as TNF-α, whereas treatment of mice with PPAR-α agonist WY-14643 significantly reduced inflammation and fibrosis progression [155, 156]. Even though several studies have shown beneficial effects of PPARs in the development of fibrosis in different organ systems, nobody has studied whether the effect is mediated by peroxisomal proliferation and their metabolic activation.

1.22. Work hypothesis and aims

We hypothesized that during idiopathic pulmonary fibrosis, different cytokines, such as TNFα and TGF-β would induce the downregulation of peroxisomal biogenesis- and lipid metabolic proteins and that stimulation of the peroxisomal compartment would improve the disease progression or alleviate the fibrotic response in patients with IPF.

In detail our specific aims were:

- To analyze peroxisomal biogenesis proteins (e.g. PEX13p, PEX14p), peroxisomal lipid metabolism (e.g. ABCD3, ACOX1), as well as peroxisomal antioxidative enzymes such as catalase and others in IPF patients in comparison to control subjects.
- To study the fibrotic response and TGF-β signaling in RNAi-mediated knockdown of peroxisomal biogenesis (PEX13) in control and IPF lung fibroblasts.
- To determine the possible impact of TGF-β and other cytokines (TNF-α, IL-6) on the regulation of peroxisomal biogenesis and metabolism in pulmonary fibrosis.
- To assess the mechanisms at cellular and molecular level for the regulation of peroxisomal gene expression by TGF-β signaling.
- To assess peroxisomal alterations in a bleomycin-induced pulmonary fibrosis mouse model.
- To analyze the eventual peroxisomal response to bleomycin treatment in TβRII KO mice in comparison to control littermates.
- To determine the regulation of peroxisomes by TGF-β signaling in TβRII and Smad3 knockout mice, as well as in TGF-β receptor I constitutively active mice (TβRI^{CA}).
- To study the effects of PPAR-α-induction and peroxisome proliferation on the fibrotic response.

Understanding the mechanisms by which peroxisomes support the cellular protection from external toxic agents such as reactive oxygen species or proinflammatory mediators may open new treatment strategies for pulmonary fibrosis. By using human IPF and control fibroblast cultures as well as the bleomycin-induced mouse lung fibrosis model, this study enhances the knowledge on the role of peroxisomes in IPF and provides novel insights into TGF-β and TNF-α induced dysfunction of peroxisomes, as well as in understanding the molecular pathogenesis of IPF.

2. Material and methods

2.1. Materials

2.1.1. General instruments, materials and reagents

All chemicals used in the thesis were of analytical grade purity. Detailed chemicals, reagents and consumables are specified along the methodology below.

All instruments, general materials as well as chemicals and enzymes are listed in table I.

General materials	Company name
Cell culture 6 well plate	Becton Dickinson GmbH, Heidelberg, Germany
Cell culture 12 well plate	Becton Dickinson GmbH, Heidelberg, Germany
Cover slips	R. Langenbrinck, Emmendingen, Germany
Gibco´s Dulbecco´s Modified Eagle Medium, (DMEM), High glucose	Sigma, Steinheim, Germany
Dimethyl sulfoxide (DMSO)	Invitrogen Life Technologies GmbH, Karlsruhe, Germany
Eppendorf tubes	Eppendorf AG, Hamburg, Germany
Falcon tubes	Becton Dickinson, Heidelberg, Germany
Filter tips	Braun, Melsungen, Germany
Microscope slides	R. Langenbrinck, Emmendingen, Germany
Nitrile gloves	Kimberly-Clark Professional, Koblenz-Rheinhafen, Germany
Pasteur pipettes	VWR International GmbH, Darmstadt, Germany
Petri dishes	Becton Dickinson GmbH, Heidelberg, Germany
Plastic pipettes, for cell culture (sterile)	Becton Dickinson GmbH, Heidelberg, Germany
Phosphate-buffer saline (PBS)	PAA laboratories GmbH, Pasching, Austria
Syringe filters 0.22 microns	Millipore GmbH, Schwalbach, Germany
Chemicals and enzymes	**Company name**
Agarose	Roche, Grenzach-Wyhlen, Germany
Bovine serum albumin (BSA)	Carl-Roth GmbH & Co, Karlsruhe, Germany
Disodium hydrogen phosphate (Na2HPO4)	Merck, Darmstadt, Germany
Ethanol	Riedel-de-Haën, Seelze, Germany
Ethidium bromide	Fluka, Neu-Ulm, Germany
Ethylene diamine tetraacetic acid (EDTA)	Fluka, Neu-Ulm, Germany
Fetal calf serum (FCS)	PAA laboratories GmbH, Pasching, Austria
Gibco´s 0.25% Trypsin/EDTA	Invitrogen Life Technologies GmbH, Karlsruhe, Germany
Glycine	USB Europe GmbH, Staufen, Germany
L-Glutamate	Cambrex BioScience, MD, USA
N-propyl-gallate	Sigma, Steinheim, Germany
Mowiol 4-88	Polysciences Europe GmbH, Eppelheim, Germany
Paraformaldehyde (PFA)	Sigma, Steinheim, Germany

Pencillin/ streptomycin	PAA laboratories GmbH, Pasching, Austria
Potassium dihydrogen phosphate (KH2PO4)	Carl-Roth GmbH & Co, Karlsruhe, Germany
Sodium chloride (NaCl)	Carl-Roth GmbH & Co, Karlsruhe, Germany
Taq DNA polymerase	Invitrogen, Heidelberg
Triton X-100	Sigma, Steinheim, Germany
Trypan blue	Sigma, Steinheim, Germany
Trypsin	Sigma, Steinheim, Germany
Tween 20	Fluka, Steinheim, Germany
1 kb Ladder	Promega, Germany
Potassium chloride (KCl)	Sigma, Steinheim, Germany
Tris (trishydroxymethylaminomethane)	Sigma, Steinheim, Germany
Instruments used	**Company name**
Bio-Rad electrophoresis apparatus	Bio-Rad, Heidelberg, Germany
Dish washing machine	Miele, Gütersloh, Germany
Cary 50 Bio-UV-visible spectrophotometer	Varian, Darmstadt, Germany
Gel-Doc 2000 gel documentation system	Bio-Rad, Heidelberg, Germany
Hera cell 240 incubator	Thermo Scientific Corporation, MA, USA
Hera safe, clean bench	Thermo Scientific Corporation, MA, USA
Ice machine	Manitowoc Ice UY-0140A, USA
iCycler PCR machine	Bio-Rad, Heidelberg, Germany
Leica DMRD fluorescence microscope	Leica Microsystems GmbH, Wetzlar, Germany
Leica TCS SP5 confocal laser scanning microscope	Leica Microsystems GmbH, Wetzlar, Germany
Magnetic stirrer, MR3001	Heidolph Instruments GmbH & Co.KG, Schwalbach,Germany
Microwave oven	LG Electronics GmbH, Austria
Mini centrifuge	Carl-Roth GmbH & Co, Karlsruhe, Germany
pH Meter	IKA® Werke GmbH & Co. KG, Staufen, Germany
Pipettes	Eppendorf AG, Hamburg, Germany
Pipette tips	Eppendorf AG, Hamburg, Germany
Power supply -200, 300 and 3000 Xi Bio-Rad, Heidelberg, Germany	Bio-Rad, Heidelberg, Germany
Pressure/ Vacuum Autoclave FVA/3	Fedegari, Albuzzano, Italy
SmartspecTM 3000 spectrophotometer	Bio-Rad Laboratories GmbH, München, Germany
T25 basic homogenizer	IKA, Staufen, Germany
Vortex M10	VWR International GmbH, Darmstadt, Germany
Water bath GFL 1083	GFL Gesellschaft für Labortechnik mbH, Burgwedel, Germany

Table I. General materials, chemicals, enzymes and instruments used in experiments

2.1.2. Buffers and solutions

All buffers and solutions used in this thesis are listed in table II.

Name of solution	Composition
Solutions for cell culture & morphology	
Perfusion fixative solution (PFA)	4% PFA in 1X PBS (150 mM NaCl, 13.1 mM K_2HPO_4, 5 mM KH_2PO_4), pH 7.4
10 X PBS	1.5 M NaCl, 131 mM K_2HPO_4, 50 mM KH_2PO_4, pH 7.4
Trypsin (0.01%)	Fresh 0.01 g trypsin in 100 ml of 1X PBS buffer
Blocking buffer-4% PBSA + 0.05% Tween 20	8 g BSA in 200 ml of 1X PBS and Tween 20
Dilution buffer- 1% PBSA + 0.05% Tween 20	2 g BSA in 200 ml of 1X PBS and Tween 20
Mowiol 4-88 solution	16.7 % Mowiol 4-88 (w/v) in 80 ml of 1X PBS, 40 ml of glycerol will be added, and centrifuged at 15,000U/min for 1 h, the supernatant was stored at -20°C prior use.
Anti-fading agent	2.5 % N-propyl-gallate in 1X PBS and add 50 % of glycerol
Mounting medium for immunofluorescence	3 parts of Mowiol 4-88 + 1 part of anti-fading agent
Solutions for biochemistry	
Homogenization buffer (HMB)	To 50 ml of 0.25 M sucrose and 5 mM MOPS (pH 7.4) add only before use 500 µl 100 mM EDTA + 50 µl 100% ethanol + 5 µl 2 M DTT + 50 µl 1 M aminocaproic acid and 100 µl cocktail of protease inhibitors
Cell lysis buffer (1X)	50mM Tris +150mM Nacl +1% Triton-X-100 (pH 7.4). Before use 10% protease inhibitor cocktail was added.
Resolving gel buffer A	1.5 M Tris-HCl, pH 8.8 + 0.4% SDS
Stacking gel buffer B	0.5 M Tris-HCl, pH 6.8 + 0.4% SDS
12 % resolving gel (for 4 SDS-PAGE gels)	8 ml of 30% acrylamide + 10 ml of buffer A + 2 ml of ddH_2O + 15 µl of TEMED + 130 µl of 10% APS
Stacking gel (for 4 SDS-PAGE gels)	1.25 ml of 30% acrylamide + 5 ml of buffer B + 5 ml of distilled H_2O + 15 µl of TEMED + 130 µl of 10% APS
10X Sample buffer	3.55 ml ddH_2O + 1.25 ml 0.5 M Tris-HCl, pH 6.8 + 2.5 ml 50% (w/v) glycerol + 2.0 ml 10% (w/v) SDS + a pinch of 0.05% bromophenol blue. Before use add 50 ml β-mercaptoethanol
10% Blocking buffer	10 g fat free milk powder in 100 ml of ddH_2O
10X Electrophoresis buffer	250 mM Tris + 2 M glycin + 1% SDS

20X Transfer buffer	Bis-Tris-HCl buffered (pH 6.4) polyacrylamide gel; NuPAGE transfer buffer, Invitrogen, Heidelberg, Germany
10X TBS	0.1 M Tris in 0.15 M NaCl in, pH 8.0
1X Washing buffer (TBST)	10 mM Tris/HCl, 0.15 M NaCl, 0.05% Tween 20, pH 8.0
Stripping buffer	62.5 mM Tris, 0.2 % SDS, 42°C in a water bath for 40 min pH 6.8

Table II. Chemical reagents and buffers employed in experimental setup

2.1.3. Recombinant cytokines and drugs

Recombinant cytokines and drugs used in this thesis are summarized in table III.

Cytokines, drugs	Application	Concentration	Vehicle	Company
Ciprofibrate	PPAR-α agonist	200 mM	DMSO	Sigma-Aldrich, Missouri-USA
GW6471	PPAR-α antagonist	10 mM	DMSO	Tocris, United Kingdom
Luteolin	Inhibitor of Nrf2	100 mM	Ethanol	Sigma-Aldrich, Missouri-USA
LY364947	Inhibition of TGF-β1 signaling	5 mM	DMSO	Tocris, United Kingdom
rHuIL-6	Activation of Interleukin 6	200 µg	4 ml pyrogen free ddH$_2$O	Biomol, Germany
rhTGF-β1	Activation of TGF-β1 signaling	20 µg/ml	4 mM HCl + 1 mg/ml BSA	R&D, USA
rHuTNF-α	Activation of TNF-α signaling	100 µg/ml	18 MΩ-cm H$_2$O	Biomol, Germany
SR11302	Inhibitor of activator protein-1 (AP-1)	10 mM	DMSO	Tocris, United Kingdom
WY14643	PPAR-α agonist	100 mM	DMSO	Tocris, United Kingdom

Table III. Recombinant cytokines and drugs

2.1.4. siRNA

The following siRNAs were used to knockdown peroxisomal biogenesis and as controls in table IV.

siRNA	pmol/transfection	Provider
PEX13 siRNA	150	Ambion AM16708, Darmstadt, Germany
PEX13 siRNA	150	Ambion AM16773, Darmstadt, Germany
silencer select negative RNA	150	Ambion, Cat#4390843, Darmstadt, Germany

Table IV. siRNAs applied for cell transfection

2.1.5. Luciferase reporter and expression plasmids

The following luciferase reporter and expression plasmids are shown in table V.

Plasmid	Description	Institute /Company name
COL1A2-luc	Collagen 1A2	Dr. Eunsum Jung (BioSpectrum LifeScience Institute, Korea)
pARE-luc	Antioxidant response element reporter plasmid	Dr. William E. Fahl (University of Wisconsin, Madison, WI, USA)
pAP-1-luc	Activator protein 1 reporter plasmid	Dr. Craig A. Hauser (The Burnham Institute, La Jolla, CA)
pGL2 basic	Empty vector negative Control	Promega, Madison, WI, USA
pGL3 basic	Empty vector negative Control	Promega, Madison, WI, USA
pGL4 basic	Empty vector negative Control	Promega, Madison, WI, USA
PPAR reporter luciferase Kit	PPAR reporter	Qiagen Cignal PPAR Reporter, Kit: CCS-3026L
pRL-SV40 Vector	pRL Renilla luciferase control reporter vector	Promega, Madison, WI, USA
SBE-luc	Smad binding element reporter plasmid	Dr. Bert Vogelstein (Johns Hopkins Kimmel Cancer Center Baltimore, MD, USA)
pSG5 PPAR alpha	PPAR-α expression plasmid	Addgene plasmid # 22751

Table V. Luciferase reporter and expression plasmids

2.1.6. Transfection reagents

The following transfection reagents were used for siRNA and plasmid transfection in table VI.

Reagent	Application	Company
Interferin	siRNA transfection Reagent	Peqlab, Erlangen, Germany
TransIT-LT1	plasmid transfection reagent	Mirus Bio LLC, WI, USA
Attractene	plasmid transfection reagent	Qiagen, Hilden, Germany

Table VI. Transfection reagents

2.1.7. Kits

The list of kits used in this thesis with corresponding suppliers in table VII.

Kits	Company name
Dual luciferase kit	Promega, Madison, WI, USA
Human IL-6 Quantikine ELISA Kit	R&D, Systems Inc. Minneapolis, USA
Human TGF-β1 immunoassay	R&D, Systems Inc. Minneapolis, USA
qPCR kit	Qiagen, Hilden, Germany
QIAGEN Plasmid midi kits	Qiagen, Hilden, Germany
Rneasy kit	Qiagen, Hilden, Germany
RT-PCR kit	Invitrogen, Karlsruhe, Germany
Sircol Soluble Collagen Assay	Biocolor, Northern Ireland, UK

Table VII. Molecular and cellular biology kits

2.1.8. Antibodies

The list of antibodies used for immunofluorescence, Immunohistochemistry and Western blots are summarized in table VIII.

Antigens	Species AB raised in	Dilution	Supplier
α-SMA	Mouse, monoclonal	(IF) 1:2,000 (WB) 1:2,000	Sigma, Missouri, USA Cat. A2547
ABC-transporter D3 (abcd3), mouse	Rabbit, polyclonal	(IF) 1:100	Gift from Alfred Völkl, University of Heidelberg, Germany
Acyl-CoA oxidase 1 (ACOX1), mouse	Rabbit, polyclonal	(IF) 1:1000	Gift from Paul P. van Veldhoven, Dept. of Molecular Cell Biology, Pharmacology, Catholic
Catalase (CAT), mouse	Rabbit, polyclonal	(IF) 1:2,000 (WB)1:10,000	Gift from Denis I. Crane, School of Biomol. Biophys. Sci., Griffith Univ., Nathan, Brisbane, Australia
Catalase (CAT), human	Rabbit, polyclonal	(IF) 1:250	Polyscience (Cat:23728)
Collagen I, mouse	Rabbit, polyclonal	(IF) 1:500 (WB) 1:500	Novus Biologicals, Cat. No: NB600-408
Collagen III, mouse	Rabbit, polyclonal	(IF) 1:500	Novus Biologicals, Cat. No:
Glutathione reductase (GR), mouse	Rabbit, polyclonal	(IF) 1:500	Abcam/Biozol (Cat:ab16801)
Glyceraldehyde 3-phosphate dehydrogenase (GAPDH), rabbit	Mouse, monoclonal	(WB) 1:10,000	HyTest Ltd, Turku, Finland, Cat. No: 5G4
Heme oxygenase 1 (HO-1), rat	Rabbit, polyclonal	(IF) 1:1,000	Assay Designs, Inc. Michigan, USA,Cat.no:SPA-895
Ki67, mouse	Rat, monoclonal	(IF) 1:600	Dakocytomation, Denmark, Cat, no: M7249
c-Myc, human	Mouse, monoclonal	(IHC) 1:250	Santa Cruz Biotechnology, Oregon, USA (9E10): sc-40
Nuclear factor erythroid 2-related factor 2 (Nrf2), human	Rabbit, polyclonal	(IF) 1:250	Santa Cruz Biotechnology Inc. Heidelberg, Germany, Cat. No:sc-13032
Peroxisomal biogenesis factor 13 (Pex13p), mouse	Rabbit, polyclonal	(IF) 1:2,000 (WB) 1:6,000	Gift from Denis I. Crane
Peroxisomal biogenesis factor 14 (Pex14p), mouse	Rabbit, polyclonal	(IF) 1:4,000 (IHC) 1:4000 (WB)1:10,000	Gift from Denis I. Crane
Prolyl 4-hydroxylase (PDI), mouse	Rabbit, polyclonal	(IF) 1:100	Acris (AP08767PU-N)
Smad3, mouse	Rabbit, polyclonal	(IF) 1:50	Cell signalling (Cat:9523)
Superoxide dismutase 2 (SOD2), rat	Rabbit, polyclonal	(IF) 1:5,000	Research Diagnostics, Inc., NJ, USA, Cat. No: RDI-RTSODMabR

Table VIII. Antibodies for Western blotting (WB), Immunohistochemistry (IHC) and immunofluorescence (IF)

2.1.9. Secondary antibodies and counterstaining of nuclei

The list of secondary antibodies and counterstaining of nuclei used in this thesis are presented below in table IX.

Secondary detection system	Host	Method	Dilution	Supplier
Anti Rabbit-IgG Alexa Fluor 488	Donkey	IF	1:600	Molecular Probes/Invitrogen, Cat. No: A21206
Anti-Mouse-IgG AlexaFluor555	Donkey	IF	1:1,000	Molecular Probes/Invitrogen, Cat. No: A31570
Rabbit biotinylated IgG	Goat	IHC	1:250	Rabbit Extravidin kit, Sigma, Steinheim, Germany, Cat. No: B6648
Extravidin	Rabbit	IHC	1:250	Rabbit Extravidin kit, Sigma, Steinheim, Germany, Cat. No: E8386
Anti mouse IgG alkaline phosphatase	Goat	WB	1:20,000	Sigma, Steinheim, Germany. Cat. No: A3562
Anti rabbit IgG alkaline phosphatase	Goat	WB	1:20,000	Sigma, Steinheim, Germany. Cat. No: A3562
Counterstaining of nuclei for IF				
Hoechst 33342 (1 μg/ml) nucleic acid staining	-	-	-	Molecular Probes/Invitrogen, Cat. No: 33342
TOTO-3 nucleic acid staining, 1:1,000	-	-	-	Molecular Probes/Invitrogen, Cat. No: T-3604

Table IX. Secondary antibodies and nuclear stains

2.1.10. Primers

Human and mouse primers used for RT-PCR and qRT-PCR are summarized in table X-XII.

Gene	Primer	Annealing (°C)	Length (bp)
PEX13	For: TCAGCAAGCTGAAGAAAGCA Rev: CTGCAGGCAAACATGAAAGA	61,5	434
TGF-β1	For:GGATAACACACTGCAAGTGGAC Rev: GGGTTATGCTGGTTGTACAGG	58,7	330
COL1A2	For:TCAGAACATCACCTACCACTGC Rev:GTCCAGAGGTGCAATGTCAAG	61,5	300
IL-6	For: AGGAGACTTGCCTGGTGAAA Rev: CAGGTTTCTGACCAGAAGAAGG	61,5	370
MMP2	For: TACTGGATCTACTCAGCCAGCA Rev: CTTCAGGTAATAGGCACCCTTG	61,5	300
28S rRNA	For: AAACTCTGGTGGAGGTCCGT Rev: CTTACCAAAAGTGGCCCACTA	63	250
HPRT	For: AAGCTTGCTGGTGAAAAGGA Rev: AAGCAGATGGCCACAGAACT	61,5	260

Table X. Human primers for RT-PCR

Gene	Primer	Annealing (°C)	Length (bp)
PEX13	For: CCATGTAGTTGCCAGAGCAG Rev: CATCAAGGCTAGCCAGAAGC	61,5	140
PEX14	For: CTGCCTTTGGCTTTGATCTC Rev: CGTGGTGTCACGGTAGTCAA	61,5	137
TGF-β1	For: GGATAACACACTGCAAGTGGAC Rev: GGGTTATGCTGGTTGTACAGG	61,5	330
COL1A2	GGTATAGGGAGCTCCAAGGACAA GCAGCCATCTACAAGAACAGTG	61,5	305
TNF-α	For*: TCTACTCCCAGGTCCTCTTCAA* Rev: *AGACTCGGCAAAGTCGAGATAG*	61,5	269
IL-6	For: AGGAGACTTGCCTGGTGAAA Rev: CAGGTTTCTGACCAGAAGAAGG	61,5	370
28S rRNA	For: AAACTCTGGTGGAGGTCCGT Rev: CTTACCAAAAGTGGCCCACTA	63	250

Table XI. Human primers for qRT-PCR

Gene	Primer	Annealing (°C)	Length (bp)
mPEX14	For: CACTGGCCTCTGTCCAAGAGCTA Rev: CTGACAGGGGAGATGTCACTGCT	61,5	298
mCatalase	For: GCAGATACCTGTGAACTGTC Rev: GTAGAATGTCCGCACCTGAG	58,7	103

Table XII. Mouse primers for qRT-PCR

2.2. Methods

2.2.1. Cell culture and tissue sections

In this thesis work, human lung tissue (cryosamples and paraffin embedded tissue) and fibroblasts from patients with IPF or control organ donors were used, obtained from the Giessen DZL-biobank (Deutsches Zentrum für Lungenforschung) at UGMLC (University of Giessen and Marburg Lung Center). Directly after lung transplantation tissue samples were snap frozen in liquid nitrogen or placed in 4% (w/v) paraformaldehyde in PBS buffer, pH 7,4. Control and IPF fibroblasts were cultured in Dulbecco's Modified Eagle's Medium (DMEM) with low glucose supplemented with 2 mM L-glutamine, 10 U of penicillin/ml, 100 µg of streptomycin/ml, 10% FBS and maintained at 37°C with 5% CO_2 for different time-points as described below.

Medium composition

The compositions of the medium and corresponding suppliers are listed in table XIII.

Product	Uses	Company
10 % Fetal Bovine Serum	Growth promoting and survival	PAA laboratories, United Kingom
1% Penicillin Streptomycin	Antibacterial agent	Gibco, USA
L-Glutamine	additive component	Merck-Millipore, Germany

Table XIII. Cell culture medium supplements

2.2.2. Isolation of control/IPF fibroblasts

Primary human control (n=10) and IPF fibroblasts (n=10) were isolated from human lung tissue biopsies obtained from patients undergoing lobectomy or pneumectomy. Tissues were cut in small slices, placed in cell culture flasks and cells regularly grown out from the tissue slices after 1 week and passaged thereafter by standard trypsinization. Isolated human lung fibroblasts were frozen in passage 3 or 4 until use. Fibroblasts were plated onto 10-cm^2 cell culture dishes and grown until confluency. They were passaged or plated for the respective experiments described below. For all experiments, fibroblasts cells were used before until the eighth passage. After passaging, cells were grown for 24 hours before undergoing any treatment with above mentioned reagents or siRNA transfection.

2.2.3. Freezing of cells

Human control and IPF lung fibroblasts were cultivated at 5% CO_2 until confluency and 37°C and passaged by trypsinization with Gibco´s 0.25% Trypsin/EDTA for 3 minutes at 37°C. After trypsinization, the cells were detached using 6 ml of fresh medium and centrifuged at 200 g for 5 min. Meanwhile the freezing solution was prepared in a ratio of 70% fresh DMEM medium, 20% of FBS and 10% of dimethyl sulfoxide (DMSO). The freezing solution was kept at 4°C for 20 minutes prior to use. The cell pellets were resuspended in the freezing solution and frozen in Nalgene cryobox filled with isopropanol at -80°C overnight. The next day, the cryotubes were transferred to liquid nitrogen for long-term storage.

2.2.4. Poly –L-lysine coating

Coverslips were placed in 12 well or 24 well Petri dishes. 10 mg of poly-L-lysine hydrobromide was dissolved in 100 ml of 0.1 M borate buffer and filtered with Millipore syringe filters of 0.22 µm. Thereafter 2 ml of the solution was added to the sterile coverslips. The incubation of Petri dishes with cover slips was done overnight under a laminar flow. After 24 h the dishes were washed twice with dd H_2O, left in ddH_2O for 5 h and thereafter washed again 2 x 5 min with dd H_2O, followed by aspiration of water drops and air drying prior to storage.

2.2.5. Mice

(The experimental work in transgenic mice and bleomycin induced pulmonary fibrosis was performed during my laboratory rotation at Saban Research Institute of Children's Hospital Los Angeles, California, USA).

C57BL/6J wild type mice, 8 wk of age, were kept under specific pathogen-free conditions at the animal facility of Children's Hospital Los Angeles. Floxed-TGF-β receptor II (*TβRII*) mice were provided by Dr. Harold Moses at Vanderbilt University [157], in which Exon 2 and Exon 3 of the *TβRII* gene were floxed [157, 158]. The mice were crossed with Tbx4-rtTA/TetO-Cre driver line [107], and lung mesenchyme-specific deletion of *TβRII* Exon 2/3 was achieved upon doxycycline administration [105]. *Smad3* null mutant (-/-) mice were bred from C57BL/6 heterozygous mice with deletion of exon 1 in the *Smad3* gene [13]. Transgenic mouse strain containing constitutively active TGF-β I receptor (*TβRI^{CA}*) were provided by Dr. Laurent Bartholin at University of Lyon [111]. LoxP-STOP-loxP-TβRI^{CA} mice were generated by using a knock-in strategy into the X chromosome-linked hypoxanthine phosphoribosyl-transferase locus (Hprt). By crossing with Tbx4-rtTA/TetO-Cre driver line, the STOP cassette was excised specifically in lung resident mesenchymal cells upon doxycycline-induced Cre expression, which resulted in *TβRI^{CA}* transgene expression under control of CAG (human cytomegalovirus enhancer and chicken β-actin) promoter [111]. Mice were monitored regularly and received food and water ad libitum (n=3 for each strain). Mice were anesthetized with isoflurane inhalation, were administered with 4 U/kg bleomycin (Sigma, St. Louis, MO) diluted in 120 µl of saline, or saline alone by intratracheal instillation using an intratracheal aerosolizer (MicroSprayer® Aerosolizer – Model IA, Penn-Century, Wyndmoor, PA on day 0 [105]. Lungs were removed for protein and mRNA isolation or

immersion fixed overnight in 4% paraformaldehyde fixative in PBS (pH 7.4) and embedded in paraffin (Paraplast Plus, St. Louis, MO) for histological analysis. Animal protocols used in the experiments were approved by the Institutional Animal Care and Use Committee at Children's Hospital Los Angeles.

2.2.6. Bleomycin-induced pulmonary fibrosis

Three female C57BL/6J control and TGF-β receptor II ($T\beta RII$) knockout mice (8-week-old), anesthetized with isoflurane inhalation, were administered with 4 U/kg bleomycin (Sigma, St. Louis, MO) diluted in 120 μl of saline, or saline alone by intratracheal instillation using an intratracheal aerosolizer (MicroSprayer® Aerosolizer – Model IA, Penn-Century, Wyndmoor, PA) on day 0 [105]. The mouse lungs were then harvested 7, 14 and 28 days post bleomycin treatment. The bleomycin dose used in the experiment was shown to produce pulmonary fibrosis consistently with a low mortality rate of the animals (10%) [13]. Lungs were immersion-fixed in 4% PFA in PBS (pH 7.4) at 4°C overnight, then dehydrated and embedded in paraffin. Paraffin sections of 5 μm thickness were cut on a sliding microtome and used for immunofluorescence staining [105].

2.2.7. Isolation of mouse fibroblasts

C57BL/6J mouse primary lung fibroblasts from *TβRII, Smad3* wild-type and knockout as well as from *TβRI* wild-type and *TβRI^{CA}* were isolated from lung tissues of pathogen-free laboratory mice. Lungs were perfused with PBS from right ventricle, and transferred the deblooded lung to a sterile dish. The minced tissue to 1 mm^3 was washed with ice-cold PBS and centrifuged at 1600 rpm for 6 min. The supernatant was discarded. Then, the minced tissue was digested with digestion solution at 37 °C for 60 min (shaking in water bath, by pipetting every 10 min). The digestion solution was prepared in Ca/Mg-free PBS, containing Dispase II 2 mg/ml (Roche), Collagenase I 1 mg/ml (Sigma), Dnase Type I 0,16 mg/mg (Sigma). The digested tissue was filtered with 70 μm cell strainer, and washed with 10 ml of DMEM/F12 medium containing 10 % FBS. Cells were centrifuged at 1600 rpm for 6 min, then washed in DMEM/F12 medium containing 10 % FBS, and centrifuged again at 1600 rpm for 6 min. Cells were resuspended in DMEM/F12 medium containing 10 % FBS, plated at the density $10^5/cm^2$ in plastic culture flask T75 for 1 h at 37 °C. The unattached cells were removed by aspirating off the medium, the plate was washed again with fresh medium and

aspirated off again. Finally DMEM/F12 containing 10 % FBS was added and cell were incubated in culture at 37 °C, 5% CO_2 for 3-5 days. Primary lung fibroblasts were used in assays of standard biochemical procedures performed with cell cultures including qRT-PCR, Western blotting and immunofluorescence staining. Epithelial and endothelial cell contamination was checked be cytokeratin staining.

2.2.8. *PEX13* siRNA transfection of control and IPF fibroblasts for Western blot- and qRT-PCR-analyses and cytokine measurements

Human control and IPF lung fibroblasts were cultured in 12-well or 24-well plates (BD Falcon #353043), at $8x10^4$ cells/well or $4x10^4$ for 24 hours in normal media (DMEM 1x, Gibco) low glucose medium supplemented with 2 mM L-glutamine, 10 U of penicillin/ml, 100 μg of streptomycin/ml, 10% FBS) and maintained until 70-80 % confluency at 37 °C with 5% CO_2. Briefly, siRNA pools for *PEX13 knockdown* (same amount of *PEX13* siRNA 1 and 2) were incubated with the Interferin siRNA Transfection Reagent (Peqlab, Cat; 13-409-10) in basal media with no serum or antibiotics and allowed to form complexes for 15 min at room temperature. The complexes were then added to the cell suspension for each well (final siRNA concentration of 15 nM). After 24 h, cells were transfected for the second time with the same pool of *PEX13* siRNA. After 72 h from the first transfection, cells were collected by centrifugation (200 g for 5 min at RT) and the pellet processed further for RNA- or protein isolation. The supernatants were used for cytokine and collagen assays. For immunofluorescence and DHE staining, cells were grown on poly-L-lysine coated coverslips. After siRNA treatment they were fixed with the above mentioned 4% PFA-fixative and processed as described in IF.

2.2.9. rhTGF-β1 treatment

The human control and IPF pulmonary fibroblasts were cultured in the same manner as described above for the rhTGF-β1 treatment studies. After 24 h, cells were challenged with 5 ng/ml rhTGF-β1 for an additional 24 h. 1 h prior to TGF-β1 treatment cells were treated with specific inhibitors: 5μM LY364947 (Tocris Cat: 2718) TGF-β1 inhibitor, 10 μM SR11302 (Tocris, Cat.No.2476) an inhibitor of activator protein-1 (AP-1) transcription factor activity, or 25 μM Luteolin (Sigma, L9283), an Nrf2 inhibitor. Cells were further processed for immunofluorescence, RNA and protein isolation and supernatants were collected for cytokine ELISA according to manufacturers´ instructions. For TGF-β1-induced ROS production

studies, cells were treated for 30-60 minutes with TGF-β1, after which they were undergoing staining with (DHE) in a final concentration of 5 μM (see below).

2.2.10. TNF-α treatment

Cells were seeded as described previously at a density of 8 x 10^4 cells/well in 12-well plates. After 24 h, they were challenged with 10 ng/ml human rHuTNF-α (Biomol Cat: 50435) for different time points: 0 h, 1 h, 4 h and 6 h duration [99]. At the end of the incubation period, the cells were processed for RNA isolation, protein analysis with Western blotting and luciferase reporter assays.

2.2.11. IL-6 treatment

IPF fibroblasts were seeded as described previously at a density of 8 x 10^4 cells/well in 12-well plates. After 24 h, they were challenged with 20 ng/ml recombinant human IL-6 (Biomol, Cat: 50435) for 6 h duration. At the end of incubation period, the cells were processed for protein analysis with Western blotting.

2.2.12. PPAR-α agonist (ciprofibrate, WY14643) and PPAR-α antagonist (GW6471) treatment

The experiments were performed on control and IPF fibroblasts from the 2nd-8th passages. Cells were seeded for 24 h in 12-well and 24-well plates as described above. Cells were then treated with ciprofibrate (Sigma-Aldrich Chemie GmbH) for 48 h with the indicated concentrations: 0 μM, 150 μM, 300 μM, 600 μM, WY14643 (Tocris, Cat.No.1312) for 48 hours with the indicated concentrations: 0 μM, 50 μM, 100 μM, 200 μM, or with GW6471 (Tocris Cat: 4618) for 24 h with the indicated concentrations: 0 μM, 5 μM, 10 μM. After respective treatments, cells were processed for immunofluorescence and protein isolation. For the experiments of TGF-β1 treatment with combined PPAR-α agonists or antagonist pretreatment, IPF cells were either pretreated with ciprofibrate (200 μM) or WY14643 (100 μM) for 48 h after which the medium was replaced with serum free medium alone or serum free medium containing the PPAR-α antagonist GW6471 (10 μM) for an additional 1 h. Fibroblasts were treated for 2 h with ciprofibrate (200 μM), WY14643 (100 μM) in serum free medium, which was followed by the addition of TGF-β1 (5ng/ml) for 24 h.

2.2.13. Immunohistochemistry

Mouse lungs from $T\beta RI$ WT and $T\beta RI^{CA}$ were fixed by perfusion via the right ventricle of the heart with 4% paraformaldehyde in PBS (pH 7.4) and embedded into paraffin. Tissue sections of 5 µM thick were used for immunohistochemistry staining. Paraffin tissue sections were deparaffinized followed by blocking of the endogenous peroxidase (3% H_2O_2 for 10 min). Sections to be stained for PEX14 and c-Myc were treated with blocking goat serum for 1 h and incubated overnight with primary antibody dissolved in PBS/BSA at 4°C. The rabbit polyclonal antibody against PEX14 and the mouse monoclonal antibody against c-Myc were used accordingly (see table VIII). The next day, sections were washed with PBS to remove unbound primary antibody, followed by incubation of sections for 1 h with biotinylated anti-mouse or anti-rabbit secondary antibody. After careful washing with PBS, the sections were incubated with Extravidin peroxidase at RT. The peroxidase activity was visualized by using diaminobenzidine for peroxidase. Nuclei were counterstained with hematoxylin. Normal rabbit IgG, bovine serum albumin, and water were used in parallel slides as negative controls.

2.2.14. Immunofluorescence

Control and IPF fibroblasts were plated on poly-L-lysine (Sigma Aldrich GmbH, Steinheim Germany) coated coverslips in 24 well plates for 24 h and thereafter treated with rhTGF-β1 (R&D Cat: 240-B), LY364947 (Tocris Cat:2718), rHuTNF-a (Biomol Cat: 50435), ciprofibrate (Sigma), WY14643 (Tocris, Cat.No.1312), GW6471 (Tocris Cat:4618) for the indicated time points as described above. Thereafter, they were subjected to an indirect immunofluorescence staining protocol as previously described [80, 159]. Briefly, cells were washed with PBS, fixed in 4% paraformaldehyde and 2% sucrose in PBS buffer pH 7.4, after which they were permeabilized using 1% glycine containing 0.02% Triton X-100 for 10 min at RT. Nonspecific binding sites were blocked with 1% BSA in PBS containing 0.05% Tween 20 for 1 h at room temperature. Then, coverslips were incubated overnight at 4 °C with the primary antibodies for single or double staining (antibody concentration see table VIII). Coverslips were then washed and incubated with appropriate secondary antibodies (see table IX). Nuclei were visualized with 1µM Hoechst 333424 and TOTO-3-iodide 1:1,000 at RT embedded in Mowiol 4-88 with N-propyl gallate as an anti-fading agent. Images were captured using a confocal laser scanning microscope (Leica TCS SP2, Leica, Germany). Pictures were processed with Adobe Photoshop version 9.

2.2.15. Isolation of total RNA from fibroblasts

The total RNA was isolated from control and IPF human lung fibroblasts as well as from transgenic mice *TβRII* WT/KO, *Smad3* WT/KO and *TβRI* WT/CA fibroblasts by using the commercial RNAasy Minikit (QIAGEN, Hilden, Germany) and QIAshredder columns (QIAGEN, Hilden, Germany). Briefly, fibroblasts were plated in 12 mm cell culture dishes until they reached 70-80% confluency. Cells were rinsed with 1xPBS twice and lysed directly with RLT lysis buffer containing 1% β-mercaptoethanol. The homogenization was done by loading the cell lysate into a QIAshredder column. The homogenate was collected from the column by 2 min of centrifugation at 14,000x g and mixed with the same volume of 70% ethanol in order to provide appropriate binding conditions prior to loading into the Rneasy Mini spin column. In the column, the total RNA was preferentially bound to the silica column. Contaminating DNA and proteins were removed by repeated sequential washes with appropriate buffers from the kit. Finally RNA was eluted from the column with RNAse free water. Samples were quantified with the Nanodrop spectrophotometer (Thermo Fisher Scientific, Waltham, Massachusetts, USA) and approximately 30 μg of RNA per sample was recovered and stored at -80°C until use.

2.2.16. cDNA synthesis

Total RNA was isolated using the Rneasy kit (Qiagen), and cDNA was synthesized by reverse transcription using the high-capacity iScript cDNA reverse transcription kit (Bio-Rad, Hercules, California, USA). To conduct the cDNA synthesis a reaction mix was prepared as shown in Table XIV.

Components	Volume per 20 μl Reaction
5x iScript reaction mix	4 μl
iScript reverse transcriptase	1 μl
Nuclease-free water	14 μl
RNA template (1 μg/μl total RNA)	1 μl

Table XIV. Reverse transcription reaction mix

The reverse transcription reaction was conducted in a thermocycler (Thermo Fisher Scientific, Waltham, Massachusetts, USA), by employing the following program: 5 minutes incubation

at 25°C, 30 minutes at 42°C and 5 minutes at 74°C. The transcribed cDNA was stored at -20°C prior to further use.

2.2.17. qRT-PCR

Total RNA isolation of drug and cytokine treated fibroblasts and cDNA synthesis was done as described above. Quantitative RT-PCR analysis was carried out using the SYBR green premix on a qPCR machine (Bio-Rad iCycler) according to the manufacturer´s instructions. Normalization was done by using *HPRT* and *28S rRNA* control primers for each template. Primers for quantitative RT-PCR analysis were designed by using Primer 3 Software. Each primer pair was tested for specificity and amplification efficiency by using gradient PCR, agarose gel electrophoresis and melting curve analysis. The relative expression, fold change of a defined gene was calculated using the ddCT method. PCR amplification of the cDNA was done with the above primers mentioned in the table X-XII. The exclusive amplification of the expected PCR product was confirmed by melting curve analysis.

DNA amplification and the reaction mix is shown in Table XV.

Content	Amount
Template, cDNA	0.15 µg (2 µl)
SYBR Green	10 µl
Primer(forward& reverse)	2 µl
Water	6 µl
Total	20 µl

Table XV. qRT-PCR reaction mixture

2.2.18. Semi-quantitative RT-PCR analysis

For semi-quantitative analysis, specific primers for respective genes were designed using the PRIMER3 program (http://www.ncbi.nlm.nih.gov/tools/primer-blast) and synthesized by Eurofins, MWG or Operon (Ebersberg, Germany). Total RNA isolation of fibroblasts and cDNA synthesis was done as described above. Amplified PCR products were analyzed by gel electrophoresis using 1-2 % agarose gels. The PCR reaction was performed using 50 ng cDNA, 100 nmol forward and reverse primers and 1 µl 5PRIME TaqDNA polymerase 5 U/µl in a final volume of 25 µl.

2.2.19. Protein isolation from human control/IPF and mouse fibroblasts

Proteins were extracted from human control and IPF fibroblasts as well as from *TβRII* WT/KO, *Smad3* WT/KO and *TβRI* WT/[CA] (constitutively active) mouse fibroblasts with cell lysis buffer (1x) as described below with CompleteTM Protease inhibitor (Roche) added shortly before use (see table II). After mixing, 100 µl of cell lysis buffer was added to each well of the 12 well/plate. Fibroblasts were scraped thoroughly from the culture plate using a cell scraper and the lysate was pipetted into a 1.5 ml Eppendorf tube on ice. Cells were incubated for 20-min on ice with intermittent vortexing, cell debris and insoluble proteins were removed by centrifuging the cell lysate for 20 min at 10,000 g at 4 ºC. The supernatant was then transferred into a new 1.5 ml Eppendorf tube on ice and stored at -20 °C prior to further use.

2.2.20. Protein isolation from mouse lung tissue

Two g of tissue samples from *TβRII* WT/KO, *Smad3* WT/KO and *TβRI* WT/CA mouse lungs were homogenized with a Potter-Elvehjem homogenizer at 1,000 rpm (1 stroke, 60 s) in 2 ml ice-cold homogenization buffer (HMB) (see table II). The quality of the homogenization process was controlled by Trypan blue staining of the lung homogenates with a light microscope. Clumps of connective tissue, nuclei and large heavy mitochondria were sedimented by centrifugation of the homogenates at $2,500 \times g$ for 20 min at 4°C. The total homogenate was processed for protein measurement. The protein concentrations of all fractions mentioned were assayed using a Bradford assay with Bio-Rad solutions according to the manufacturer's instructions.

2.2.21. Measurement of protein concentration

Briefly, the isolated protein solution was diluted 1:125 with water. To each sample and an additional blank control, 200 µl of Bio-Rad Bradford solution was added. Then, 4 µl of the protein sample or the buffer (same dilution) was added to each sample duplicates. This was followed by 15 min incubation period at RT. The absorption was read in a plate reader at 570 nm. The concentration of the protein in each sample was calculated by using a newly prepared protein standard curve.

2.2.22. SDS-PAGE and Western blotting

Control and IPF fibroblasts were washed with 1x PBS, lysed and the protein quantification done with the Bradford protein assay (Bio-Rad, Munich, Germany) as described above [159]. Thirty µg of protein samples were separated by SDS-PAGE (12% gel) for ca. 2 h at 110 mV until the bromophenol blue marker reached the bottom of the gel. The gels with separated protein samples were further processed to blotting onto polyvinylidene difluoride membranes (PVDF, Millipore). Membranes were blocked with 5% skim milk or 5% BSA (depending on the following antibody steps), 50 mM Tris HCl (pH 7.6), 150 mM NaCl, and 0.05% Tween 20 for 1 hr at RT or at 4 °C overnight. The primary antibodies were diluted in the appropriate blocking buffer, using dilutions described in table VIII, and incubated overnight at 4°C overnight. On the following day, the membrane was washed three times 15 min in PBST. For secondary antibody detection, alkaline phosphatise-labelled goat anti-rabbit IgG or anti-mouse IgG alkaline phosphatase (DPC Bierman) were used accordingly (see table IX). Antigen-antibody complexes were visualized with chemiluminescence detection using the Immun-Star alkaline phosphatase substrate from Bio-Rad according to the manufacturer's instructions. The bands were visualized by exposing the blots to Kodak Biomax Films and quantified with a Bio-Rad Gel Doc 2000 system (Bio-Rad, Germany).

2.2.23. Transfection and dual luciferase assay

Control and IPF fibroblasts were cultured overnight. Transfection of plasmid DNA into the cells was performed by lipofection with TransIT-LT1 (Mirus Bio) as described previously [160] or Attractene transfection reagent as described in the manufacturer´s instructions (Qiagen). Cells were transfected with 1 µg of the firefly luciferase reporter plasmids in co-transfection with 1µg of the indicated renilla luciferase expression vectors. Empty vector controls were run in parallel by using the appropriate empty vector plasmid in co-transfection experiments with the renilla luciferase expression vectors. Cells were transfected with plasmids and after 24 h treated with respective drugs and cytokines for indicated time-points. For the PPAR reporter assay, cells were cotransfected with PPAR-α expression plasmid and the CIGNAL PPAR reporter construct and after 24 h treated with the respective cytokines and drugs for the indicated times as mentioned above. Cells were lysed with the luciferase lysis reagent (Promega), and firefly or renilla luciferase activities were determined with the appropriate substrates of the dual luciferase reporter assay system (Promega) as described in the manufacturer's instructions.

2.2.24. Measurement of reactive oxygen species

Generation of reactive oxygen species (ROS) was performed with dihydroethidine (DHE) at a final concentration of 5 μM. DHE is oxidized by superoxide to its fluorescent product ethidine. Ethidine is trapped intracellularly after it is oxidized, thus allowing quantitative estimations of the intracellular ROS level [161]. Control and IPF fibroblasts were grown on coverslips and transfected with *PEX13* siRNA, control siRNA, or treated respectively with the above mentioned drugs and cytokines (see table III). DHE was added to the cells and incubated for 20 minutes. Thereafter cells were washed with 1x PBS and fixed with 4% paraformaldehyde in PBS, pH 7.4 for 20 minutes at RT. The coverslips were mounted for measuring cellular ethidine fluorescence under a confocal laser scanning microscope (Leica TCS SP2, Leica, Germany) (40X objective). Ethidine fluorescence intensity was quantified individually in all cells using the Leica Confocal Software program (Leica, Bensheim, Germany). One hundred cells per sample were evaluated. The measured values represent the mean fluorescence intensity (MFI) of ethidine per cell.

2.2.25. Sircol Collagen Assay

To examine the release of collagens into the cell culture medium, control and IPF fibroblasts were grown in 12 well plates for 24 hours, followed by *PEX13* siRNA or control siRNA transfections using Interferin (4 μl or 2 μl). After 72 hours, the supernatants were collected and collagen production was analyzed by using the Sircol Assay protocol according to the manufacturer´s instructions (Biocolor).

2.2.26. Cytokine ELISAs

Control and IPF fibroblasts were transfected with *PEX13* or control siRNA and 72 hours after transfection the supernatants were collected and levels of secreted cytokines were analysed using the human TGF-β1 immunoassay, or the human IL-6 Quantikine ELISA Kit. In addition, cells were also treated with rHuTGF-β1, LY364947, ciprofibrate, GW6471 as mentioned above for 24 hours and the secreted levels of IL-6 were analyzed in the collected supernatants at the respective time-points with the Quantikine ELISA kit according to the manufacturer's instructions.

2.2.27. Statistics

All values are expressed as means ± SEM where n = 3 or 4. An unpaired Student's t-test or ANOVA test using SPSS Software were used to assess the difference between two groups. Image J was used for quantification of RT-PCR expression. Differences were considered statistically significant when $P<0.05$.

3. Results

The results of this thesis have been published in part in the *Proceedings of the National Academy of Sciences* of the United States of America (PNAS) and the pubmed ID of the following paper is: PMID: 25848047

Oruqaj G, Karnati S, Vijayan V, Kotarkonda LK, Boateng E, Zhang W, Ruppert C, Günther A, Shi W, Baumgart-Vogt E. **(2015).** Compromised peroxisomes in idiopathic pulmonary fibrosis, a vicious cycle inducing a higher fibrotic response via TGF-β signaling. Proc Natl Acad Sci U S A. 2015 Apr 21;112(16):E2048-57. Doi: 10.1073/pnas.1415111112.

3.1. General function of peroxisomes in maintaining oxidant/antioxidant balance and their implication in lung inflammatory conditions

Oxidant and antioxidant imbalance in the lung is associated with various respiratory inflammatory diseases such as asthma, idiopathic pulmonary fibrosis, adult respiratory distress syndrome, COPD, pneumonia, lung transplantation and lung cancer [162-164]. Interestingly, peroxisomes are organelles that are intimately involved in ROS metabolism, since they contain various antioxidative enzymes such as catalase, and they are involved in the synthesis of polyunsaturated fatty acids and plasmalogens, which were suggest to trap ROS release [80, 112]. This thesis, was therefore based on the hypothesis that peroxisomal metabolism might be altered in the lung of IPF patients, and peroxisome induction would attenuate the fibrotic response, thus affecting the molecular pathogenesis of this devastating disease.

3.2. Peroxisome biogenesis, lipid metabolism and redox balance are compromised in IPF patients

First, lung samples of control subjects and IPF patients were analyzed for peroxisomal alterations. As mentioned above, catalase is the major peroxisomal antioxidative enzyme, therefore the first experiments were performed with anti-catalase antibodies on paraffin-embedded lung tissue slices. Moreover, an anti-PEX14p antibody was used since this protein was described as the optimal marker to visualize peroxisomes [165]. Stainings of paraffin-embedded tissue sections of human lung biopsies of controls and IPF patients revealed that

the peroxisomal number-as shown by PEX14p staining was reduced in fibroblasts in tissue sections of IPF lungs (Fig. 10). Moreover, catalase was strongly downregulated in fibroblasts of fibrotic areas of IPF lung samples (Fig. 10).
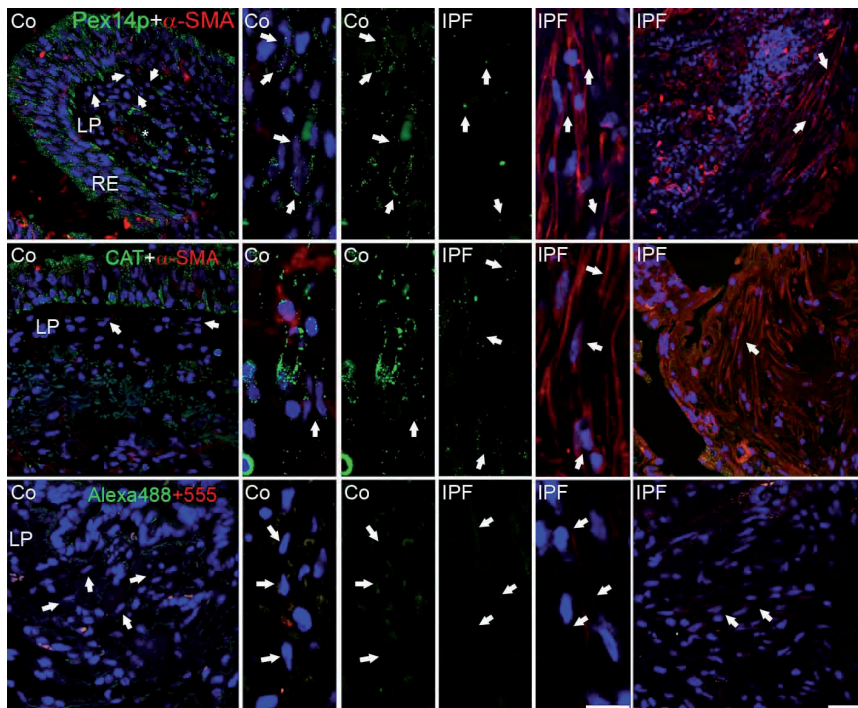

Fig. 10. Peroxisomal proteins PEX14p and catalase were compromised in human lung biopsies of control and IPF tissues. Immunofluorescence for PEX14p and catalase (CAT) in control and IPF lung tissue. Negative control for the secondary antibody reaction with donkey anti-rabbit Alexa488 and donkey anti-mouse Alexa555. Co: control, IPF: idiopathic pulmonary fibrosis. RE (Respiratory epithelium), LP (Lamina propria), Arrows: fibroblasts in the lamina propria. Scale bar: 10 μm.

Next, we analyzed whether isolated lung fibroblasts from these human IPF patients would retain the phenotype in cell culture. Indeed, these cells expressed higher levels of α-SMA (Fig. 11A) and exhibited increased mRNA levels of the pro-fibrotic markers *TGF*-β1, *COL1A2* and *IL-6* (Fig. 11B) compared to the fibroblasts isolated from controls. The pro-fibrotic phenotype was also confirmed by increased TGF-β signaling in IPF cells via luciferase reporter assay studies using an SBE-luciferase reporter plasmid (Fig. 11C).
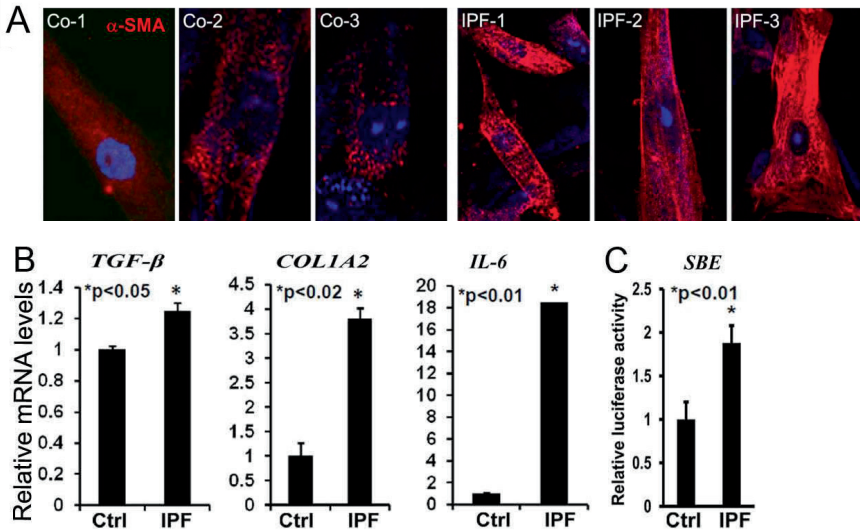
Fig. 11. IPF fibroblasts retain their fibrotic phenotype in cell culture. (A) Single immunofluorescence of the fibrotic marker α-SMA in control and IPF fibroblasts. (B) Expression of *TGF-β1, Col1A2* and *IL-6* mRNAs in control and IPF fibroblasts. (C) Luciferase reporter activity of *SBE* (Smad binding element) in control and IPF fibroblasts. The activity of firefly luciferase was measured in cell lysates and normalized to the activity of renilla luciferase. E.V-empty vector. Co: control, IPF: idiopathic pulmonary fibrosis. Data represent means ± SD of three independent experiments. *P* value was calculated by unpaired Student t-test. Scale bar: 10 μm.

Analysis of protein abundance by immunofluorescence revealed that the peroxisomal biogenesis protein PEX13p and the metabolic proteins catalase, ACOX1 and ABCD3 were strongly reduced in IPF fibroblasts with retained pro-fibrotic phenotype, suggesting that peroxisomal functions in maintaining "redox balance and lipid metabolism" in IPF fibroblasts are disturbed (Fig. 12A-B). The downregulation of the peroxisomal biogenesis protein PEX13p was confirmed by Western blot (Fig. 12A). Similarly, a reduced expression of the *PEX13* gene was observed at the mRNA level between control and IPF fibroblasts by qRT-PCR analysis (Fig. 12A). Since, catalase (Fig. 12B) was downregulated, we hypothesized that IPF fibroblasts might have an impaired anti-oxidant response. DHE staining revealed that IPF fibroblasts exhibited a higher ROS production in comparison to control fibroblasts (Fig. 12D). Downregulation of catalase and ACOX1 in IPF fibroblasts were also demonstrated at mRNA level (Fig. 12C). Interestingly, a series of anti-oxidative enzymes such as SOD1, heme

Downregulation of catalase and ACOX1 in IPF fibroblasts were also demonstrated at mRNA level (Fig. 12C). Interestingly, a series of anti-oxidative enzymes such as SOD1, heme oxygenase (HO-1), glutathione reductase (GR), and the redox sensitive transcription factor Nrf2 were also decreased in IPF fibroblasts (Fig. 13A-D). Moreover, reporter gene analyses showed that Nrf2 binding element (ARE)-driven luciferase activity was significantly decreased in IPF fibroblasts (5-fold reduction) ($p<0.05$) (Fig. 13E), whereas the luciferase activity of the AP1 reporter construct was not significantly changed in IPF fibroblasts in basal unstimulated conditions (Fig. 13E). Taken together, these results indicate that in IPF tissues as well as in IPF fibroblasts peroxisomal proteins were significantly downregulated and IPF fibroblast exhibit a disturbed antioxidant response.
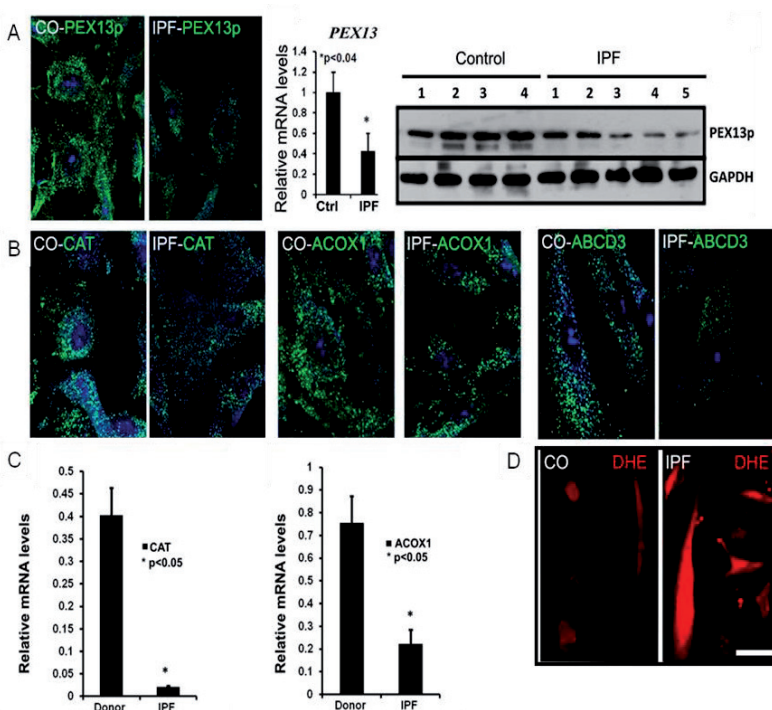
Fig. 12. Affected peroxisomal biogenesis, lipid metabolism and antioxidative response in IPF fibroblasts. (A) Expression of *PEX13* at mRNA and protein level by immunofluorescence staining and Western blotting in both control and IPF fibroblasts. (B) Immunofluorescence staining of the peroxisomal proteins catalase, ACOX1 and ABCD3 in control and IPF fibroblasts. (C) Expression of *catalase* and *ACOX1* mRNAs in both control and IPF fibroblasts. (D) Generation of reactive oxygen species (ROS) detection with dihydroethidine (DHE) in

49
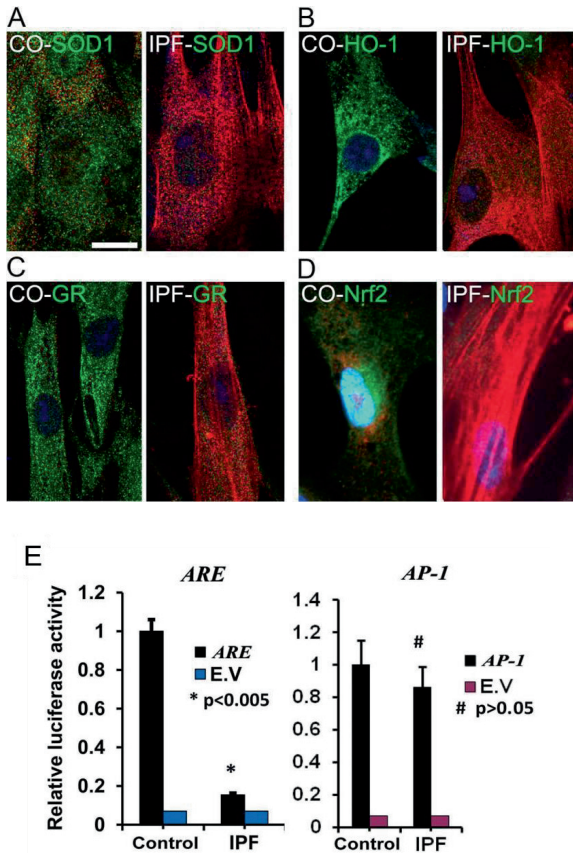
Fig. 13. Diminished antioxidative response in IPF fibroblasts. (A-D) Double immunofluorescence of the antioxidative enzymes SOD1, HO-1, GR and the redox-sensitive transcription factor Nrf2 together with the fibrotic marker α-SMA in donor and IPF fibroblasts. (E) Luciferase reporter activity of ARE and AP1 promoter elements in control and IPF fibroblasts. The activity of firefly luciferase was measured in cell lysates and normalized to the activity of renilla luciferase. E.V-luciferase empty vector. SOD1: superoxide dismutase, HO-1: heme oxygenase-1, GR: glutathione reductase, Nrf2: nuclear factor erythroid 2–related factor 2. CO: Control, IPF: idiopathic pulmonary fibrosis. Data represent means ± SD of three independent experiments. *P* value calculated by unpaired Student t-test. Scale bar (A-D): 10 µm.

3.3. PEX13p knockdown activates Smad-dependent TGF-β1 pathway and increases COL1 production

Abrogation of peroxisomal proteins in IPF subjects may be a collateral effect due to persistent fibrosis or could also be a crucial factor that contributes to the pathogenesis of this devastating condition. To address this question, PEX13p, one of the peroxin proteins involved in peroxisomal biogenesis, was knocked down using a siRNA mediated approach. The strong knockdown of *PEX13* expression in both control and IPF fibroblasts was verified by quantitative RT-PCR and Western blot analysis (Fig. 14A and B), and disruption of peroxisomal biogenesis, leading in consequence to mistargeting of catalase into the cytoplasm (Fig. 14C). Interestingly, disruption of the peroxisomal biogenesis triggered the production of the pro-fibrotic markers *COL1A2* and *TGF-β1* at mRNA level and of the COL1 protein in Western blot analysis (Fig. 14A and B).
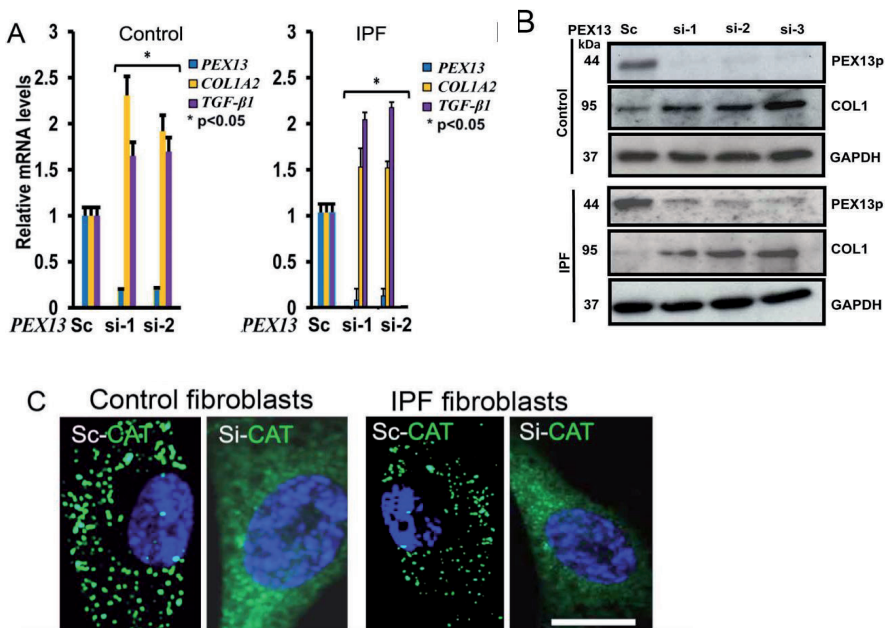
Fig. 14. Increased fibrotic response in *PEX13* siRNA treated control and IPF fibroblasts. (A) RT-qPCR analysis of peroxisome biogenesis *PEX13* and fibrotic markers *TGF-β1* and *COL1A2* in *PEX13* siRNA transfected fibroblasts. The expressions of *28S rRNA* and of the *HPRT1* gene were used as controls for normalization, *p<0.005. (B) Western blots depicting the abundance of the peroxisomal biogenesis protein PEX13p and collagen I in *PEX13* knockdown. The abundance of GAPDH was used as control. Sc (scrambled siRNA control), si-1 (siRNA *PEX13*-1), si-2 (siRNA *PEX13*-2), si-3 (siRNA *PEX13* 1 plus 2). (C) Mistargeting of the peroxisomal matrix enzyme catalase into the cytoplasm in control and IPF fibroblast due to the *PEX13* knockdown. Scale bar: 10 µm. Data represent means ± SD of three independent experiments. *P* value was calculated by unpaired Student t-test.

The peroxisome deficiency was associated with increased TGF-β1 in the culture medium and activation of TGF-β1 signaling in fibroblasts shown by *SBE* luciferase reporter activation (Fig. 15A and B). Moreover, increased collagen levels were produced in the medium and the *COL1A2* promoter activity was increased in the fibroblasts with *PEX13* knockdown (Fig. 15C and D). It is noteworthy that also control fibroblasts exhibit an increased fibrotic phenotype after peroxisomal knockdown, even though to a lesser extent in comparison to the transfected IPF fibroblasts (Fig. 15A-D).
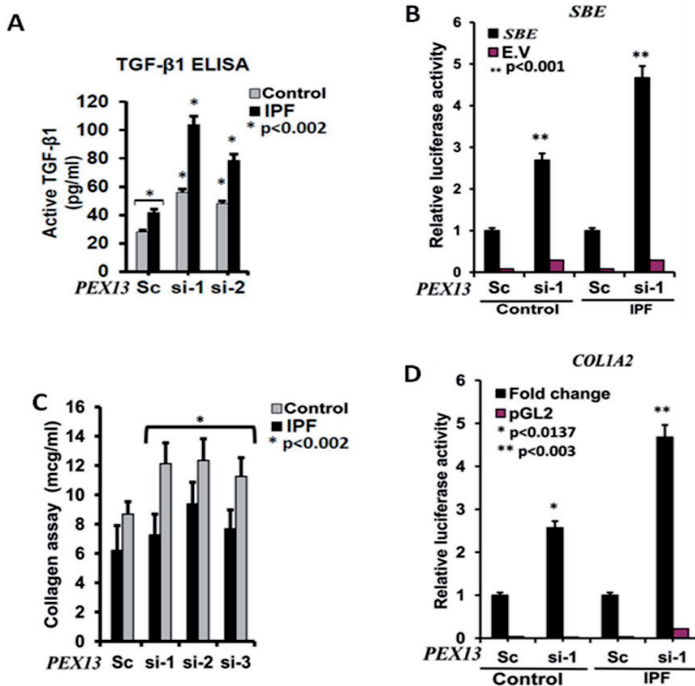
Fig. 15. Activation of TGF-β1 Smad pathway in *PEX13* siRNA treated control and IPF fibroblasts. (A) TGF-β1 release in supernatant measured by TGF-β1 ELISA. (B) *SBE* luciferase reporter assay in siRNA treated control and IPF fibroblasts. (C) Collagen Sircol assay, measuring the production of collagen released in the medium by control and IPF fibroblasts. (D) *COL1A2* luciferase reporter assay in siRNA treated control and IPF fibroblasts. The activity of firefly luciferase was measured in cell lysates and normalized to the activity of renilla. E.V-empty vector. Sc (scrambled siRNA control), si-1 (siRNA *PEX13*-1), si-2 (siRNA *PEX13*-2), si-3 (siRNA *PEX13* 1, 2). Data represent means ± SD of three independent experiments. *P* value was calculated by unpaired Student t-test.

Additionally, *PEX13* knockdown also led to the intracellular elevation of pro-fibrotic markers/proteins such as collagen I, collagen 3A1 (COL3A1) and prolyl 4-hydroxylase beta polypeptide (PDI) as revealed by immunofluorescence studies (Fig. 16A and B). Moreover, increased mRNA levels of matrix metalloproteinase 2 (MMP2) were detected in *PEX13* knockdown, an enzyme that has been implicated in excessive TGF-β1 activation (Fig. 17A and E). The increased fibrotic response of *TGF-β1* and *COL1A2* was also observed with semi-

quantitative RT-PCR with a *PEX13* knockdown in IPF fibroblasts (Fig. 17A-D). PEX13 knockdown studies in control fibroblasts exhibited the same patterns as the ones of IPF (data not shown). To summarize, these results indicate that the downregulation of peroxisomes in both control and IPF fibroblasts leads to an increased fibrotic phenotype in these cells associated with an increased production of collagen and TGF-β1 as well as an activation of TGF-β signaling.
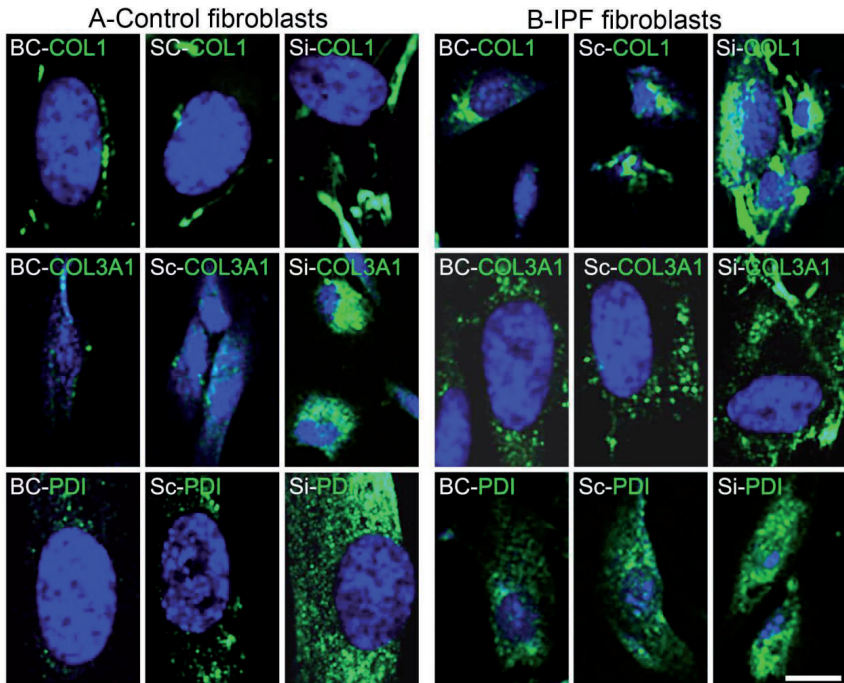
Fig. 16. Higher abundance of fibrotic marker proteins COL1, COL3A1 and PDI induced by the *PEX13* knockdown. (A-B) Depiction of the fibrotic marker proteins collagen I (COL1), collagen III (COL3A1) and prolyl 4-hydroxylase (PDI) by immunofluorescence staining in *PEX13* knockdown control and IPF fibroblast cultures. Nuclei were stained with 1 μM Hoechst 33342. Scale bar: 10 μm.
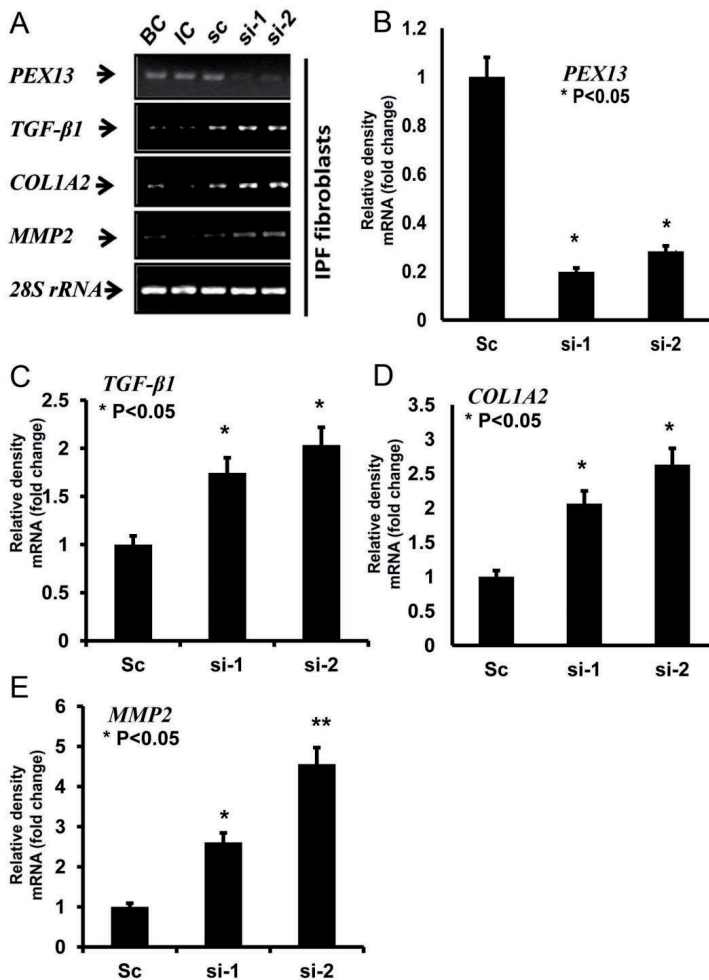
Fig. 17. Increased fibrotic response and elevated MMP2 mRNA in *PEX13* knockdown of IPF fibroblasts.
(A) Expression of *PEX13*, *TGF-β1*, *COL1A2* and *MMP2* at mRNA level shown by RT-PCR in IPF fibroblasts.
Expression of *28S rRNA* gene was used as control. (B-E) Quantification of mRNA expression from depicted
genes in (A). BC: basal control, IC: interferin control, Sc: scrambled control, si-1: siRNA-1, si-2: siRNA-2. Data
represent means ± SD of three independent experiments. *P* value was calculated by unpaired Student t-test.

3.4. Knockdown of peroxisomes leads to elevated ROS, increased ARE/AP1 transcriptional activity and pro-inflammatory cytokines in fibroblasts

As shown above in Fig. 12, IPF fibroblasts exhibit an increased production of ROS. Since peroxisomes are able to produce and scavenge ROS [80] and are downregulated in IPF fibroblasts, we questioned whether they are involved in the cellular ROS production observed. Indeed, the knockdown of *PEX13* led to an increase in the production of ROS as measured by dihydroethidine staining both in control as well as IPF fibroblasts (Fig. 18A). However, unlike in the basal conditions of IPF fibroblasts (Fig. 13E), the acute downregulation of PEX13 increased ROS production, and was paralleled with increased ARE and AP-1 promoter activity (Fig. 18B). Moreover, a high antioxidative response was induced leading to the upregulation of antioxidative enzymes such as HO-1, GR and abundance of the redox-sensitive transcription factor Nrf2 (Fig. 19A and B).
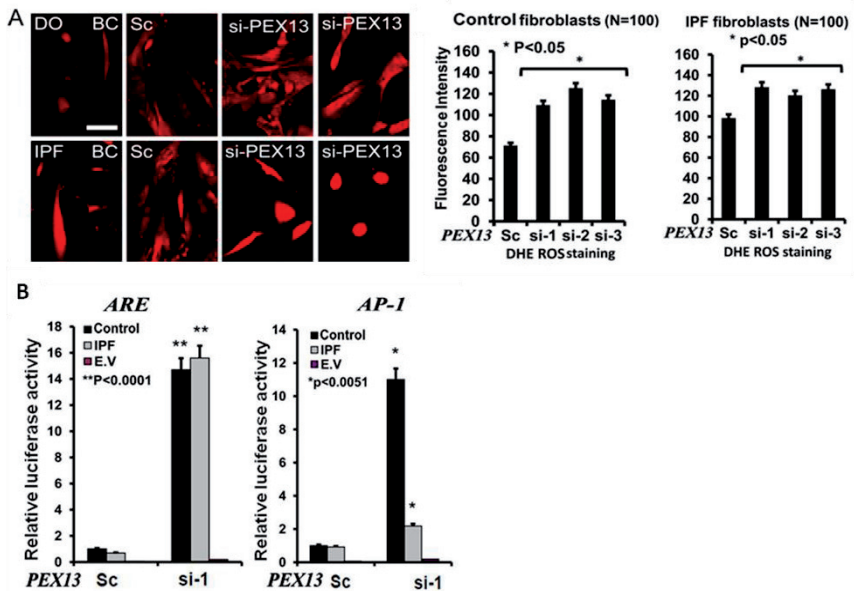
Fig. 18. Induction of ROS and activation of *ARE, AP1* transcriptional elements in *PEX13* knockdown control and IPF fibroblasts. (A) Detection of generated reactive oxygen species (ROS) with dihydroethidine (DHE) and quantification of the DHE staining in *PEX13* siRNA-treated control and IPF fibroblasts, (N-number of cells for quantification). (B) ARE and AP-1 element luciferase reporter assays in *PEX13* knockdown control and IPF fibroblasts, (si vs. Sc). (E.V-empty vector). The activity of firefly luciferase was measured in cell lysates and normalized to the activity of renilla. Sc (scrambled siRNA control), si-1 (siRNA *PEX13*-1), si-2 (siRNA *PEX13*-2). Data represent means ± SD of three independent experiments. *P* value was calculated by unpaired Student t-test.
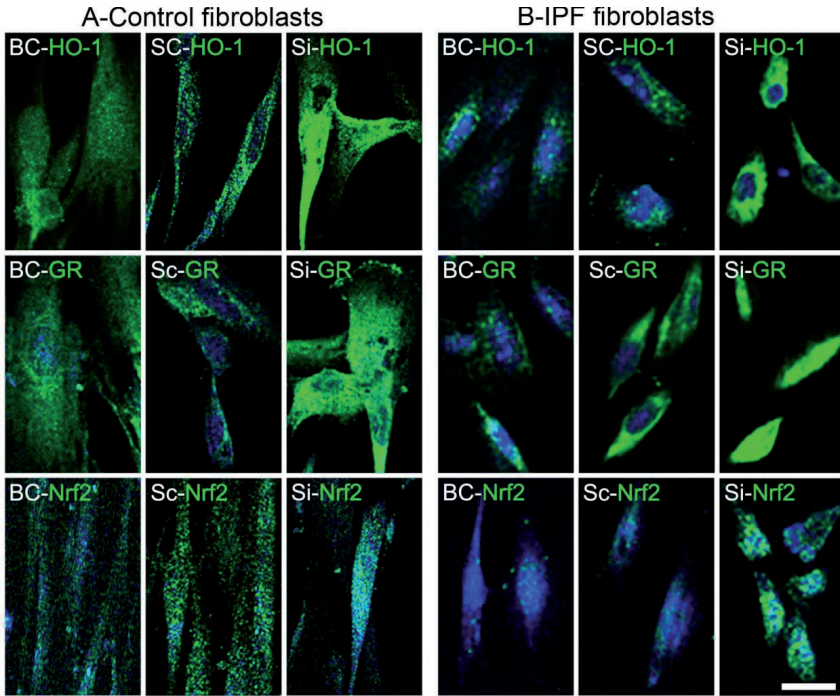
Fig. 19. Antioxidative response in *PEX13* siRNA treated fibroblasts. (A and B) Antioxidative response in *PEX13* knockdown control and IPF fibroblasts, depicted by immunofluorescence staining for heme oxygenase-1 (HO-1), glutathione reductase (GR) and Nrf2. BC: basal control, Sc: scrambled control, si: siRNA. Scale bar: 10 µm.

Next, we analyzed the effect of the *PEX13* knockdown on the production of pro-inflammatory cytokines such as TNF-α and IL-6, which have been proposed to play an important role in the pathogenesis of fibrosis. At the mRNA level both *TNF-α* and *IL-6* were significantly induced in *PEX13* knockdown control and IPF fibroblasts in comparison to the respective cells transfected with the negative control siRNA (Fig. 20A). IL-6 was readily detectable and also significantly increased in the culture supernatants of *PEX13* knockdown fibroblasts (Fig. 20B). In contrast, by using the same supernatants under similar experimental conditions for a TNF-α ELISA, the concentration of this cytokine was too low for reliable detection (data not shown). In summary, knockdown of peroxisomes leads to increased ROS production and IL-6 release in both control and IPF fibroblasts.

Fig. 20. Induction of cytokine production in *PEX13* knockdown control and IPF fibroblasts. (A) qRT-PCR analysis of mRNA expression for cytokines (TNF-α and IL-6) in *PEX13* knockdown of control and IPF fibroblasts. (B) Human IL-6 secretory levels measured by the Quantikine ELISA in *PEX13* siRNA treated control and IPF fibroblasts. Sc (scrambled siRNA control), si-1 (*PEX13*-1 siRNA), si-2 (*PEX13*-2 siRNA), Data represent means ± SD of three independent experiments. *P* value was calculated by unpaired Student t-test.
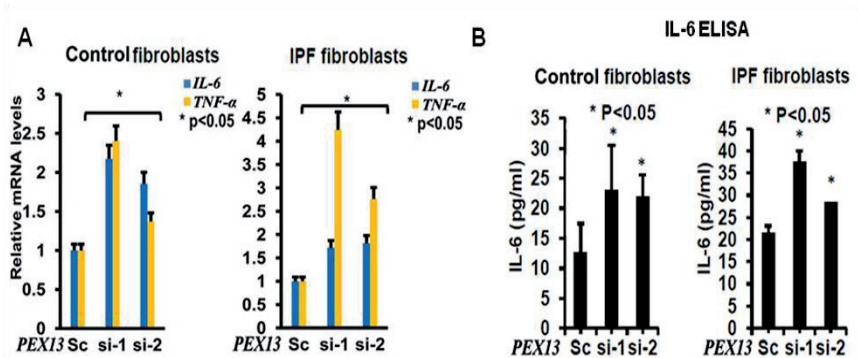
3.5. TGF-β1 signaling downregulates peroxisomal biogenesis proteins in IPF fibroblasts

By considering the pivotal role of TGF-β1 in the pathogenesis of lung fibrosis, we thought to examine the possibility that it might modulate the expression of the *PEX13* gene, and that activated TGF-β signaling could account for impaired peroxisome biogenesis and metabolism in IPF. The fibrotic response of TGF-β1 treatment was demonstrated by the upregulation of *COL1A2* and *IL*-6 mRNAs, which were blocked specifically with the TGF-β1 receptor inhibitor LY364947 (Fig. 21A). Elevated levels of IL-6 in culture supernatants of lung fibroblasts treated with TGF-β1 and inhibition of the same cytokine with the TGF-β1 receptor inhibitor LY364947 were confirmed by ELISA (Fig. 22A). Similarly, the activation of the TGF-β1-Smad pathway in these cells was also confirmed by increased *SBE* luciferase reporter activity, increased TGF-β1 mRNA (Fig. 22B and D, Fig. 21A) and by increased Smad3 translocation into nucleus (Fig. 22C). We then analyzed whether the expression of the *PEX13* gene would be affected by TGF-β1 stimulation. Interestingly, TGF-β1 treatment indeed resulted in the downregulation of the *PEX13* mRNA and protein, suggesting that TGF-β1 inhibits peroxisomal biogenesis (Fig. 21B-C and 22D-E). This effect was reversed when

TGF-β signaling was specifically blocked using the TGF-β1 receptor inhibitor LY364947 (Fig. 21B-C and 22D-E). TGF-β1 treatment also increased ROS production in these fibroblasts (Fig. 21D).
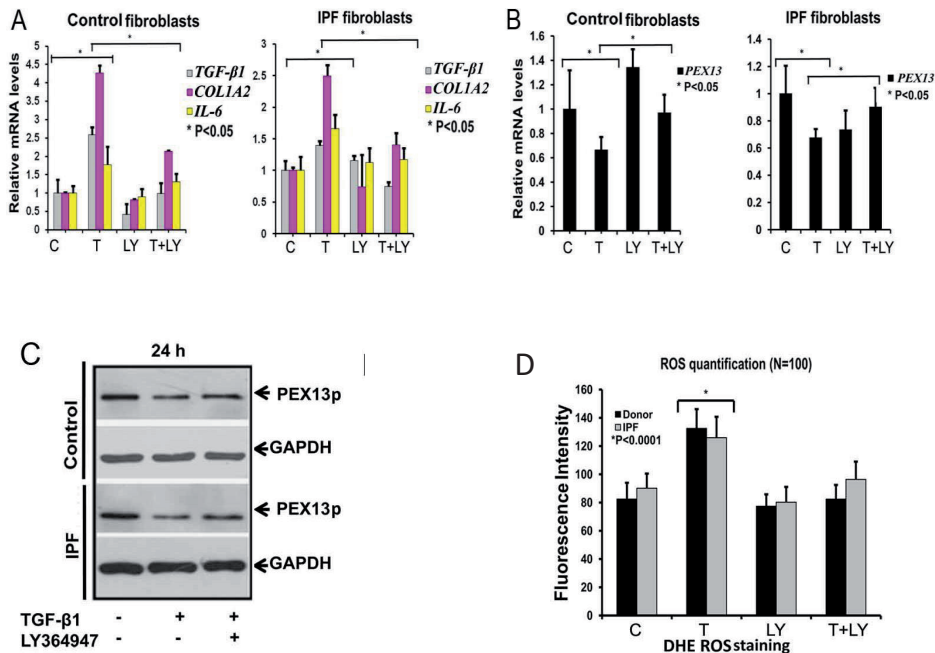
Fig. 21. TGF-β1 signaling suppresses the *PEX13* mRNA expression and protein abundance in control/IPF fibroblasts. Confluent control and IPF fibroblasts were pretreated with 5 µM LY364947 (TGF-β1 inhibitor) for 1 h, followed by a stimulation with 5 ng/ml TGF-β1, or combined for 24 h. RNA expression of *TGF-β1, COL1A2, IL-6* and *PEX13* was examined by real-time qRT-PCR (A and B). The results were normalized with *28S rRNA* and *HPRT* mRNA. (C) Total protein was isolated following 24 h incubation with TGF-β1, LY364947 or combinations and subjected to Western blotting for PEX13p. GAPDH was used as loading control. (D) Detection of TGF-β1 induced reactive oxygen species (ROS) with dihydroethidine (DHE) in control and IPF fibroblasts. C: control, T: TGF-β1, LY: LY364947, T + LY: TGF-β-1 + LY364947. Data represent means ± SD of three independent experiments. *P* value was calculated by unpaired Student t-test.
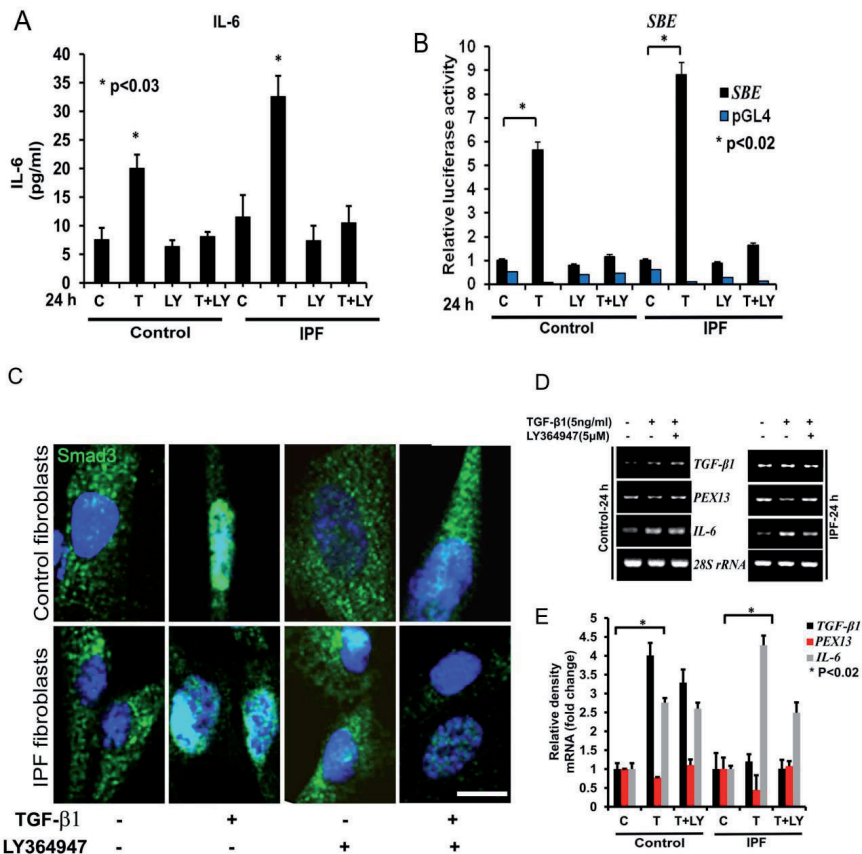
Fig. 22. TGF-β induction affects *PEX13* in control and IPF fibroblasts. (A) IL-6 secretory levels measured by ELISA after treatment with TGF-β1 (5 ng/ml) and LY364947 (5 μm) in control and IPF fibroblasts. C: control, T: TGF-β1, LY: LY364947, T+LY: TGF-β1 + LY364947 (B) SBE dual-luciferase reporter gene assay. The activity of firefly luciferase was measured in cell lysates and normalized to the one of renilla luciferase. Data represent the results of at least three experiments performed in triplicates. (C) Total Smad3 protein staining of TGF-β1 treated control and IPF fibroblasts. (D) Depiction of *PEX13, TGF-β1* and *IL-6* mRNA levels with RT-PCR, followed by quantification. Data represent means ± SD of three independent experiments. *P* value was calculated by unpaired Student t-test. Scale bar: 10 μm.

## 3.6. Downregulation of peroxisomal proteins in bleomycin-induced pulmonary fibrosis is abrogated in TβRII bleomycin-treated knockout mice

To extend and confirm these findings to the *in vivo* situation, lung mesenchyme-specific TGF-β receptor II knockout mice were used. Since the anti-PEX13p antibody does not work properly for the staining of PFA-fixed paraffin-embedded tissue [165], an antibody against PEX14p, a binding partner of PEX13p in the docking complex of the peroxisomal membrane that was also reduced in IPF lungs (Fig. 1), was used. Indeed, bleomycin treatment in control mice downregulated peroxisomes (PEX14p) on day 7 after treatment, followed by a recovery on day 14 and 28 in comparison to day 7, however, upto a lower protein abundance than in appropriate control animals (Fig. 23). Strikingly, bleomycin treatment in TGF-β receptor II knockout mice did not induce the downregulation of peroxisomes as detected by staining with PEX14p, indicating a direct relation for TGF-β-induced signaling in the downregulation of peroxisomes (Fig. 23). Accordingly, also the downregulation of other peroxisomal enzymes such as ACOX1 and the antioxidative enzyme catalase on day 7 after bleomycin treatement were abrogated in *TβRII* knockout mice, suggesting a possible link between TGF-β signaling and regulation of peroxisomal metabolism (Fig. 24, 25). In summary, these findings indicate that TGF-β1 signaling downregulates peroxisomes in bleomycin-induced pulmonary fibrosis, whereas abrogation of the *TβRII* prevents the reduction of peroxisome abundance on the peak of inflammation on day 7 after bleomycin treatment, and so prevents the development of fibrosis.

Fig. 23. The reduction of PEX14p in the bleomycin-induced mouse model of lung fibrosis is abrogated by *TβRII* knockout. Double immunofluorescence of PEX14p and α-SMA in the bleomycin-induced mouse model of pulmonary fibrosis. Ctrl: Control, WT: wild-type, RII-KO: TGF-β receptor II knockout, Bleo: Bleomycin. Data represent the results of at least three reproducible experiments. Scale bar: 10 μm.
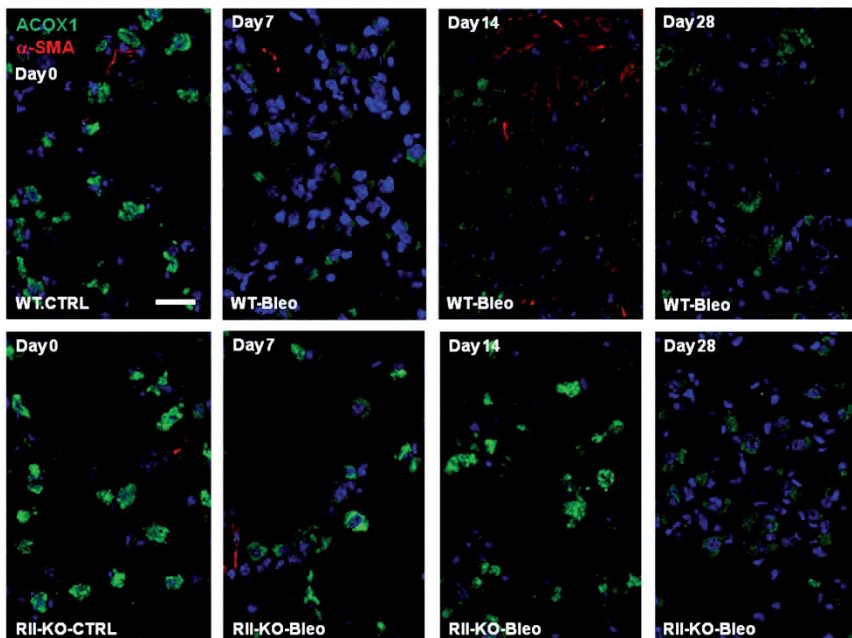
Fig. 24. The downregulation of ACOX1, a peroxisomal lipid metabolic enzyme in the bleomycin-induced mouse model of lung fibrosis is abrogated by the *TβRII* knockout. Double immunofluorescence of Acyl-CoA oxidase 1 (ACOX1) and α-SMA in bleomycin induced mouse model of pulmonary fibrosis. Ctrl: Control, WT: wild-type, RII-KO: TGF-β receptor II knockout (TβRII), Bleo: Bleomycin. Data represent the results of at least three reproducible experiments. Scale bar: 10 μm.

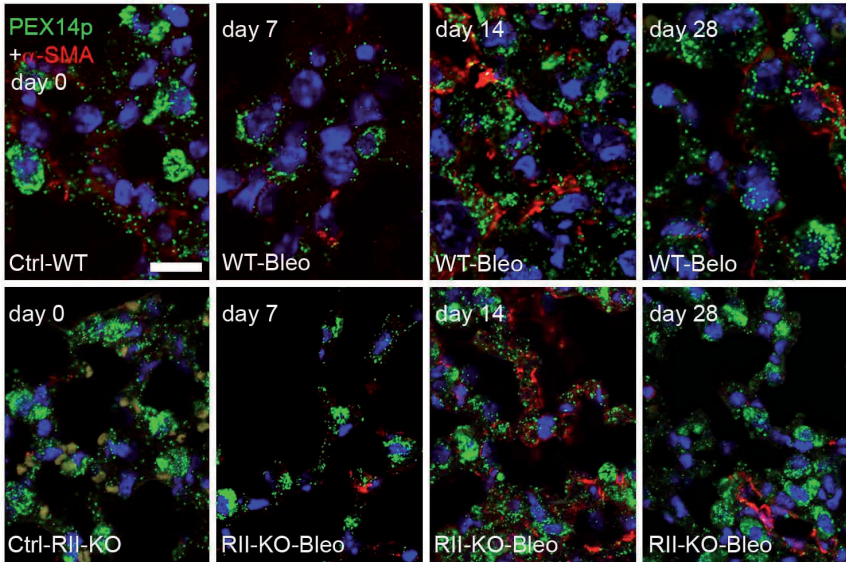**Fig. 25. The downregulation of the peroxisomal antioxidative enzyme catalase in the bleomycin-induced mouse model of lung fibrosis is abrogated by the *TβRII* knockout**. Double immunofluorescence of catalase and α-SMA in the bleomycin-induced mouse model of pulmonary fibrosis. Ctrl: Control, WT: wild-type, RII-KO: TGF-β receptor II knockout (TβRII), Bleo: Bleomycin. Data represent the results of at least three reproducible experiments. Scale bar: 10 µm.
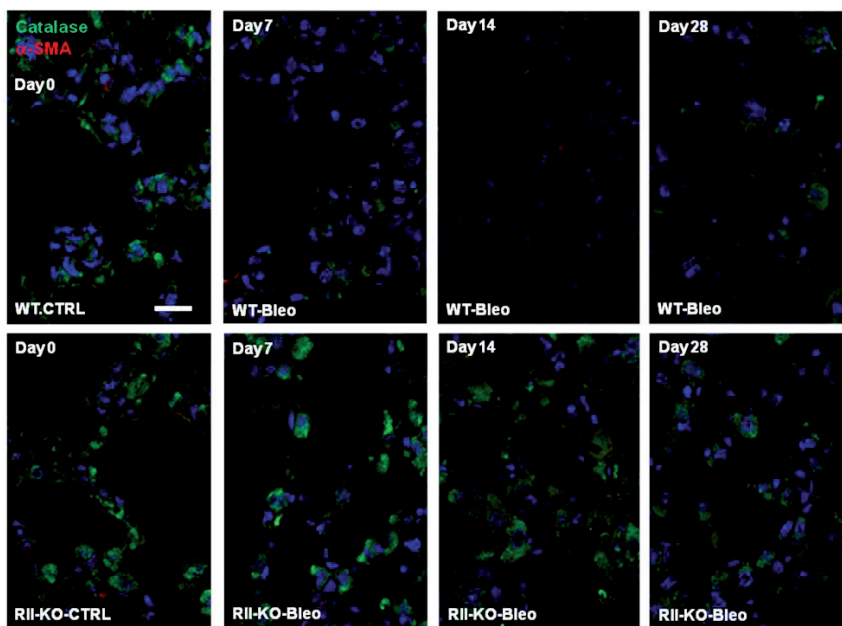
3.7. AP-1 signaling is involved in TGF-β1-mediated downregulation of PEX13 in human IPF fibroblasts

Reports from literature indicate a cross-talk between TGF-β1 signaling and the transcriptional factor AP-1 [166]. In this study was also demonstrated an upregulation of AP-1 in *PEX13* knockdown fibroblasts [11]. Hence, we questioned if the transcriptional factor AP-1, normally activated during pro-fibrotic and pro-inflammatory responses, would also play a role in the observed TGF-β1 mediated PEX13 downregulation. For a comparison, we also used the luciferase reporter vector *(ARE)* to test the activity of the ROS-activated transcriptional factor Nrf2. Indeed, stimulation with TGF-β1 induced the activity of the *AP-1* luciferase reporter construct (Fig. 26A) but the activity of the ARE-luciferase construct remained unchanged (Fig. 26B). Further, the AP-1 specific inhibitor SR11302 partially blocked the TGF-β1 stimulated activity of both the *AP-1*-luciferase construct and the *ARE*-luciferase construct (Fig. 26A, B). This was explainable, as the AP-1 binding element shares the consensus sequence of the Nrf2 binding element but not vice versa. The luciferase reporter assays revealed that the inhibitor luteolin used generally as Nrf2 inhibitor is not specific since it also inhibits the TGF-β1-induced activation of *AP-1* (Fig. 26A) in addition to the inhibition of *ARE* luciferase (Fig. 26B). Interestingly, pretreatment of cells with an AP-1 specific inhibitor SR11302 or the Nrf2/AP-1 inhibitor luteolin blocked the TGF-β1-mediated SBE activation, indicating a role for AP-1 in the TGF-β1-mediated Smad-dependent pathway (Fig. 26C). Moreover, pretreatment with SR11302 and luteolin also reversed the TGF-β1-mediated downregulation of the PEX13p protein (Fig. 26D). To summarize, these findings suggest that the pro-fibrotic cytokine TGF-β1 might downregulate *PEX13* through the transcriptional factor *AP-1*.
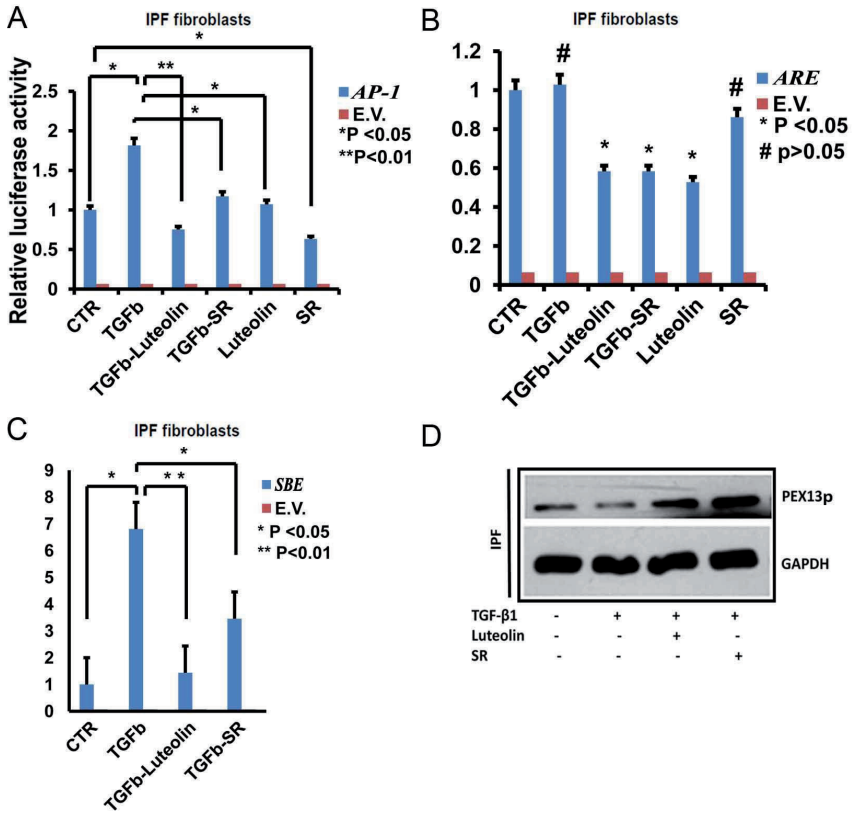
Fig. 26. AP-1 signaling is activated in TGF-β1-mediated downregulation of *PEX13* in human IPF fibroblasts. Confluent IPF fibroblasts were pretreated for 1 h with 25 µM luteolin or 10 µM SR11302 (SR). Then, cells were challenged with 5 ng/ml TGF-β1 for 24 h as indicated in the figure. (A-C) *AP1, ARE* and *SBE* luciferase reporter assays in IPF fibroblasts. The activity of firefly luciferase was measured in cell lysates and normalized to the activity of renilla luciferase. E.V-empty vector. (D) Protein analysis of PEX13p in IPF fibroblasts treated with TGF-β1, luteolin or SR11302. GAPDH was used as loading control. Luteolin: Nrf2 inhibitor, SR11302: AP-1 inhibitor. Data represent means ± SD of three independent experiments. *P* value was calculated by unpaired Student t-test.

3.8. Pro-inflammatory cytokines TNF-α and IL-6 also suppress the peroxisome biogenesis protein PEX13p in human IPF fibroblasts

In a complex disease condition such as IPF, factors other than TGF-β1 may also contribute to the downregulation of peroxisomal genes *in vivo*. Macrophage-mediated TNF-α production might play an important paracrine role in this process. To determine whether TNF-α affects peroxisome biogenesis, IPF fibroblasts were treated with 10 ng/ml TNF-α for the indicated time points (Fig. 27A and B). TNF-α induced a significant downregulation of the *PEX13* mRNA as early as 1 h (Fig. 27A), as well as the protein abundance of PEX13p after 6 h (Fig. 27B). Similar to TGF-β1, TNF-α also induced the activity of the *AP-1* luciferase construct and increased the luciferase activity of the *ARE*-luciferase construct (Fig. 27C). Interestingly, the AP-1 inhibitor SR11302 reversed the TNF-α-mediated downregulation of PEX13p (Fig. 27D). Finally, treatment with the pro-inflammatory cytokine IL-6 also induced the downregulation of PEX13p (Fig. 27E). In summary, pro-inflammatory cytokines (TNF-α and IL-6) downregulate PEX13p in IPF fibroblasts. Moreover, TNF-α-mediated downregulation of PEX13p is partially mediated through AP-1 signaling.
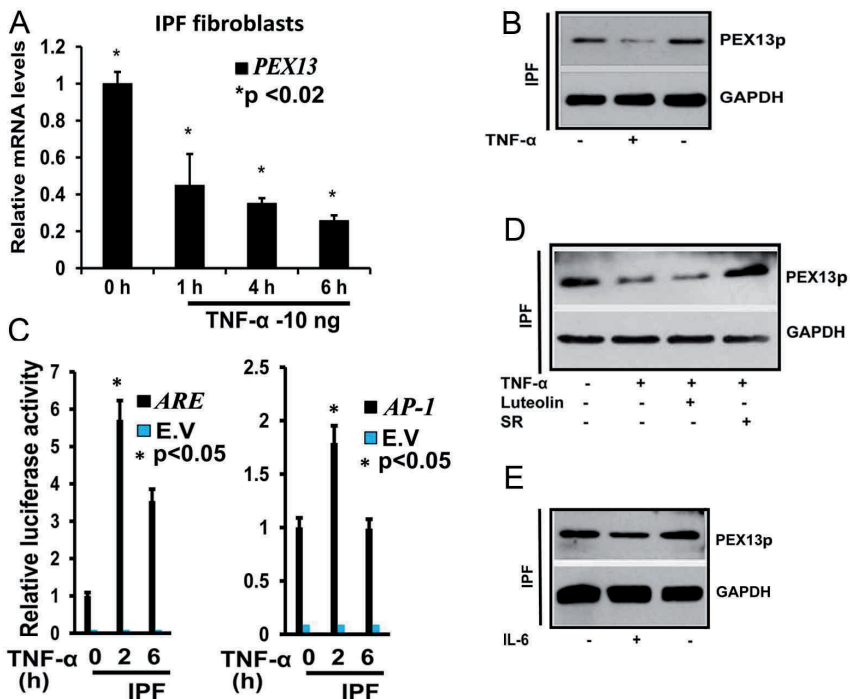
Fig. 27. TNF-α downregulates peroxisome biogenesis by induction of AP1 in human IPF fibroblasts. (A) IPF fibroblasts were treated with 10 ng/ml TNF-α for the indicated time points, and the expression of *PEX13* mRNA was determined by using qRT-PCR. (B) IPF fibroblasts were treated with 10 ng/ml TNF-α for 6 h, and cells were lysed for Western blot analysis. As loading control GAPDH was used (C) *ARE* and *AP-1* dual luciferase reporter assays of IPF fibroblasts treated with 10 ng/ml TNF-α for indicated times. The activity of firefly luciferase was measured in cell lysates and normalized to the activity of renilla luciferase. (D) IPF fibroblasts were treated with 10 ng/ml TNF-α for 6 h; cells were pretreated 1 h before with Nrf2 inhibitor Luteolin and AP-1 inhibitor SR11302 (SR), PEX13p abundance was analyzed with Western blotting. GAPDH was used as loading control (E) IPF fibroblasts were treated with 20 ng/ml IL-6 and PEX13p abundance was analyzed with Western blotting. GAPDH was used as loading control. E.V-empty vector. Data represent means ± SD of three independent experiments. *P* value was calculated by unpaired Student t-test.

3.9. PPAR-α agonists proliferate peroxisomes and inhibit the TGF-β1-induced pro-fibrotic response in IPF fibroblasts

As demonstrated above, reduced peroxisome biogenesis is associated with an increased pro-fibrotic response as shown by the activation of TGF-β1 signaling and collagen production. This raises the possibility that increasing the peroxisomal biogenesis may be beneficial as a treatment strategy in IPF. To evaluate the hypothesis we used two structurally distinct PPAR-α agonists (ciprofibrate and WY14643), classical peroxisome proliferators, and investigated the relationship between peroxisome proliferation and TGF-β1-induced myofibroblast differentiation (as shown by α-SMA abundance) and upregulation of the collagen I protein. Treatment with either ciprofibrate or WY14643 for 48 h resulted in proliferation of peroxisomes as detected by PEX14p staining (Fig. 28A). The peroxisomal biogenesis protein PEX13p was also induced after treatment of IPF cells with ciprofibrate or WY14643 (Fig. 28B). PPAR-α has been shown to exert multiple effects on cellular targets which are independent of peroxisome proliferation, wherefore it is important to distinguish the peroxisome-dependent anti-fibrotic effects of PPAR-α agonists. To do this, the experimental setup (mentioned in detail in the methods) contained two different controls 1) IPF cells which were pretreated with PPAR-α agonists for 48 h after which the medium was replaced with the PPAR-α antagonist to block endogenous PPAR- α activation. Ideally, these cells then contain proliferated peroxisomes but further PPAR-α activation is blocked. 2) IPF cells which were pretreated with PPAR-α agonists only for 2 h prior to TGF-β1 stimulation and hence will exhibit an activation of PPAR-α but no peroxisome proliferation due to the insufficiently short time period of drug treatment. The concentrations of PPAR-α agonists and antagonists that were used for this approach activated and inhibited the PPAR-response-element (PPRE)-luciferase reporter construct respectively (Fig. 29A). Interestingly, IPF cells pretreated with ciprofibrate or WY14643 for 48 h showed a significant reduction in the TGF-β1-induced myofibroblast differentiation represented by the abundance of the α-SMA protein. The strongest reduction was observed in the cells pretreated with PPAR-α agonist for 48 h followed by pretreatment with PPAR-α antagonist for 1 h prior to the addition of TGF-β1 (Fig. 29B and 29C). Whereas, pretreatment with PPAR-α agonist for 2 h prior to TGF-β1 stimulation did not block the TGF-β1-induced α-SMA protein. Similarly, the TGF-β1-induced COL1 protein was also blocked by the addition of the PPAR-α agonists (treated for 48 h) followed by 1 h antagonist, but not in IPF cells solely pretreated with PPAR-α agonists for 2 h or 48 h (Fig. 29B, C). In summary, these findings suggest that in IPF cells with

proliferated peroxisomes the TGF-β1-induced upregulation of myofibroblast differentiation and the COL1 protein is blocked.
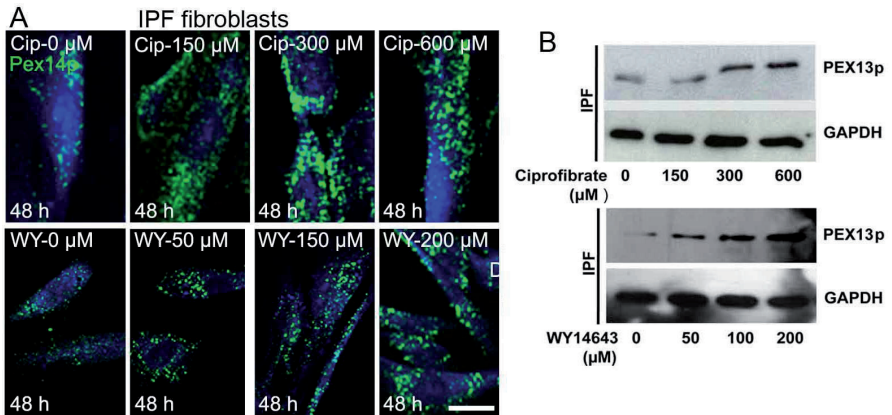
Fig. 28. Peroxisome proliferation by PPAR-α agonists ciprofibrate and WY14643 in IPF fibroblasts. (A) Staining of IPF fibroblasts treated with ciprofibrate or WY14643 for 48h at the indicated concentrations with the peroxisomal marker PEX14p. (B) Western blot analysis of PEX13p in IPF cells treated with ciprofibrate or WY14643 for 48 h. CTRL: control, GW: GW6471, CIP: ciprofibrate, WY: WY14643. Data represent the results of at least three reproducible experiments. Scale bar: 10 µm.
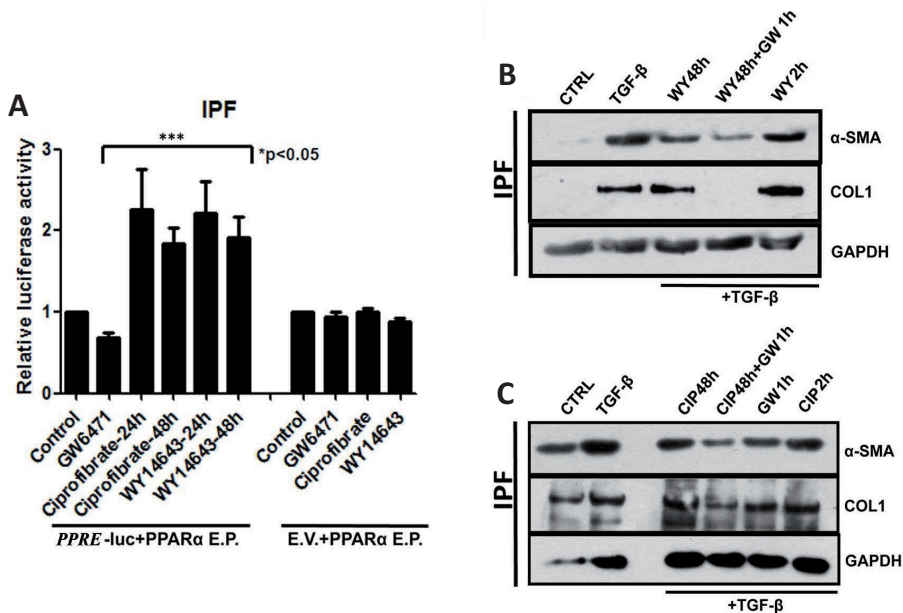
Fig. 29. Peroxisome proliferation by PPAR-α agonists ciprofibrate and WY14643 blocks the TGF-β1-induced pro-fibrotic response in IPF fibroblasts. (A) IPF cells co-transfected with PPAR-α expression plasmid (PPAR-α E.P.) and PPRE-luciferase-reporter vector (PPRE)/or empty vector (E.V) were treated with ciprofibrate (200 μM) or WY14643 (100 μM) or GW6471 (10 μM) for the indicated times after which the firefly luciferase activity was measured in cell lysates and normalized to the activity of renilla luciferase. (B, C) Western blot analysis of IPF cells pretreated with WY14643 (100 μM) or ciprofibrate (200 μM) and/or GW6471 (10 μM) for the indicated times followed by treatment with TGF-β1 (5 ng/ml) for another 24 h. Note: After 48 h treatment of WY14643 or ciprofibrate, the medium was replaced with fresh serum free medium before stimulation with TGF-β1. Whereas, the medium was not replaced before the addition of TGF-β1 in cells pretreated with WY14643 or ciprofibrate for 2 h or GW6471 for 1 h. CTRL: control, GW: GW6471, CIP: ciprofibrate, WY: WY14643. Data represent the results of at least three reproducible experiments. Statistical analysis for luciferase assays were performed by ANOVA.

3.10. Peroxisome proliferation by a PPAR-α activator exerts a protective effect against the fibrotic response through suppression of ROS production and the inhibition of the IL-6 release

As mentioned in the studies above, reduced peroxisome biogenesis is associated with increased TGF-β1 activation and subsequently to ROS generation. Therefore, we investigated the relationship between ciprofibrate treatment, ROS and cytokine release and collagen production. Indeed, proliferation of peroxisomes and increase of PEX14p staining was observed after ciprofibrate treatment (Fig. 30A-B). Ciprofibrate also increased *PEX13* mRNA expression (Fig. 30E). In contrast, *COL1A2* expression was significantly reduced at the mRNA level upon ciprofibrate treatment (Fig. 30E). Consistent reduced ROS production (Fig. 30A-C) and decreased IL-6 secretion were also detected upon ciprofibrate treatment (Fig. 30D). Taken together, peroxisome proliferation by the PPAR-α agonist exerts protective effects through diminishing ROS and reducing the IL-6 release.
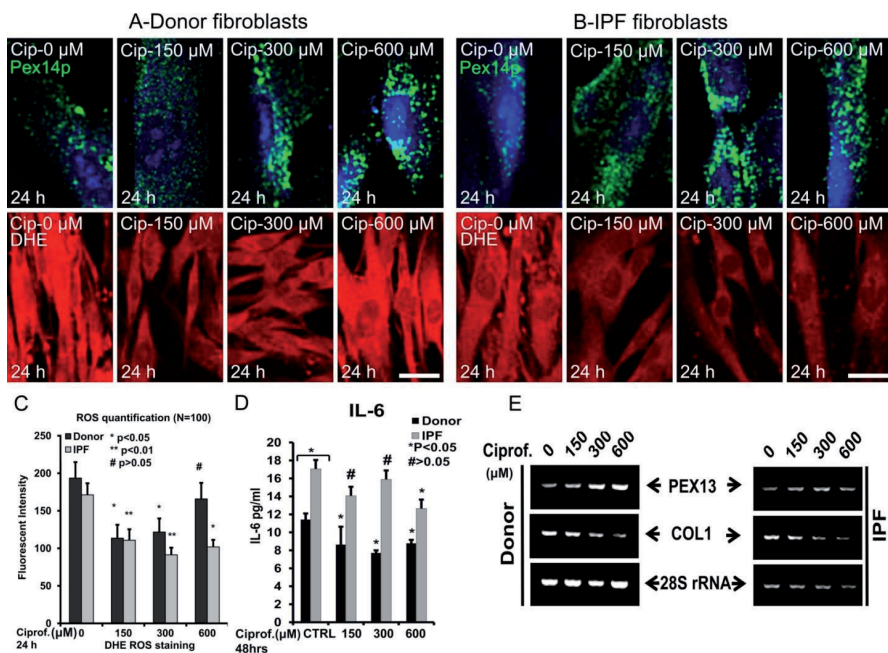
Fig. 30. PPAR-α agonist ciprofibrate induces peroxisome proliferation, decreases fibrotic markers COL1 and reduces ROS and IL-6 levels in control and IPF fibroblasts. (A-B) Immunofluorescence for PEX14p of control and IPF fibroblasts treated with ciprofibrate at indicated concentrations and times. (A-C) ROS generation detected by DHE staining and its quantification. (D) IL-6 production measured by ELISA as described above. (E) RT-PCR analysis for *PEX13, COL1A2* mRNAs in ciprofibrate-treated control and IPF fibroblasts. Data represent means ± SD of three independent experiments. *P* value was calculated by unpaired Student t-test. Scale bar: 10 µm.

3.11. Peroxisome proliferation by a PPAR-α activator inhibits cell proliferation in control and IPF fibroblasts

Activation of PPAR-α is reported to inhibit cardiac fibrosis through suppression of the ET-1 pathway in vivo [167]. This inhibitory effects of fenofibrate may be caused by upregulation of p27[Kip1] via suppression of c-jun expression and may be related to the cell cycle of cardiac fibroblasts [167]. Also in our study, we showed that ciprofibrate treatment significantly decreased the number of proliferating cells in both control and IPF fibroblasts (Fig. 31A-B).

74

Therefore, we speculated that this inhibition of proliferation might contribute to the alleviation of fibrosis progression by blocking fibroblast/myofibroblast differentiation.
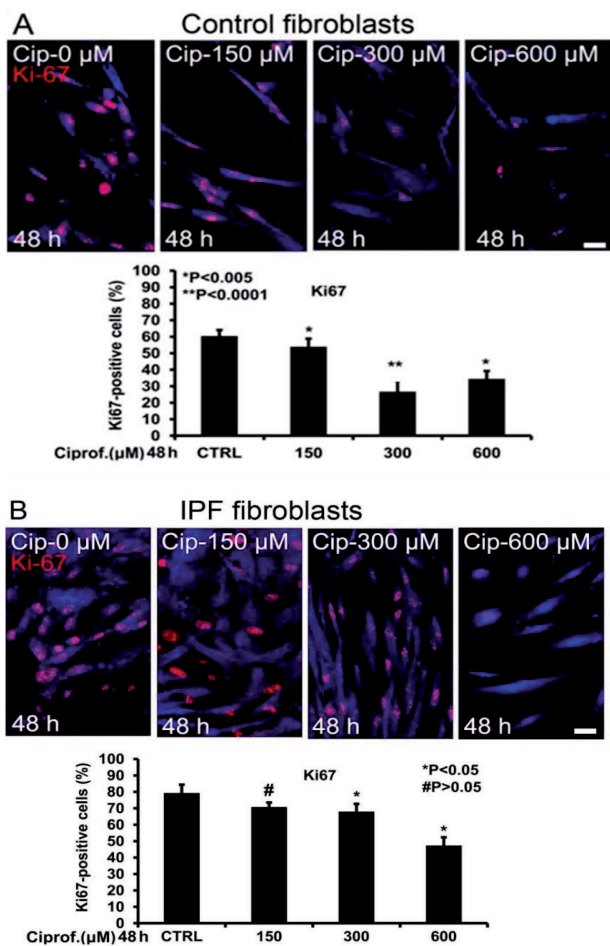
Fig. 31. Peroxisome proliferation by PPAR-α agonist ciprofibrate inhibits cell proliferation in control and IPF fibroblasts. Confluent control and IPF fibroblasts were treated with ciprofibrate with indicated concentrations and times. (A-B) Identification and quantification of fibroblast proliferation by Ki67 staining in control and IPF subjects. Data represent means ± SD of three independent experiments. *P* value was calculated by unpaired Student t-test. Scale bar: 25 μm.

3.12. PPAR-α inhibitor GW6471 blocks peroxisome proliferation and promotes myofibroblast differentiation as well as ROS release in control and IPF fibroblasts

In order to further investigate whether the effects of ciprofibrate on reduction of the fibrotic response would be dependent on the PPAR-α mediated proliferation of peroxisomes, the PPAR-α antagonist GW6471 was applied in our study. Treatment of control and IPF fibroblasts with GW6471 for 24 h with two different concentrations (5 and 10 µM) increased the fibrotic response, shown by increased α-SMA expression in control and IPF fibroblasts (Fig. 32A and B). Inhibition of peroxisome proliferation by GW6471 resulted in the increase of ROS production in both control and IPF fibroblasts (Fig. 32C). These results suggest that inhibition of the peroxisome proliferation and PPAR-α by GW6471 would aggravate the fibrogenesis process in control and IPF fibroblasts.
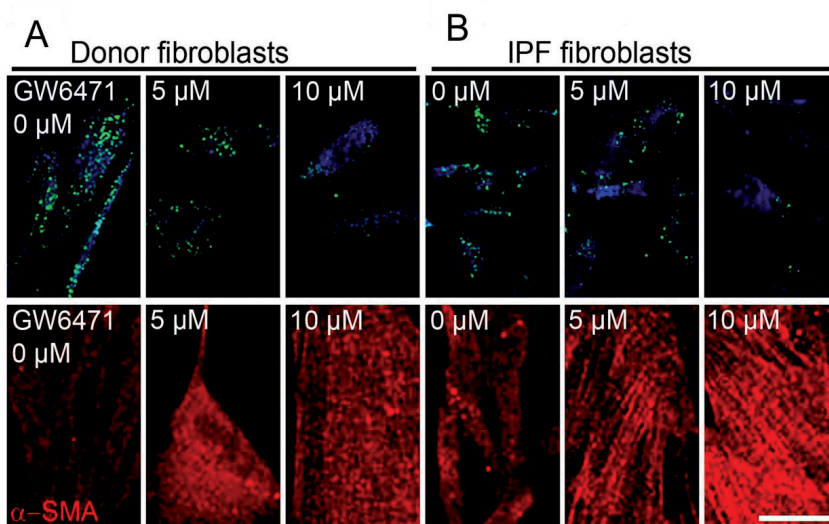

Fig. 32. PPAR-α inhibitor GW6471 blocks peroxisome proliferation and increases profibrotic response. (A-B) Single immunofluorescence staining for PEX13 and α-SMA in 24 h GW6471-treated control and IPF fibroblasts. Data represent the results of at least three experiments performed in triplicates. Scale bar: 10 µm
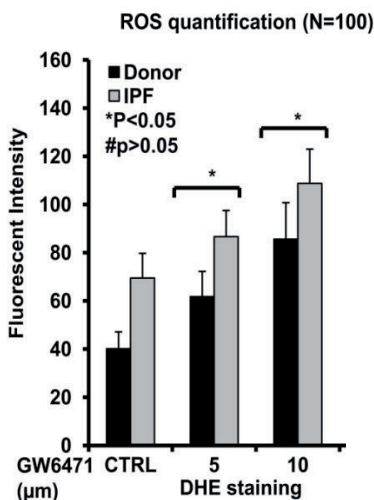
Fig. 33. PPAR-α inhibitor GW6471 increases ROS generation in control and IPF fibroblasts. ROS quantification by DHE staining in 24 h GW6471-treated control and IPF fibroblasts. Data represent means ± SD of three independent experiments. *P* value was calculated by unpaired Student t-test.

3.13. Upregulation of peroxisomal proteins in wild-type and *TβRII* knockout mice

In order to further investigate the role of TGF-β signaling on peroxisome regulation, fibroblast cultures and lung tissue of *TβRII* knockout mice were used to compare the peroxisomal compartment to corresponding wild-type littermates. Consistent with the *in vitro* findings, the peroxisome biogenesis protein PEX13 as well as the peroxisomal lipid metabolic enzyme ACOX1 and antioxidative enzyme catalase were enormously upregulated in *TβRII* knockout mice, in bronchial epithelium as well as in alveolar region of lung tissue as well as in lung fibroblasts isolated from mentioned subjects, suggesting a suppressing effect of TGF-β signaling on peroxisomal proteins (Fig. 34A-B and 36A-B). The upregulation of peroxisomal proteins PEX13p and PEX14p were also shown by Western blot analysis (Fig. 35).
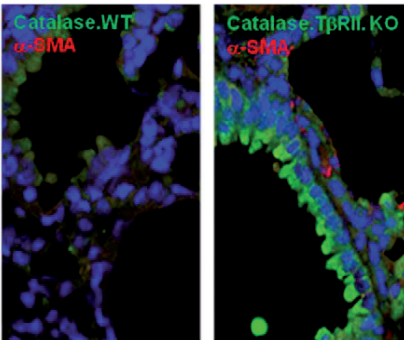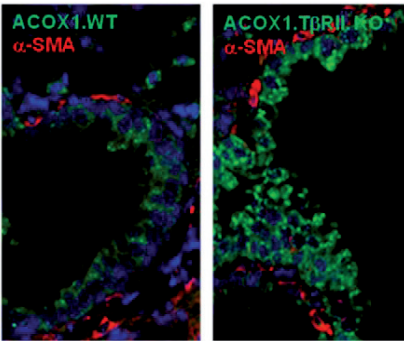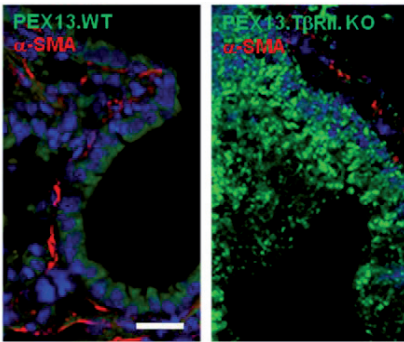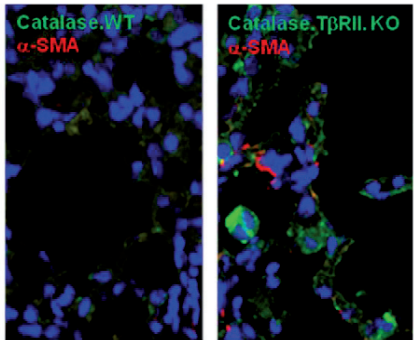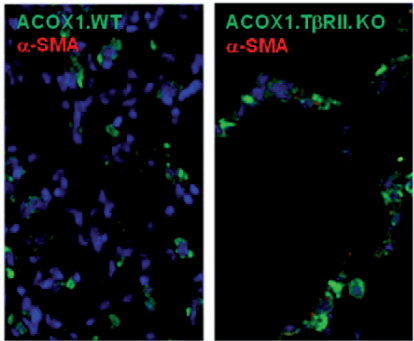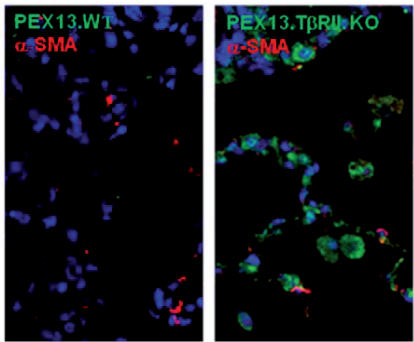
Fig. 34. Increased abundance of peroxisomal proteins in *TβRII* knockout mice. (A-B) Double immunofluorescence staining for PEX13, ACOX1 and Catalase with α-SMA in wild-type and *TβRII* knockout lung tissue sections. Data is a representative of at least three reproducible experiments. Scale bar: 10 μm.
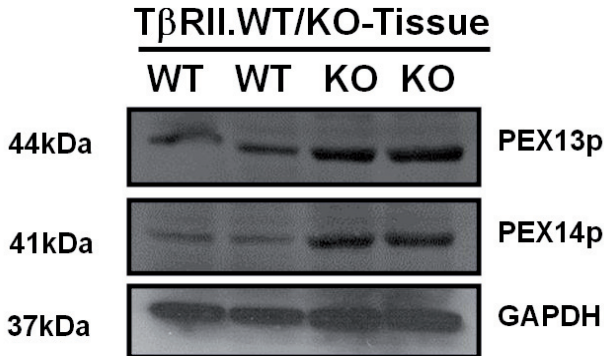
Fig. 35. Increased abundance of peroxisomal proteins in *TβRII* knockout mice. Western blot analysis of PEX13p, PEX14p in wild-type and *TβRII* knockout lung tissue. GAPDH was used as loading control. Data is a representative of at least three reproducible experiments.

Similar alterations of peroxisomal proteins were also observed at the cellular level in cultures of isolated fibroblasts from wild-type and *TβRII* knockout mice. A tremendous increase in the abundance of peroxisomal biogenesis proteins PEX13p and PEX14p was observed in *TβRII* knockout fibroblasts (Fig. 36, Fig. 37). The *TβRII* knockout was demonstrated by TβRII staining and by Western blott in fibroblast culture (Fig. 36). The similar changes of increase in abundance of peroxisomal proteins were observed at mRNA level and by Western blot analysis in fibroblast cultures (Fig. 37). Since the *TβRII*-KO is a mesenchymal specific knockout, the knockout of this receptor includes the majority of mesenchyme derived cells (Fig. 36). These findings strongly suggest that TGF-β signaling might be involved in regulation of peroxisomal proteins, possibly by interacting with downstream transcription factors of TGF-β Smad dependent and independent signaling.
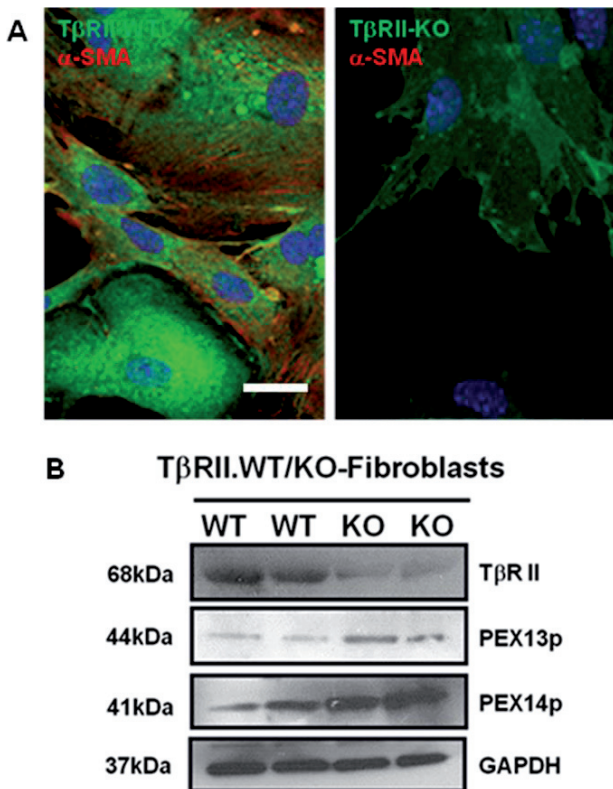
Fig. 36. Upregulation of peroxisomal proteins in *TβRII* knockout mice. (A) Double immunofluorescence staining of TβRII with α-SMA in wild-type and *TβRII* knockout lung fibroblasts. (B) Western blot analysis for TβRII, PEX13p and PEX14p in wild-type and *TβRII* knockout lung fibroblasts. GAPDH was used as loading control. Data is a representative of at least three reproducible experiments. Scale bar: 10 μm.

Fig. 37. Upregulation of peroxisomal proteins in *TβRII* knockout mice. (A) Double immunofluorescence staining of PEX14p with α-SMA in wild-type and *TβRII* knockout lung fibroblasts. (B) mRNA expression of *PEX14* in *TβRII* knockout mice was analysed with real time qRT-PCR. The results were normalized with *28S rRNA* and *HPRT* mRNA. Data is a representative of at least three reproducible experiments. Data represent means ± SD of three independent experiments. *P* value was calculated by unpaired Student t-test. Scale bar: 10 µm.

3.14. Upregulation of peroxisomal proteins in wild-type and *Smad3* knockout mice

In order to investigate the possible regulation of peroxisomal proteins by TGF-β signaling, and in particular by TGF-β Smad-dependent pathway, general *Smad3* knockout mice were used. Similar to mice with completely disturbed TβRII signaling, *Smad3* knockout mice exhibited an increased abundance of the peroxisomal proteins involved in organelle

biogenesis (PEX14p), peroxisomal lipid metabolism (ABCD3, ACOX1) as well as peroxisomal antioxidative response (catalase) (Fig. 38A and 39A-B). Similar changes of the peroxisomal biogenesis protein PEX13p and the antioxidative enzyme catalase were observed with Western blot analysis (Fig. 38B). The Smad3-KO was verified by using an anti-Smad3 antibody (Fig. 38B).
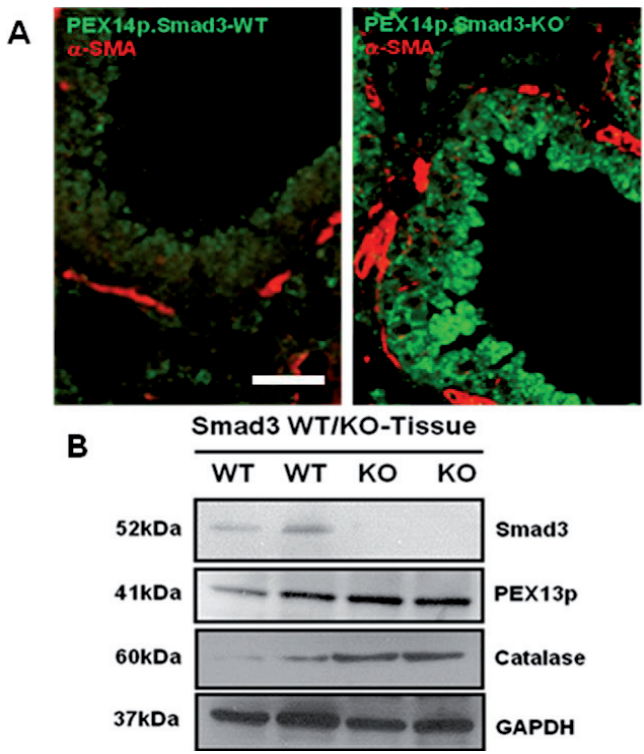
Fig. 38. Upregulation of peroxisomal proteins in *Smad3* knockout mice. (A) Double immunofluorescence staining of PEX14p with α-SMA in wild-type and *Smad3* knockout lung tissue sections. (B) Western blot analysis of Smad3, PEX13p and catalase in wild-type and *Smad3* knockout lung tissue. GAPDH was used as loading control. Data is a representative of at least three reproducible experiments. Scale bar: 10 µm

A   B

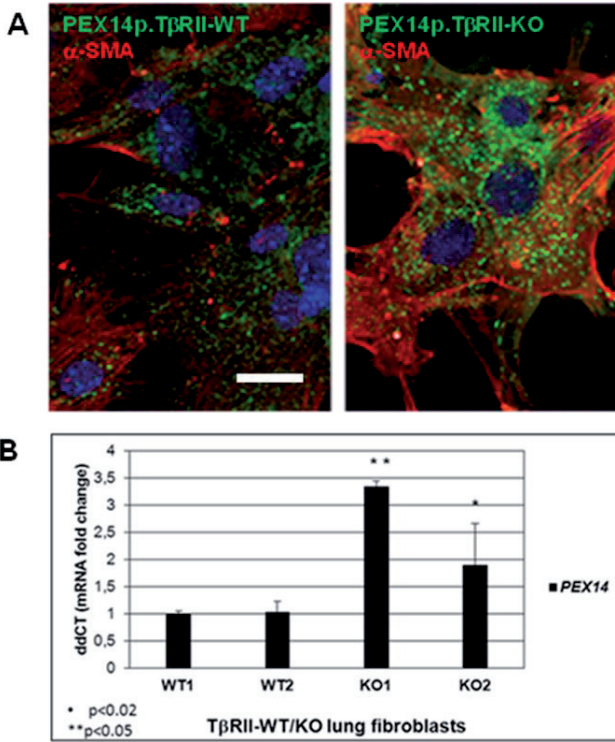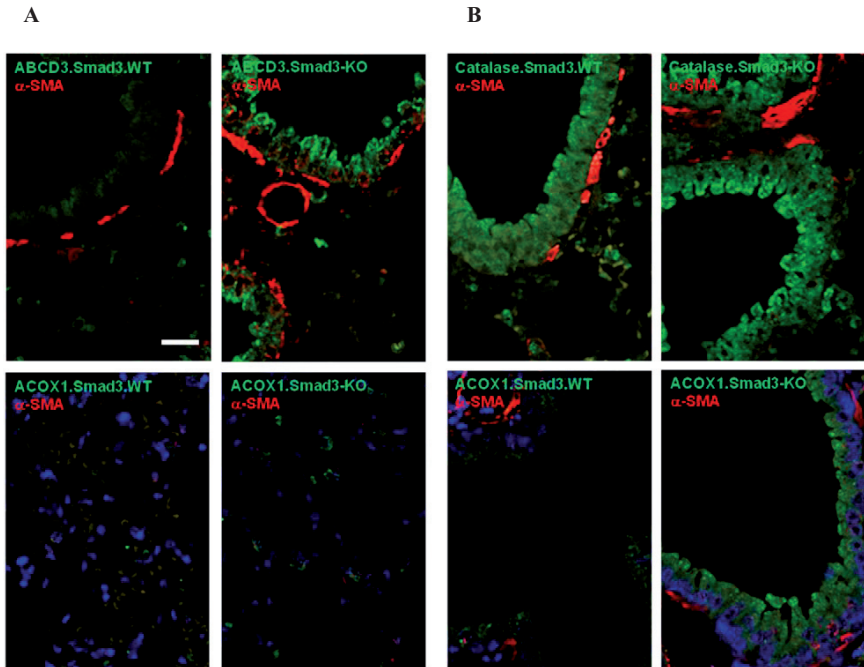**Fig. 39. Upregulation of peroxisomal proteins in *Smad3* knockout mice**. (A-B) Double immunofluorescence staining of ABCD3, ACOX1 and Catalase with α-SMA in wild-type and *Smad3* knockout lung tissue sections. Data is a representative of at least three reproducible experiments. Scale bar: 10 µm.

To confirm, that the TGF-β regulation of peroxisomal proteins also occurs in primary cell culture, fibroblasts were isolated from wild-type and *Smad3* knockout mice mouse lungs. Indeed, the expression of peroxisomal biogenesis protein PEX13p was similarly upregulated in *Smad3* knockout fibroblasts as shown by Western blot analysis (Fig. 40). Moreover, the mRNA levels for *PEX14* and *catalase* were upregulated in *Smad3* knockout fibroblasts (Fig. 40). The increase of PEX13p abundance in the Western blots corroborates the morphological results obtained in *Smad3*-KO lungs and coincides with the downregulation of collagen I (Fig. 40).

83
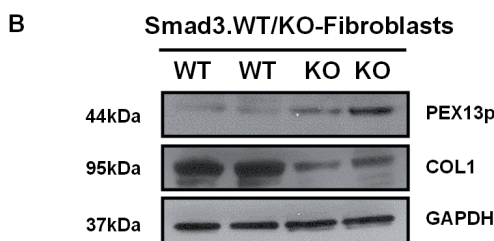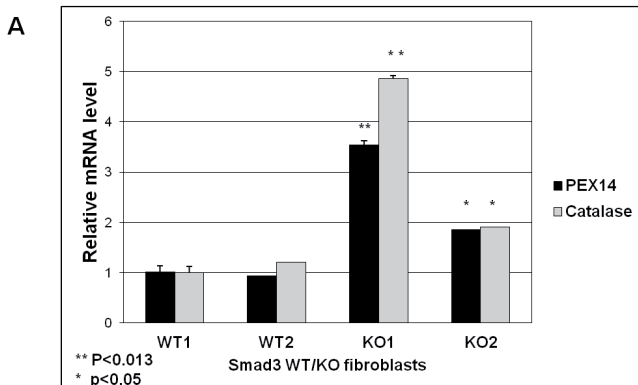
Fig. 40. Upregulation of the peroxisomal biogenesis protein PEX13p in *Smad3* knockout mouse lung fibroblasts. (A) mRNA expression of *PEX14* and *catalase* in *Smad3* knockout mice was analysed with real time qRT-PCR. The results normalized with *28S rRNA* and *HPRT* mRNA. (B) Western blot analysis of PEX13p and collagen I in wild-type and *Smad3* knockout mice lung fibroblasts. GAPDH was used as loading control. Data represent means of ± SD of three independent experiments. *P* value was calculated with unpaired Student t-test.

3.15. Upregulation of TGF-β signaling via constitutively active TβR-I activation leads to reduction of peroxisomal biogenesis in the lung of one month old mice

The TGF-beta receptor I (TβRI) is crucial in activation of Smad-dependent regulation of gene transcription. Therefore, a transgenic mouse expressing a constitutively active TGF-β type I receptor (TβRI/ALK5) was used to investigate the Smad-dependent regulation of the peroxisomal biogenesis protein PEX14p. TβRI[CA] is c-myc tagged at the C-terminal end to be able to assess the TGF-β receptor I overexpression. The peroxisomal biogenesis protein PEX14p was strongly downregulated in the lung of one-month-old mice in cells

84

overexpressing the TβRI^{CA} as shown by immunocytochemistry staining (Fig. 41). The downregulation of PEX14p was also observed by Western blot analysis in lung homogenates of one-month-old TβRI^{CA} mice, whereas in lung homogenates of 3-month-old animals TβR-I activation upregulated the peroxisomal biogenesis protein PEX14p (Fig. 42). Taken together, TGF-β participates in regulation of peroxisomal biogenesis proteins possibly via Smad-dependent signaling.
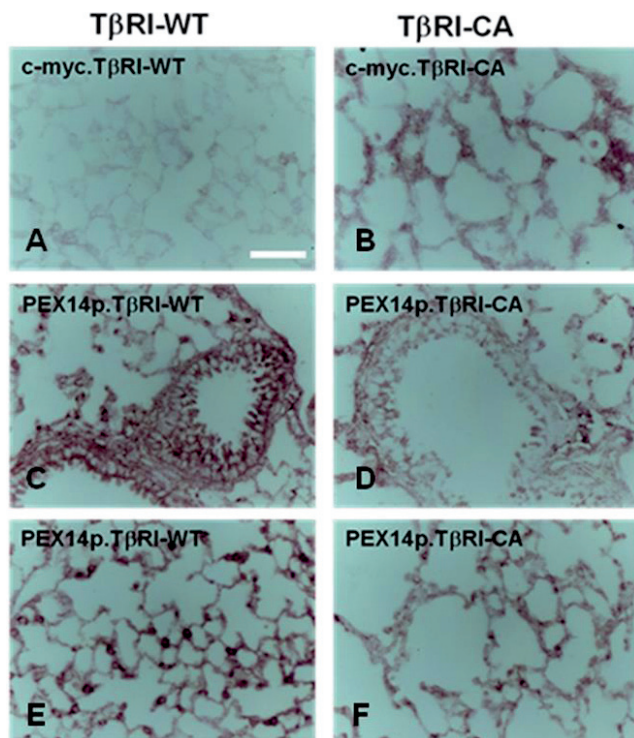
Fig. 41. Downregulation of peroxisomal biogenesis protein PEX14p in *TβRI* constitutively active mice. Immunochemistry staining of lung tissue paraffin sections from one-month-old wild-type and *TβRI^{CA}* mice. (A-B) IHC staining for the c-myc-tagged *TβRI* revealed the higher abundance of this receptor in the *TβRI^{CA}* mice. (C-F) PEX14p staining was strongly downregulated in lung tissue of mice with TGF-β receptor I overexpression in bronchioli and the alveolar region in comparison to wild-type animals. *TβRI* WT: TGF-β receptor 1 wild-type, *TβRI^{CA}*: TGF-β receptor I constitutively active. Data is a representative of at least three reproducible experiments. Scale bar: 10 μm.

TβRI.WT/CA-Tissue

	WT 1M	CA 1M	WT 3M	CA 3M	
41kDa					PEX14p
95kDa					COL1
37kDa					GAPDH
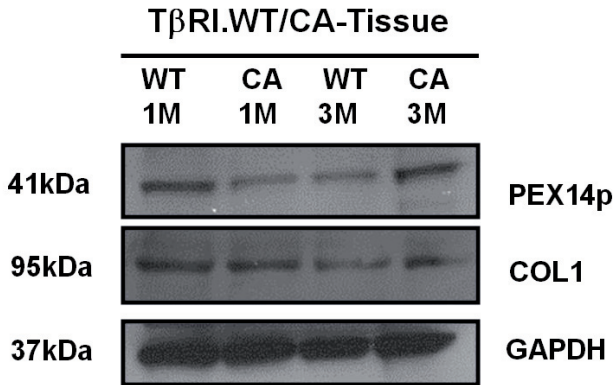
Fig. 42. Alterations of peroxisomal biogenesis protein PEX14p in *TβRI^CA* mice. Western blot analysis of PEX13p and collagen 1 in wild-type and *TβRI^CA* mouse lung tissue homogenates of 1- month and 3-month-old animals. GAPDH was used as loading control. TβRI WT: TGF-β receptor 1 wild-type, TβRI^CA: TGF-β receptor 1 constitutively active, 1M: 1-month, 3M: 3-month. Data is a representative of at least three reproducible experiments.

4. Discussion

The findings demonstrated in this thesis revealed a novel mechansim and provide compelling evidence that peroxisomes are protective organelles against the development or progression of lung fibrosis by scavenging ROS and participating in metabolism of lipid mediators, thus inhibiting the release of cytokines that trigger TGF-β signaling. Importantly, it was demonstrated that in lung tissue samples of IPF patients as well as in IPF fibroblast cultures peroxisomal proteins are downregulated. Furthermore, siRNA-mediated downregulation of the peroxisomal biogenesis protein PEX13p elicits a pro-fibrotic response, via activation of TGF-β signaling. Accordingly, treatment of IPF fibroblasts with PPAR-α agonists such as ciprofibrate or WY1463 increased the peroxisomal abundance and decreased the TGF-β1-induced myofibroblast differentiation. The findings also indicate that dysfunctional peroxisomes lead to increased cellular ROS production in IPF cells. Most importantly, *in vivo* findings in our bleomycin-induced *TβRII* knockout mouse model studies, loss of TGF-β signaling prevented the bleomycin-induced downregulation of peroxisomal proteins such as PEX14p, ACOX1 and catalase. As demonstrated in this thesis, downregulation of peroxisomes is mediated via TGF-β signaling, a pivotal cytokine important in pathogenesis of IPF and a crucial regulator of peroxisome biogenesis and metabolism.

4.1. Role of peroxisomes in maintaining oxidant/antioxidant balance and their implication in lung inflammatory conditions and idiopathic pulmonary fibrosis

It is well known that the lung is one of the organs most exposed to the various forms of reactive oxygen species due to its high oxygen environment [113]. Oxidant and antioxidant imbalance in the lung is associated with various respiratory inflammatory diseases such as asthma, idiopathic pulmonary fibrosis, adult respiratory distress syndrome, COPD, pneumonia, lung transplantation and lung cancer [162-164]. Especially, lung inflammatory diseases such as asthma and COPD as well as IPF as restrictive pulmonary disease are characterized by elevated reactive oxygen species (ROS) released from inflammatory cells, and oxidative stress plays an important role in the pathogenesis of these diseases [11, 164]. Moreover, scavenging or diminishing ROS was demonstrated also to protect mice from bleomycin-induced lung fibrosis [83]. Peroxisomes are present in different pulmonary cell types and exhibit strong heterogeneity in their abundance and enzyme composition [80].

Peroxisomes produce high amounts of hydrogen peroxide, but also possess the most efficient antioxidative enzyme catalase, which scavenges hydrogen peroxide, thus helping to maintain the cellular oxidant/antioxidant balance [168]. Catalase as an important peroxisomal antioxidative enzyme was diminished in idiopathic pulmonary fibrosis as well as inhibited in bleomycin-induced pulmonary fibrosis, suggesting a protective role against inflammation and the development of lung fibrosis [11, 169]. Interestingly, ROS production is enormously increased in cases of downregulation of the antioxidative enzymes such as catalase and MnSOD in airway smooth muscle (ASM) [170]. In this respect, the protective role of peroxisomes in pulmonary fibrosis is closely associated with their functions in scavenging ROS species thus preventing excessive ROS generation and subsequent inflammatory reactions [5, 80, 120]. Accordingly, our findings also indicate that dysfunctional peroxisomes lead to increased cellular ROS production in IPF cells. This is in concordance with previous studies showing that the deficiency of peroxisomal proteins leads to increased ROS production and oxidative stress [114, 171].

4.2. TGF-β1 is a crucial pathogenic factor in development of IPF and ROS induction, and an important regulator of peroxisome biogenesis and metabolism

In this respect, TGF-β1 is thought to be a crucial pathogenic factor for the development of IPF by inducing epithelial cell death, ROS production and consequently deposition of extracellular matrix production and foci formation [82, 83, 85, 172]. Moreover, TGF-β1, a key cytokine in proinflammatory and fibrotic processes is found to be upregulated in airway smooth muscle (ASM) in patients with asthma and COPD, as well as in lung fibroblasts of patients with idiopathic pulmonary fibrosis [11, 170]. In addition, TGF-β1 also triggers ROS release through NADPH oxidases or direct activation of NADPH oxidase 4 (Nox4) by other mechanisms, induces enormous ROS generation in airway smooth muscle of asthma patients as well as in myofibroblasts of IPF patients [5, 170]. In this thesis is demonstrated the role of peroxisomal proteins in attenuating the fibrotic response, and in particular the impact of TGF-β signaling on regulation of peroxisome biogenesis and metabolim. It is of particular interest to emphasize that in the observed findings lung tissue samples as well as fibroblasts of IPF patients exhibit reduced peroxisomal protein abundance, mimicking some molecular pathogenic mechanisms of Zellweger syndrome, a peroxisomal disorder with complete absence or reduced number of peroxisomes, and progressive development of hepatic fibrosis

[115]. We hypothesized that a continuous trigger would be necessary to induce this consistent downregulation of peroxisomes in IPF fibroblast cultures since peroxisomal biogenesis would complement for this downregulation over time. Based on our findings that the SBE-luciferase activity was higher in IPF cells in their basal state and contained increased concentrations of TGF-β1 in the cell culture medium (Fig. 11C and 15A), we propose that the persistent activation of TGF-β signaling in these cells might be responsible for the downregulation of peroxisomal proteins in IPF subjects. This hypothesis is also supported by the *in vivo* findings in our bleomycin-induced *TβRII* knockout mouse model studies, in which loss of TGF-β signaling prevented the bleomycin-induced downregulation of peroxisomal proteins such as PEX14p, ACOX1 and catalase (Fig. 23, 24, 25). In addition, peroxisomal proteins were strongly upregulated in *TβRII* knockout mice and *Smad3* knockout mice, indicating a suppressive effect of TGF-β signaling on peroxisomal metabolism. Since the *TβRII* knockout mice are mesenchymal specific knockout and no general KO mice, the majority of mesenchyme-derived cells contain the knockout such as fibroblasts, therefore few other cell types exhibit a slight expression of TβRII in the knockout animals. Consistent with these findings, TβRI constitutively active mice (TβRI[CA]) inducing continuous TGF-β signaling activation exhibit a reduced abundance of the peroxisomal biogenesis protein PEX14p in 1-month-old mice. The upregulation of peroxisomes in lung samples of 3-month-old mice in TβRI[CA] suggests the involvement of compensatory mechanisms regulating the peroxisome-related gene expression, under continuous stress conditions to escape from the acute suppressive effect of TGF-β signaling. To our knowledge, this is the first study to show a direct role of TGF-β signaling in the regulation of peroxisome-related genes, possibly by interacting with downstream transcription factors of TGF-β signaling (e.g. Smad3, Smad4).

4.3. Pro-inflammatory cytokines TNF-α and IL-6 inhibit the peroxisome biogenesis protein PEX13p via AP-1 signaling

Furthermore, downregulation of the peroxisomal genes by the pro-inflammatory cytokine TNF-α has been shown previously in the liver [133]. In this thesis, we extended our knowledge on the molecular mechanisms leading to the TNF-α mediated downregulation of peroxisomes by showing that TNF-α mediates this effect through activation of AP-1 (Fig. 27C-D). It is known that TNF-α^{-/-} mice develop less liver fibrosis in comparison to littermate controls, exhibit reduced levels of α-SMA, a marker for activated myofibroblasts, and

reduced TGF-β1 mRNA [173]. Consistent with our findings are the existing evidences from the literature that TNF-α is crucial in initiation and progression of the fibrotic processes via AP-1 in Swiss 3T3 fibroblasts [99, 101]. Similarly, the interplay between Smad-dependent TGF-β signaling and AP-1 that we observed in our study [11] has also been reported in numerous studies and are still contradictory. In one study, the transcriptional factor AP-1 was reported to be essential for ROS-mediated TGF-β1 activation and TGF-β1-induced IL-6 production [174] which is in line with our finding that AP-1 signaling activates Smad-dependent SBE activation (Fig. 26C) [11]. In contrast to this, Verrecchia and colleagues reported that the Jun family of AP-1 factors acts as inhibitor of Smad-dependent signaling [166]. The AP-1 family of transcriptional factors is a broad class of transcriptional factors that can form hetero and homo dimmers and were shown to be both pro-fibrotic and anti-fibrotic, based on the specific factors activated in different conditions [175, 176]. Further studies to specifically identify the AP-1 factors activated due to peroxisomal dysfunction are required to understand this observed pro-fibrotic nature in our experimental conditions. In addition to TNF-α also other proinflammatory cytokines were reported to play a role in the molecular pathogenesis of lung fibrosis [5, 177]. In agreement with this notion are the findings of this thesis that *PEX13* knockdown in fibroblasts induces activation of TGF-β signaling, increased ROS, collagen and IL-6 production. Several studies have reported that ROS and the release of pro-inflammatory cytokines are the main triggers of TGF-β signaling pathway, shown also in bleomycin-induced lung fibrosis mouse model at the peak of inflammation on day 7 [5, 177]. Interestingly, in our bleomycin model the strongest downregulation of peroxisomes was also observed at day 7 (Fig. 23), which is consistent with our *in vitro* findings that pro-inflammatory cytokines TNF-α and IL-6 downregulate peroxisomes in IPF fibroblasts (Fig. 27D-E). IL-6 is known to mediate many inflammatory processes in the lung and has been implicated in the pathogenesis of a variety of respiratory disorders and the possible association between IL-6 and development of fibrosis was described [178, 179]. In addition, IL-6 plays an important role in development of BLM-induced lung inflammation and subsequent fibrotic changes through the activation of TGF−β signaling [104]. ROS interferes with many cellular functions and results in activation of the master regulators of the cellular response to oxidative stress such as Nrf2 and NF-κB and the induction of the anti-oxidative machinery [180]. Although we were able to identify the activation of Nrf2 in our *PEX13* knockdown fibroblasts based on the *ARE*-luciferase activity, luteolin which is commonly used in studies as an Nrf2 inhibitor was also found to inhibit the transcriptional factor *AP-1*. Hence

at present we cannot conclude that the observed effect of luteolin on *SBE* activation is solely dependent on its ability as an Nrf2 inhibitor.

4.4. Proliferation of peroxisomes by PPAR-α agonists inhibit the TGF-β1-induced pro-fibrotic response, myofibroblast differentiation and fibroblast proliferation

Finally, we also show that pretreatment of IPF cells with PPAR-α agonists for longer time-points reduced the TGF-β1-induced collagen and myofibroblast differentiation, provided that the endogenous PPAR-α activation during TGF-β1 stimulation is blocked. This is particularly interesting because several independent studies that reported anti-fibrotic effects of PPAR-α agonists have not considered peroxisome proliferation by these agonists. This is largely due to the vast amount of accumulating evidence in the literature describing the broad anti-fibrotic and anti-inflammatory properties of PPAR-α. In particular are the studies which report that PPAR−α agonists i) prevent cardiac fibrosis by inhibiting the proliferation of cardiac fibroblasts through suppression of ET-1 pathway [167], ii) reduced the lung injury induced by bleomycin [155] and iii) inhibit TGF-β induced transcription of β5 integrin in vascular smooth muscle cells [181]. The inhibiting effects of fenofibrate on cardiac fibroblast proliferation may be caused by upregulation of p27^{Kip1} by suppression of c-jun expression and may be related to the cell cycle of cardiac fibroblasts [167]. Consistent with this study above, ciprofibrate inhibits fibroblast proliferation in control and IPF fibroblasts. Furthermore, PPAR-α as a transcription factor mediates peroxisome proliferation in rodent liver, and a functional PPRE is found about 8.4 kb downstream of the *PEX11α* promoter [119], encoding a protein involved in peroxisome proliferation [119, 132]. Lack of specific and potent peroxisome proliferators that are independent of specific PPAR-activation is one of the main technical limitations in distinguishing the beneficial effects of peroxisome proliferation. Although the findings presented here suggest that peroxisome proliferation rather than the endogenous PPAR-α activation mediates the anti-fibrotic effects observed, we cannot rule out the possibility of other molecular targets being altered during this 48 h pretreatment with PPAR-α agonists. Similarly, it should also be taken into consideration that the PPAR-α antagonist, GW6471 used in this study might also interfere in the activation/regulation of other PPAR family members, leading to secondary effects, which could result in the inhibitory effect observed on TGF-β1-induced α-SMA and collagen. Future

studies have to be carried out to confirm the specificity of this PPAR-α antagonist and to get more insights into the complex interactions of distinct PPARs on the PPREs of dependent genes, e.g. genes for peroxisomal proteins. Our study also highlights the necessity to design and synthesize new drugs with selective peroxisome proliferation activity, independent of PPARs, to resolve the technical difficulties in studying the beneficial effects of peroxisome proliferation in disease models.

4.5. Concluding remarks

Taken together, activation of TGF-β signaling during lung injury and subsequent induction and release of pro-inflammatory mediators such as TNF-α, ROS and IL-6 in IPF, leads to the downregulation of peroxisomes (e.g. PEX13) via AP-1 transcription factor, thus enabling the persistence of a fibrotic phenotype, which in turn generates more ROS and elevates secretion of proinflammatory cytokines (e.g. IL-6) (Fig. 43). Moreover, the activation of TGF-β signaling (Smad-dependent pathway) in peroxisome downregulation through *PEX13* knockdown promotes the increase of extracellular matrix production and generation of a fibrotic phenotype (Fig. 43). In summary, this study identifies a functionally relevant and potentially possible target for future development of new viable therapeutic approaches "the peroxisome", and significantly extends the role of this organelle in the maintenance of normal cellular function by scavenging ROS, metabolizing lipid mediators, and by protecting against inflammatory processes, leading eventually to exacerbations in patients with pulmonary fibrosis.
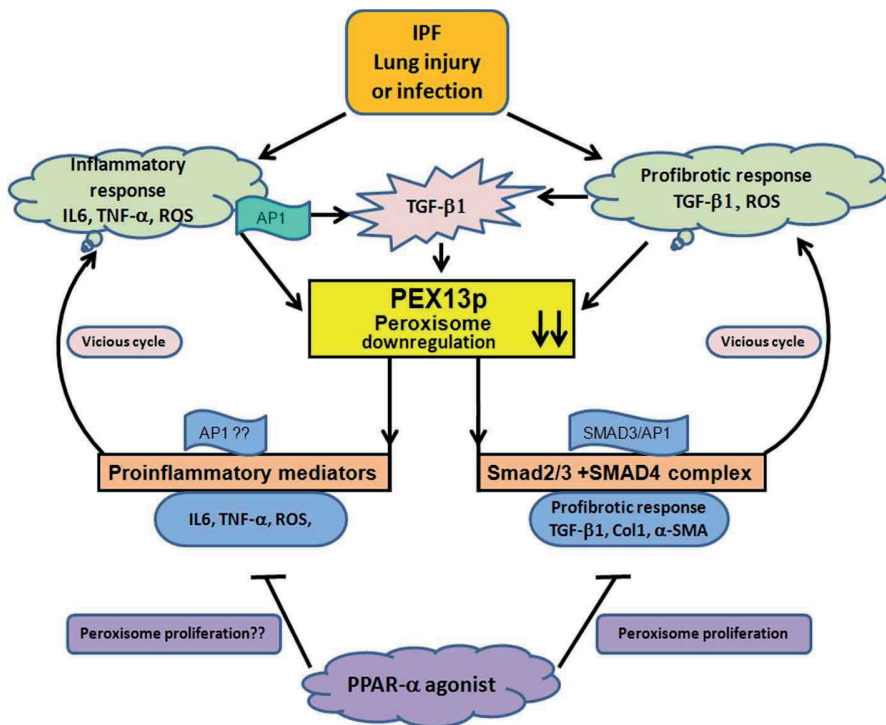
Fig. 43. Mechanism: Schematic illustration of TGF-β1 effects on peroxisome function, described as proposed model in this study. In idiopathic pulmonary fibrosis, lung injury leads to the production of pro-inflammatory mediators such as TNF-α, IL-6 and ROS and the activation of pro-fibrogenic TGF-β- and AP-1 signaling. This leads to downregulation of peroxisomes (e.g. PEX13p), which in turn induces more ROS, promotes secretion of cytokines such as IL-6 and triggers the activation of TGF-β1 and AP-1 signaling in a vicious cycle thus enabling the persistence of a fibrotic phenotype and inflammatory exacerbation phases in IPF patients. In addition, this vicious cycle also leads to increased production of collagen. In contrast, treatment with PPAR-α agonists induce the proliferation of peroxisomes and inhibit the pro-fibrogenic mechanisms such as myofibroblast differentiation (α-SMA) and collagen release [11].

5. Summary

Idiopathic pulmonary fibrosis (IPF) is a chronic devastating disease, and its pathogenic mechanisms remain incompletely understood. In this disease, the lung undergoes dramatic pathological remodelling and myofibroblasts with high α-smooth muscle actin (α-SMA) content secrete huge amounts of extracellular matrix. However, altered peroxisome functions in IPF pathogenesis have never been investigated. Proinflammatory mediators and reactive oxygen species (ROS) accumulation were shown as pathogenetic mechanisms of this yet incurable disease. Since peroxisomes are involved in both the degradation of proinflammatory lipid mediators (eicosanoids) as well as ROS metabolism, alterations in the protective capacity of this organelle might contribute to the pathogenesis of IPF. In addition, children with Zellweger Syndrome, the most severe peroxisomal biogenesis defect, develop chronic liver fibrosis and cirrhosis, suggesting that the peroxisomal metabolism is essential for the protection against fibrotic organ degeneration. In the experimental part of this thesis the hypothesis was tested, 1) whether the peroxisomal compartment and corresponding gene expression is altered in IPF, 2) whether the downregulation of peroxisomal biogenesis and metabolism in IPF promotes further excessive secretion of extracellular matrix proteins and proinflammatory mediators and 3) whether proinflammatory and profibrotic cytokines influence peroxisomal abundance and metabolism. Moreover, the molecular mechanisms leading to the alterations of the peroxisomal compartment were investigated. In addition, a bleomycin induced lung fibrosis mouse model was used to analyze peroxisomal biogenesis, antioxidative and lipid metabolic proteins at various time-points after bleomycin treatment. The molecular mechanisms and specific involvement of peroxisomal proteins in TGF-β1 induced ECM production were investigated. Finally the effect of TGF-β1 on the peroxisomal compartment in TGF-beta receptor II knockout (*TβRII)* and *Smad3* knockout mice as well in transgenic constitutively active *TβRI^{CA}* overexpressing mice was studied. In this thesis, the peroxisomal compartment as well as peroxisomal metabolic proteins were analyzed in parallel to several cell type-specific markers in paraffin sections of different lung tissue samples of human controls in comparison to IPF patients. In addition, primary cultures of lung fibroblasts of the same individuals were used for morphological, biochemical and molecular biological analysis of peroxisomal protein alterations. Moreover, control and IPF fibroblast were challenged with TGF-β1, TNF-α, IL−6 and *PEX13* siRNA to analyze the impact of peroxisomes on the molecular pathogenesis of IPF. To confirm this *in vitro* findings the bleomycin induced lung fibrosis mouse model and *TβRII* mice were used to study peroxisome

biogenesis and metabolism *in situ* in these animal models. By comparing peroxisome-related protein and gene expression in lung tissue and isolated lung fibroblasts between human control and IPF patients, we found that IPF lungs exhibited a significant down-regulation of peroxisomal biogenesis and metabolism (e.g. PEX13p, catalase, ABCD3 and acyl-CoA oxidase 1). Moreover, *in vivo* the bleomycin-induced downregulation of peroxisomes was abrogated in *TβRII* mice indicating a role for TGF-β signaling in the regulation of peroxisomes. Furthermore, *in vitro* treatment of IPF fibroblasts with the pro-fibrotic factors TGF-β1 or TNF-α was found to downregulate peroxisomes via the AP-1 signaling pathway. Therefore, the molecular mechanisms by which reduced peroxisomal functions contribute to enhanced fibrosis were further studied. Direct down-regulation of *PEX13* mRNA by RNAi 1) induced the activation of Smad-dependent TGF-β signaling, accompanied by increased ROS production, 2) resulted in the release of cytokines (e.g. IL-6, TGF-β) and excessive production of collagen I and III. In contrast, treatment of fibroblasts with ciprofibrate or WY14643, PPAR-α activators, induced peroxisome proliferation and reduced the TGF-β-induced myofibroblast differentiation and collagen protein in IPF cells.

Overall in this thesis it could be proven that the peroxisomal compartment is severely affected and compromised in IPF, mediated by TGF-β1 signaling and the action of proinflammatory cytokines (TNF-α and IL-6) via AP-1 signal transduction. TGF-β1 downregulates peroxisomes via the Smad-dependent pathway, which results in reduced ability of cells to scavenge ROS, degrade proinflammatory lipid mediators (eicosanoids) and subsequently inducing a vicious cycle, leading to the aggravation of IPF. Thus, TGF-β1 and TNF-α may exacerbate the clinical conditions and intensify the fibrotic response in patients with IPF upon inflammation and lung injury by the downregulation of peroxisomal biogenesis and metabolism (e.g. PEX13, ACOX1).

6. Zusammenfassung

Die Ideopathische Lungenfibrose (IPF) ist eine schwerwiegende chronische Lungenerkrankung, deren Pathomechanismus bis heute noch nicht vollständig aufgeklärt wurde. Im Verlauf dieser Erkrankung wird die Lungenstruktur dramatisch pathologisch umgebaut und Myofibroblasten mit einem hohen Gehalt an α-glatten Muskelzellaktin (α-SMA) sezernieren riesige Mengen extrazelluläre Matrix. Die Ansammlung von proinflammatorischen Mediatoren und reaktiven Sauerstoffspezies (ROS) ist bisher als pathogener Faktor dieser nach wie vor unheilbaren Krankheit, nachgewiesen worden. Da Peroxisomen sowohl in den Abbau von proinflammatorischen Lipidmediatoren (Eicosanoide) als auch in den ROS-Stoffwechsel eingebunden sind, könnten Veränderungen der peroxisomalen Schutzfunktion zur molekularen Pathogenese der IPF beitragen. Weiterhin entwickeln Kinder mit Zellweger Syndrom, den schwersten Phänotyps der peroxisomalen Biogenese Defekte (PBD), chronische Leberfibrose bzw. Zirrhose, was für die essentielle Bedeutung des peroxisomalen Stoffwechsels zum Schutz vor fibrotischen Organveränderungen spricht. Im experimentalen Teil dieser Dissertation wurde geprüft, 1) ob das peroxisomale Kompartiment und die dazugehörige Genexpression bei IPF verändert ist, 2) ob die Herrunterregulierung der peroxisomalen Biogenese und des peroxisomalen Stoffwechsels die Sekretion extrazellulärer Matrixproteine und inflammatorische Mediatoren steigert und 3) ob proinflammatorische und profibrotische Zytokine die Anzahl Peroxisomen und deren Stoffwechsel beeinflussen. Außerdem wurden die molekularen Mechanismen, die zur Veränderungen des peroxisomalen Kompartiments führen, untersucht. Zusätzlich wurde ein Bleomycin-induziertes Lungenfibrose-Mausmodell benutzt, um die peroxisomale Biogenese sowie Proteine des antioxidativen Stoffwechsels des Lipidmetabolismus zu verschiedenen Zeitpunkten nach der Bleomycinbehandlung zu analysieren. Weiterhin wurden die Mechanismen und die spezifische Beteiligung peroxisomaler Proteine bei der TGF-β1 induzierten Produktion extrazellulärer Matrixkomponenten untersucht. Zuletzt wurde der Effekt von TGF-β1 auf das peroxisomale Kompartment in *TβRII-*, und *SMAD3-*Knockoutmäusen, sowie in transgenen TβR-I überexprimierenden produzierenden Mäusen (*TβRI^{CA}*), beobachtet. In dieser Dissertation wurden das peroxisomale Kompartment und peroxisomale Stoffwechselproteine parallel zu zelltyp-spezifischen Markern in Paraffinschnitten von verschiedenen Lungengewebsproben von gesunden Kontrollen und IPF Patienten analysiert. Zusätzlich wurden Primärkulturen von Lungenfibroblasten von Kontrollen und IPF Patienten benutzt, um sie morphologisch, biochemisch und

molekularbiologisch auf peroxisomale Veränderungen zu untersuchen. Weiterhin wurden Primärkulturen von gesunden und IPF Patienten mit TGF-β1, TNF-α, IL–6 und *PEX13* siRNA behandelt, um den Einfluss von Peroxisomen auf die molekulare Pathogenese der IPF besser zu verstehen. Um die in vitro Ergebnisse zu bestätigen, wurden die Biogenese und der Stoffwechsel in der Peroxisomen *in situ* in Wildtyp Mäusen mit Bleomycin induzierten Lungenfibrose im Vergleich zu TGF-beta Rezeptor II Knockoutmäuse *(TβRII)* untersucht. Beim Vergleich peroxisomen-assoziierter Protein-und Genexpression in Lungengewebe und isolierten Fibroblasten gesunder Kontrollen und IPF Patienten fiel auf dass die Biogenese und der Stoffwechsel der Peroxisomen signifikant herunterreguliert wurden (z.B. PEX13p, Katalase, ABCD3 und Acyl-CoA-Oxidase 1). Ferner wurde die Bleomycin-induzierte Herunterregulierung der Peroxisomen in TβRII Knockoutmäusen aufgehoben, was auf eine wichtige Rolle von TGF-beta auf die Regulierung der Peroxisomen hinweist. Zusätzlich wurde nach Behandlung mit den profibrotischen Faktoren, TGF-β1 oder TNF-α in IPF Fibroblasten eine Herunterregulierung der Peroxisomen durch den AP-1 Signalweg beobachtet. Deswegen wurden die Mechanismen, duch die eine Verringerung der Peroxsiomen zu vermehrten Fibrose beitragen, im Detail untersucht. Eine direkte Herunterregulierung der *PEX13* mRNA via RNAi 1) induzierte die Aktivierung des Smad-abhängigen TGF-β Signalwegs und wurde begleitet von einer gesteigerten ROS-Produktion, 2) resultierte in der Freisetzung von Zytokinen (z.B. IL-6, TGF-β1) und der übermäßigen Produktion von Kollagen I und III. Im Gegensatz dazu führte eine Behandlung mit Ciprofibrat oder WY14643, beides PPAR-α-Aktivatoren, zu einer Proliferation der Peroxisomen und der reduzierten TGF-β-induzierten Myofibroblastendifferentiation, sowie zu verringerten Kollagenmengen in IPF-Zellen.

Zusammenfassend konnte in dieser Dissertation nachgewiesen werden, dass Peroxisomen bei der ideopathischen Lungenfibrose stark verändert und beeinträchtigt sind, und dieser Prozess durch TGF-β1 und dem Einfluss von proinflammatorischen Zytokinen (TNF-α und IL-6) mittels der AP-1 Signaltransduktion ausgelöst wird. TGF-β1 reguliert Peroxisomen mittels des Smad-abhängigen Signalwegs herunter, was in einer verminderten Fähigkeit, zu intrazellulären ROS-Abwehr mündet. Zusätzlich werden proinflammatorische Mediatoren (Eicosanoide) nicht mehr abgebaut, was in einen Teufelskreis mündet und zur Verschlechterung der ideopathischen Lungenfibrose führt. Somit scheinen TGF-β1 and TNF-α zur Exazerbation der klinischen Symptome und der verstärkten Fibrose von IPF Patienten durch die Herunterregulierung der peroxisomalen Biogenese und des peroxisomalen Stoffwechsels (z.B. PEX13, ACOX1) beizutragen.

7. References

1. Bjoraker, J.A., et al., *Prognostic significance of histopathologic subsets in idiopathic pulmonary fibrosis.* Am J Respir Crit Care Med, 1998. **157**(1): p. 199-203.
2. King, T.E., Jr., A. Pardo, and M. Selman, *Idiopathic pulmonary fibrosis.* Lancet. **378**(9807): p. 1949-61.
3. Dempsey, O.J., *Clinical review: idiopathic pulmonary fibrosis--past, present and future.* Respir Med, 2006. **100**(11): p. 1871-85.
4. Mura, M., et al., *Predicting survival in newly diagnosed idiopathic pulmonary fibrosis: a 3-year prospective study.* Eur Respir J. **40**(1): p. 101-9.
5. Cui, Y., et al., *Oxidative stress contributes to the induction and persistence of TGF-beta1 induced pulmonary fibrosis.* Int J Biochem Cell Biol, 2011. **43**(8): p. 1122-33.
6. Katzenstein, A.L. and J.L. Myers, *Idiopathic pulmonary fibrosis: clinical relevance of pathologic classification.* Am J Respir Crit Care Med, 1998. **157**(4 Pt 1): p. 1301-15.
7. Kuhn, C. and J.A. McDonald, *The roles of the myofibroblast in idiopathic pulmonary fibrosis. Ultrastructural and immunohistochemical features of sites of active extracellular matrix synthesis.* Am J Pathol, 1991. **138**(5): p. 1257-65.
8. Pardo, A. and M. Selman, *Molecular mechanisms of pulmonary fibrosis.* Front Biosci, 2002. **7**: p. d1743-61.
9. Walters, D.M., H.Y. Cho, and S.R. Kleeberger, *Oxidative stress and antioxidants in the pathogenesis of pulmonary fibrosis: a potential role for Nrf2.* Antioxid Redox Signal, 2008. **10**(2): p. 321-32.
10. Gao, F., et al., *Extracellular superoxide dismutase in pulmonary fibrosis.* Antioxid Redox Signal, 2008. **10**(2): p. 343-54.
11. Oruqaj, G., et al., *Compromised peroxisomes in idiopathic pulmonary fibrosis, a vicious cycle inducing a higher fibrotic response via TGF-beta signaling.* Proc Natl Acad Sci U S A. **112**(16): p. E2048-57.
12. Warburton, D., W. Shi, and B. Xu, *TGF-beta-Smad3 signaling in emphysema and pulmonary fibrosis: an epigenetic aberration of normal development?* Am J Physiol Lung Cell Mol Physiol, 2013. **304**(2): p. L83-5.
13. Zhao, J., et al., *Smad3 deficiency attenuates bleomycin-induced pulmonary fibrosis in mice.* Am J Physiol Lung Cell Mol Physiol, 2002. **282**(3): p. L585-93.
14. Coward, W.R., G. Saini, and G. Jenkins, *The pathogenesis of idiopathic pulmonary fibrosis.* Ther Adv Respir Dis. **4**(6): p. 367-88.
15. Williams, K., et al., *Identification of spontaneous feline idiopathic pulmonary fibrosis: morphology and ultrastructural evidence for a type II pneumocyte defect.* Chest, 2004. **125**(6): p. 2278-88.
16. Sisson, T.H., et al., *Targeted injury of type II alveolar epithelial cells induces pulmonary fibrosis.* Am J Respir Crit Care Med. **181**(3): p. 254-63.
17. Eickelberg, O. and G.J. Laurent, *The quest for the initial lesion in idiopathic pulmonary fibrosis: gene expression differences in IPF fibroblasts.* Am J Respir Cell Mol Biol. **42**(1): p. 1-2.
18. Strieter, R.M. and B. Mehrad, *New mechanisms of pulmonary fibrosis.* Chest, 2009. **136**(5): p. 1364-70.
19. Eickelberg, O., et al., *Molecular mechanisms of TGF-(beta) antagonism by interferon (gamma) and cyclosporine A in lung fibroblasts.* FASEB J, 2001. **15**(3): p. 797-806.
20. Gauldie, J., M. Jordana, and G. Cox, *Cytokines and pulmonary fibrosis.* Thorax, 1993. **48**(9): p. 931-5.
21. Konigshoff, M., et al., *WNT1-inducible signaling protein-1 mediates pulmonary fibrosis in mice and is upregulated in humans with idiopathic pulmonary fibrosis.* J Clin Invest, 2009. **119**(4): p. 772-87.

22. Selman, M., et al., *Gene expression profiles distinguish idiopathic pulmonary fibrosis from hypersensitivity pneumonitis.* Am J Respir Crit Care Med, 2006. **173**(2): p. 188-98.

23. White, E.S., et al., *Negative regulation of myofibroblast differentiation by PTEN (Phosphatase and Tensin Homolog Deleted on chromosome 10).* Am J Respir Crit Care Med, 2006. **173**(1): p. 112-21.

24. Xia, H., et al., *Pathological integrin signaling enhances proliferation of primary lung fibroblasts from patients with idiopathic pulmonary fibrosis.* J Exp Med, 2008. **205**(7): p. 1659-72.

25. Tanjore, H., et al., *Contribution of epithelial-derived fibroblasts to bleomycin-induced lung fibrosis.* Am J Respir Crit Care Med, 2009. **180**(7): p. 657-65.

26. Rock, J.R., et al., *Multiple stromal populations contribute to pulmonary fibrosis without evidence for epithelial to mesenchymal transition.* Proc Natl Acad Sci U S A. **108**(52): p. E1475-83.

27. Kubo, H., et al., *Anticoagulant therapy for idiopathic pulmonary fibrosis.* Chest, 2005. **128**(3): p. 1475-82.

28. Collard, H.R., et al., *Acute exacerbations of idiopathic pulmonary fibrosis.* Am J Respir Crit Care Med, 2007. **176**(7): p. 636-43.

29. Homma, S., et al., *Cyclosporin treatment in steroid-resistant and acutely exacerbated interstitial pneumonia.* Intern Med, 2005. **44**(11): p. 1144-50.

30. Zisman, D.A., et al., *A controlled trial of sildenafil in advanced idiopathic pulmonary fibrosis.* N Engl J Med. **363**(7): p. 620-8.

31. Taniguchi, H., et al., *Pirfenidone in idiopathic pulmonary fibrosis.* Eur Respir J. **35**(4): p. 821-9.

32. Richeldi, L., et al., *Efficacy and safety of nintedanib in idiopathic pulmonary fibrosis.* N Engl J Med, 2014. **370**(22): p. 2071-82.

33. Piguet, P.F. and C. Vesin, *Treatment by human recombinant soluble TNF receptor of pulmonary fibrosis induced by bleomycin or silica in mice.* Eur Respir J, 1994. **7**(3): p. 515-8.

34. Raghu, G., et al., *Treatment of idiopathic pulmonary fibrosis with etanercept: an exploratory, placebo-controlled trial.* Am J Respir Crit Care Med, 2008. **178**(9): p. 948-55.

35. Demedts, M., et al., *High-dose acetylcysteine in idiopathic pulmonary fibrosis.* N Engl J Med, 2005. **353**(21): p. 2229-42.

36. Germano, D., et al., *Prominin-1/CD133+ lung epithelial progenitors protect from bleomycin-induced pulmonary fibrosis.* Am J Respir Crit Care Med, 2009. **179**(10): p. 939-49.

37. Wang, D., et al., *Transplantation of human embryonic stem cell-derived alveolar epithelial type II cells abrogates acute lung injury in mice.* Mol Ther. **18**(3): p. 625-34.

38. Thabut, G., et al., *Survival after bilateral versus single-lung transplantation for idiopathic pulmonary fibrosis.* Ann Intern Med, 2009. **151**(11): p. 767-74.

39. Xaubet, A., et al., *Transforming growth factor-beta1 gene polymorphisms are associated with disease progression in idiopathic pulmonary fibrosis.* Am J Respir Crit Care Med, 2003. **168**(4): p. 431-5.

40. Fernandez, I.E. and O. Eickelberg, *The impact of TGF-beta on lung fibrosis: from targeting to biomarkers.* Proc Am Thorac Soc. **9**(3): p. 111-6.

41. Ward, P.A. and G.W. Hunninghake, *Lung inflammation and fibrosis.* Am J Respir Crit Care Med, 1998. **157**(4 Pt 2): p. S123-9.

42. Massague, J., *TGFbeta in Cancer.* Cell, 2008. **134**(2): p. 215-30.

43. Cutroneo, K.R., et al., *Therapies for bleomycin induced lung fibrosis through regulation of TGF-beta1 induced collagen gene expression.* J Cell Physiol, 2007. **211**(3): p. 585-9.

44. Dancer, R.C., A.M. Wood, and D.R. Thickett, *Metalloproteinases in idiopathic pulmonary fibrosis.* Eur Respir J. **38**(6): p. 1461-7.

45. Bargagli, E., et al., *Oxidative stress in the pathogenesis of diffuse lung diseases: a review.* Respir Med, 2009. **103**(9): p. 1245-56.

46. Crawford, S.E., et al., *Thrombospondin-1 is a major activator of TGF-beta1 in vivo.* Cell, 1998. **93**(7): p. 1159-70.

47. Hinz, B., *Tissue stiffness, latent TGF-beta1 activation, and mechanical signal transduction: implications for the pathogenesis and treatment of fibrosis.* Curr Rheumatol Rep, 2009. **11**(2): p. 120-6.

48. Margadant, C. and A. Sonnenberg, *Integrin-TGF-beta crosstalk in fibrosis, cancer and wound healing.* EMBO Rep. **11**(2): p. 97-105.

49. Shi, Y. and J. Massague, *Mechanisms of TGF-beta signaling from cell membrane to the nucleus.* Cell, 2003. **113**(6): p. 685-700.

50. Feng, X.H. and R. Derynck, *Specificity and versatility in tgf-beta signaling through Smads.* Annu Rev Cell Dev Biol, 2005. **21**: p. 659-93.

51. Raghu, G., et al., *Collagen synthesis by normal and fibrotic human lung fibroblasts and the effect of transforming growth factor-beta.* Am Rev Respir Dis, 1989. **140**(1): p. 95-100.

52. Madri, J.A. and H. Furthmayr, *Collagen polymorphism in the lung. An immunochemical study of pulmonary fibrosis.* Hum Pathol, 1980. **11**(4): p. 353-66.

53. Monboisse, J.C., et al., *Collagen activates superoxide anion production by human polymorphonuclear neutrophils.* Biochem J, 1987. **246**(3): p. 599-603.

54. Wei, J.G., et al., *[Relationship between bleomycin-induced pulmonary fibrosis and vascular endothelial cell injury].* Zhonghua Lao Dong Wei Sheng Zhi Ye Bing Za Zhi, 2004. **22**(5): p. 354-7.

55. Fontana, L., et al., *Fibronectin is required for integrin alphavbeta6-mediated activation of latent TGF-beta complexes containing LTBP-1.* FASEB J, 2005. **19**(13): p. 1798-808.

56. Kornblihtt, A.R., K. Vibe-Pedersen, and F.E. Baralle, *Human fibronectin: molecular cloning evidence for two mRNA species differing by an internal segment coding for a structural domain.* EMBO J, 1984. **3**(1): p. 221-6.

57. Taipale, J., J. Saharinen, and J. Keski-Oja, *Extracellular matrix-associated transforming growth factor-beta: role in cancer cell growth and invasion.* Adv Cancer Res, 1998. **75**: p. 87-134.

58. Kinnula, V.L., et al., *Oxidative stress in pulmonary fibrosis: a possible role for redox modulatory therapy.* Am J Respir Crit Care Med, 2005. **172**(4): p. 417-22.

59. Krieg, T. and M. Heckmann, *Regulatory mechanisms of fibroblast activity.* Recenti Prog Med, 1989. **80**(11): p. 594-8.

60. Grinnell, F., *Fibroblasts, myofibroblasts, and wound contraction.* J Cell Biol, 1994. **124**(4): p. 401-4.

61. Hung, C., et al., *Role of lung pericytes and resident fibroblasts in the pathogenesis of pulmonary fibrosis.* Am J Respir Crit Care Med. **188**(7): p. 820-30.

62. Ramos, C., et al., *Fibroblasts from idiopathic pulmonary fibrosis and normal lungs differ in growth rate, apoptosis, and tissue inhibitor of metalloproteinases expression.* Am J Respir Cell Mol Biol, 2001. **24**(5): p. 591-8.

63. Derdak, S., et al., *Differential collagen and fibronectin production by Thy 1+ and Thy 1- lung fibroblast subpopulations.* Am J Physiol, 1992. **263**(2 Pt 1): p. L283-90.

64. Phan, S.H., *The myofibroblast in pulmonary fibrosis.* Chest, 2002. **122**(6 Suppl): p. 286S-289S.

65. Pache, J.C., et al., *Myofibroblasts in diffuse alveolar damage of the lung.* Mod Pathol, 1998. **11**(11): p. 1064-70.

66. Vaughan, M.B., E.W. Howard, and J.J. Tomasek, *Transforming growth factor-beta1 promotes the morphological and functional differentiation of the myofibroblast.* Exp Cell Res, 2000. **257**(1): p. 180-9.

67. Wilson, M.S. and T.A. Wynn, *Pulmonary fibrosis: pathogenesis, etiology and regulation.* Mucosal Immunol, 2009. **2**(2): p. 103-21.

68. Zeisberg, M. and R. Kalluri, *Cellular mechanisms of tissue fibrosis. 1. Common and organ-specific mechanisms associated with tissue fibrosis.* Am J Physiol Cell Physiol, 2013. **304**(3): p. C216-25.

69. Bienkowski, R.S. and M.G. Gotkin, *Control of collagen deposition in mammalian lung.* Proc Soc Exp Biol Med, 1995. **209**(2): p. 118-40.

70. Eickelberg, O., et al., *Transforming growth factor-beta1 induces interleukin-6 expression via activating protein-1 consisting of JunD homodimers in primary human lung fibroblasts.* J Biol Chem, 1999. **274**(18): p. 12933-8.

71. Kim, K.K., et al., *Alveolar epithelial cell mesenchymal transition develops in vivo during pulmonary fibrosis and is regulated by the extracellular matrix.* Proc Natl Acad Sci U S A, 2006. **103**(35): p. 13180-5.

72. Willis, B.C., et al., *Induction of epithelial-mesenchymal transition in alveolar epithelial cells by transforming growth factor-beta1: potential role in idiopathic pulmonary fibrosis.* Am J Pathol, 2005. **166**(5): p. 1321-32.

73. Yu, L., M.C. Hebert, and Y.E. Zhang, *TGF-beta receptor-activated p38 MAP kinase mediates Smad-independent TGF-beta responses.* EMBO J, 2002. **21**(14): p. 3749-59.

74. Bhowmick, N.A., et al., *Transforming growth factor-beta1 mediates epithelial to mesenchymal transdifferentiation through a RhoA-dependent mechanism.* Mol Biol Cell, 2001. **12**(1): p. 27-36.

75. Yamashita, C.M., et al., *Matrix metalloproteinase 3 is a mediator of pulmonary fibrosis.* Am J Pathol. **179**(4): p. 1733-45.

76. Green, M.J., et al., *Serum MMP-3 and MMP-1 and progression of joint damage in early rheumatoid arthritis.* Rheumatology (Oxford), 2003. **42**(1): p. 83-8.

77. Selman, M., et al., *Accelerated variant of idiopathic pulmonary fibrosis: clinical behavior and gene expression pattern.* PLoS One, 2007. **2**(5): p. e482.

78. Swiderski, R.E., et al., *Differential expression of extracellular matrix remodeling genes in a murine model of bleomycin-induced pulmonary fibrosis.* Am J Pathol, 1998. **152**(3): p. 821-8.

79. Zuo, F., et al., *Gene expression analysis reveals matrilysin as a key regulator of pulmonary fibrosis in mice and humans.* Proc Natl Acad Sci U S A, 2002. **99**(9): p. 6292-7.

80. Karnati, S. and E. Baumgart-Vogt, *Peroxisomes in mouse and human lung: their involvement in pulmonary lipid metabolism.* Histochem Cell Biol, 2008. **130**(4): p. 719-40.

81. Waghray, M., et al., *Hydrogen peroxide is a diffusible paracrine signal for the induction of epithelial cell death by activated myofibroblasts.* FASEB J, 2005. **19**(7): p. 854-6.

82. Thannickal, V.J., et al., *Ras-dependent and -independent regulation of reactive oxygen species by mitogenic growth factors and TGF-beta1.* FASEB J, 2000. **14**(12): p. 1741-8.

83. Kondrikov, D., et al., *Reactive oxygen species-dependent RhoA activation mediates collagen synthesis in hyperoxic lung fibrosis.* Free Radic Biol Med. **50**(11): p. 1689-98.

84. Kliment, C.R. and T.D. Oury, *Oxidative stress, extracellular matrix targets, and idiopathic pulmonary fibrosis.* Free Radic Biol Med. **49**(5): p. 707-17.

85. Manoury, B., et al., *The absence of reactive oxygen species production protects mice against bleomycin-induced pulmonary fibrosis.* Respir Res, 2005. **6**: p. 11.

86. Hecker, L., et al., *NADPH oxidase-4 mediates myofibroblast activation and fibrogenic responses to lung injury.* Nat Med, 2009. **15**(9): p. 1077-81.

87. Fattman, C.L., et al., *Enhanced bleomycin-induced pulmonary damage in mice lacking extracellular superoxide dismutase.* Free Radic Biol Med, 2003. **35**(7): p. 763-71.

88. Kinnula, V.L. and M. Myllarniemi, *Oxidant-antioxidant imbalance as a potential contributor to the progression of human pulmonary fibrosis.* Antioxid Redox Signal, 2008. **10**(4): p. 727-38.

89. McKeown, S., et al., *MMP expression and abnormal lung permeability are important determinants of outcome in IPF.* Eur Respir J, 2009. **33**(1): p. 77-84.

90. Koli, K., et al., *Transforming growth factor-beta activation in the lung: focus on fibrosis and reactive oxygen species.* Antioxid Redox Signal, 2008. **10**(2): p. 333-42.

91. Jobling, M.F., et al., *Isoform-specific activation of latent transforming growth factor beta (LTGF-beta) by reactive oxygen species.* Radiat Res, 2006. **166**(6): p. 839-48.

92. Fatma, N., et al., *Impaired homeostasis and phenotypic abnormalities in Prdx6-/-mice lens epithelial cells by reactive oxygen species: increased expression and activation of TGFbeta.* Cell Death Differ, 2005. **12**(7): p. 734-50.

93. Jochum, W., E. Passegue, and E.F. Wagner, *AP-1 in mouse development and tumorigenesis.* Oncogene, 2001. **20**(19): p. 2401-12.

94. Wagner, E.F. and R. Eferl, *Fos/AP-1 proteins in bone and the immune system.* Immunol Rev, 2005. **208**: p. 126-40.

95. Johnson, R.S., et al., *A null mutation at the c-jun locus causes embryonic lethality and retarded cell growth in culture.* Genes Dev, 1993. **7**(7B): p. 1309-17.

96. Angel, P. and M. Karin, *The role of Jun, Fos and the AP-1 complex in cell-proliferation and transformation.* Biochim Biophys Acta, 1991. **1072**(2-3): p. 129-57.

97. Avouac, J., et al., *Inhibition of activator protein 1 signaling abrogates transforming growth factor beta-mediated activation of fibroblasts and prevents experimental fibrosis.* Arthritis Rheum, 2012. **64**(5): p. 1642-52.

98. Palumbo, K., et al., *The transcription factor JunD mediates transforming growth factor {beta}-induced fibroblast activation and fibrosis in systemic sclerosis.* Ann Rheum Dis. **70**(7): p. 1320-6.

99. Sullivan, D.E., et al., *TNF-alpha induces TGF-beta1 expression in lung fibroblasts at the transcriptional level via AP-1 activation.* J Cell Mol Med, 2009. **13**(8B): p. 1866-76.

100. Ortiz, L.A., et al., *Expression of TNF and the necessity of TNF receptors in bleomycin-induced lung injury in mice.* Exp Lung Res, 1998. **24**(6): p. 721-43.

101. Verjee, L.S., et al., *Unraveling the signaling pathways promoting fibrosis in Dupuytren's disease reveals TNF as a therapeutic target.* Proc Natl Acad Sci U S A, 2013. **110**(10): p. E928-37.

102. Selman, M., et al., *Idiopathic pulmonary fibrosis: pathogenesis and therapeutic approaches.* Drugs, 2004. **64**(4): p. 405-30.

103. Moodley, Y.P., et al., *Inverse effects of interleukin-6 on apoptosis of fibroblasts from pulmonary fibrosis and normal lungs.* Am J Respir Cell Mol Biol, 2003. **29**(4): p. 490-8.

104. Saito, F., et al., *Role of interleukin-6 in bleomycin-induced lung inflammatory changes in mice.* Am J Respir Cell Mol Biol, 2008. **38**(5): p. 566-71.

105. Luo, Y., et al., *A novel profibrotic mechanism mediated by TGFbeta-stimulated collagen prolyl hydroxylase expression in fibrotic lung mesenchymal cells.* J Pathol. **236**(3): p. 384-94.

106. Li, M., et al., *Epithelium-specific deletion of TGF-beta receptor type II protects mice from bleomycin-induced pulmonary fibrosis.* J Clin Invest. **121**(1): p. 277-87.

107. Zhang, W., et al., *Spatial-temporal targeting of lung-specific mesenchyme by a Tbx4 enhancer.* BMC Biol. **11**: p. 111.

108. Bonniaud, P., et al., *Smad3 null mice develop airspace enlargement and are resistant to TGF-beta-mediated pulmonary fibrosis.* J Immunol, 2004. **173**(3): p. 2099-108.

109. Wrana, J.L., et al., *Mechanism of activation of the TGF-beta receptor.* Nature, 1994. **370**(6488): p. 341-7.

110. Wieser, R., J.L. Wrana, and J. Massague, *GS domain mutations that constitutively activate T beta R-I, the downstream signaling component in the TGF-beta receptor complex.* EMBO J, 1995. **14**(10): p. 2199-208.

111. Bartholin, L., et al., *Generation of mice with conditionally activated transforming growth factor beta signaling through the TbetaRI/ALK5 receptor.* Genesis, 2008. **46**(12): p. 724-31.

112. Karnati, S. and E. Baumgart-Vogt, *Peroxisomes in airway epithelia and future prospects of these organelles for pulmonary cell biology.* Histochem Cell Biol, 2009. **131**(4): p. 447-54.

113. Rahman, I., et al., *Is there any relationship between plasma antioxidant capacity and lung function in smokers and in patients with chronic obstructive pulmonary disease?* Thorax, 2000. **55**(3): p. 189-93.

114. Ahlemeyer, B., M. Gottwald, and E. Baumgart-Vogt, *Deletion of a single allele of the Pex11beta gene is sufficient to cause oxidative stress, delayed differentiation and neuronal death in mouse brain.* Dis Model Mech, 2012. **5**(1): p. 125-40.

115. Steinberg, S.J., et al., *Peroxisome biogenesis disorders.* Biochim Biophys Acta, 2006. **1763**(12): p. 1733-48.

116. Baes, M., et al., *A mouse model for Zellweger syndrome.* Nat Genet, 1997. **17**(1): p. 49-57.

117. Li, X., et al., *PEX11 beta deficiency is lethal and impairs neuronal migration but does not abrogate peroxisome function.* Mol Cell Biol, 2002. **22**(12): p. 4358-65.

118. Boor, P., et al., *The peroxisome proliferator-activated receptor-alpha agonist, BAY PP1, attenuates renal fibrosis in rats.* Kidney Int, 2011. **80**(11): p. 1182-97.

119. Shimizu, M., et al., *Tissue-selective, bidirectional regulation of PEX11 alpha and perilipin genes through a common peroxisome proliferator response element.* Mol Cell Biol, 2004. **24**(3): p. 1313-23.

120. Rahman, I. and W. MacNee, *Regulation of redox glutathione levels and gene transcription in lung inflammation: therapeutic approaches.* Free Radic Biol Med, 2000. **28**(9): p. 1405-20.

121. Distel, B., et al., *A unified nomenclature for peroxisome biogenesis factors.* J Cell Biol, 1996. **135**(1): p. 1-3.

122. Lazarow, P.B. and Y. Fujiki, *Biogenesis of peroxisomes.* Annu Rev Cell Biol, 1985. **1**: p. 489-530.

123. Goldman, B.M. and G. Blobel, *Biogenesis of peroxisomes: intracellular site of synthesis of catalase and uricase.* Proc Natl Acad Sci U S A, 1978. **75**(10): p. 5066-70.

124. Eckert, J.H. and R. Erdmann, *Peroxisome biogenesis.* Rev Physiol Biochem Pharmacol, 2003. **147**: p. 75-121.

125. Fujiki, Y., et al., *Peroxisome biogenesis in mammalian cells.* Front Physiol. **5**: p. 307.

126. Liu, Y., et al., *PEX13 is mutated in complementation group 13 of the peroxisome-biogenesis disorders.* Am J Hum Genet, 1999. **65**(3): p. 621-34.

127. Wiese, S., et al., *Proteomics characterization of mouse kidney peroxisomes by tandem mass spectrometry and protein correlation profiling.* Mol Cell Proteomics, 2007. **6**(12): p. 2045-57.

128. Islinger, M., et al., *Insights into the membrane proteome of rat liver peroxisomes: microsomal glutathione-S-transferase is shared by both subcellular compartments.* Proteomics, 2006. **6**(3): p. 804-16.

129. Schrader, M. and H.D. Fahimi, *Mammalian peroxisomes and reactive oxygen species.* Histochem Cell Biol, 2004. **122**(4): p. 383-93.

130. Karnati, S., et al., *Mammalian SOD2 is exclusively located in mitochondria and not present in peroxisomes.* Histochem Cell Biol, 2013. **140**(2): p. 105-17.

131. Moser, H.W., *[Disorders associated with alterations in single peroxisomal proteins, including X-linked adrenoleukodystrophy].* Rev Neurol, 1999. **28 Suppl 1**: p. S55-8.

132. Colasante, C., et al., *Peroxisomes in cardiomyocytes and the peroxisome / peroxisome proliferator-activated receptor-loop.* Thromb Haemost, 2015. **113**(3).

133. Beier, K., A. Volkl, and H.D. Fahimi, *TNF-alpha downregulates the peroxisome proliferator activated receptor-alpha and the mRNAs encoding peroxisomal proteins in rat liver.* FEBS Lett, 1997. **412**(2): p. 385-7.

134. Beier, K. and H.D. Fahimi, *Environmental pollution by common chemicals and peroxisome proliferation: efficient detection by cytochemistry and automatic image analysis.* Prog Histochem Cytochem, 1991. **23**(1-4): p. 150-63.

135. Schrader, M., et al., *Peroxisome-mitochondria interplay and disease.* J Inherit Metab Dis. **38**(4): p. 681-702.

136. Rahman, I., *Antioxidant therapies in COPD.* Int J Chron Obstruct Pulmon Dis, 2006. **1**(1): p. 15-29.

137. Immenschuh, S. and E. Baumgart-Vogt, *Peroxiredoxins, oxidative stress, and cell proliferation.* Antioxid Redox Signal, 2005. **7**(5-6): p. 768-77.

138. Baumgart, E., et al., *Mitochondrial alterations caused by defective peroxisomal biogenesis in a mouse model for Zellweger syndrome (PEX5 knockout mouse).* Am J Pathol, 2001. **159**(4): p. 1477-94.

139. Hunt, M.C., V. Tillander, and S.E. Alexson, *Regulation of peroxisomal lipid metabolism: the role of acyl-CoA and coenzyme A metabolizing enzymes.* Biochimie. **98**: p. 45-55.

140. Wanders, R.J. and H.R. Waterham, *Biochemistry of mammalian peroxisomes revisited.* Annu Rev Biochem, 2006. **75**: p. 295-332.

141. Wierzbicki, A.S., et al., *Refsum's disease: a peroxisomal disorder affecting phytanic acid alpha-oxidation.* J Neurochem, 2002. **80**(5): p. 727-35.

142. Jansen, G.A., et al., *Phytanoyl-coenzyme A hydroxylase deficiency -- the enzyme defect in Refsum's disease.* N Engl J Med, 1997. **337**(2): p. 133-4.

143. Foulon, V., et al., *Breakdown of 2-hydroxylated straight chain fatty acids via peroxisomal 2-hydroxyphytanoyl-CoA lyase: a revised pathway for the alpha-oxidation of straight chain fatty acids.* J Biol Chem, 2005. **280**(11): p. 9802-12.

144. Eaton, S., K. Bartlett, and M. Pourfarzam, *Mammalian mitochondrial beta-oxidation.* Biochem J, 1996. **320 (Pt 2)**: p. 345-57.

145. Reddy, J.K. and T. Hashimoto, *Peroxisomal beta-oxidation and peroxisome proliferator-activated receptor alpha: an adaptive metabolic system.* Annu Rev Nutr, 2001. **21**: p. 193-230.

146. Belvisi, M.G. and D.J. Hele, *Peroxisome proliferator-activated receptors as novel targets in lung disease.* Chest, 2008. **134**(1): p. 152-7.

147.   Lakatos, H.F., et al., *The Role of PPARs in Lung Fibrosis.* PPAR Res, 2007. **2007**: p. 71323.

148.   Moras, D. and H. Gronemeyer, *The nuclear receptor ligand-binding domain: structure and function.* Curr Opin Cell Biol, 1998. **10**(3): p. 384-91.

149.   Belvisi, M.G., D.J. Hele, and M.A. Birrell, *Peroxisome proliferator-activated receptor gamma agonists as therapy for chronic airway inflammation.* Eur J Pharmacol, 2006. **533**(1-3): p. 101-9.

150.   Becker, J., et al., *Regulation of inflammation by PPARs: a future approach to treat lung inflammatory diseases?* Fundam Clin Pharmacol, 2006. **20**(5): p. 429-47.

151.   Osumi, T., J.K. Wen, and T. Hashimoto, *Two cis-acting regulatory sequences in the peroxisome proliferator-responsive enhancer region of rat acyl-CoA oxidase gene.* Biochem Biophys Res Commun, 1991. **175**(3): p. 866-71.

152.   Rizzo, G. and S. Fiorucci, *PPARs and other nuclear receptors in inflammation.* Curr Opin Pharmacol, 2006. **6**(4): p. 421-7.

153.   Cuzzocrea, S., et al., *Peroxisome proliferator-activated receptor-alpha contributes to the anti-inflammatory activity of glucocorticoids.* Mol Pharmacol, 2008. **73**(2): p. 323-37.

154.   Delayre-Orthez, C., et al., *PPARalpha downregulates airway inflammation induced by lipopolysaccharide in the mouse.* Respir Res, 2005. **6**: p. 91.

155.   Genovese, T., et al., *ROLE OF ENDOGENOUS AND EXOGENOUS LIGANDS FOR THE PEROXISOME PROLIFERATOR-ACTIVATED RECEPTOR alpha IN THE DEVELOPMENT OF BLEOMYCIN-INDUCED LUNG INJURY.* Shock, 2005. **24**(6): p. 547-55.

156.   Bowden, D.H., *Unraveling pulmonary fibrosis: the bleomycin model.* Lab Invest, 1984. **50**(5): p. 487-8.

157.   Chytil, A., et al., *Conditional inactivation of the TGF-beta type II receptor using Cre:Lox.* Genesis, 2002. **32**(2): p. 73-5.

158.   Sauer, B., *Manipulation of transgenes by site-specific recombination: use of Cre recombinase.* Methods Enzymol, 1993. **225**: p. 890-900.

159.   Nenicu, A., et al., *Peroxisomes in human and mouse testis: differential expression of peroxisomal proteins in germ cells and distinct somatic cell types of the testis.* Biol Reprod, 2007. **77**(6): p. 1060-72.

160.   Vijayan, V., et al., *Bruton's tyrosine kinase is required for TLR-dependent heme oxygenase-1 gene activation via Nrf2 in macrophages.* J Immunol, 2011. **187**(2): p. 817-27.

161.   Ahlemeyer, B., et al., *Differential expression of peroxisomal matrix and membrane proteins during postnatal development of mouse brain.* J Comp Neurol, 2007. **505**(1): p. 1-17.

162.   Rahman, I. and F. Kelly, *Biomarkers in breath condensate: a promising new non-invasive technique in free radical research.* Free Radic Res, 2003. **37**(12): p. 1253-66.

163.   Yao, H., et al., *Redox regulation of lung inflammation: role of NADPH oxidase and NF-kappaB signalling.* Biochem Soc Trans, 2007. **35**(Pt 5): p. 1151-5.

164.   Kirkham, P. and I. Rahman, *Oxidative stress in asthma and COPD: antioxidants as a therapeutic strategy.* Pharmacol Ther, 2006. **111**(2): p. 476-94.

165.   Grant, P., et al., *The biogenesis protein PEX14 is an optimal marker for the identification and localization of peroxisomes in different cell types, tissues, and species in morphological studies.* Histochem Cell Biol, 2013. **140**(4): p. 423-42.

166.   Verrecchia, F., et al., *Smad3/AP-1 interactions control transcriptional responses to TGF-beta in a promoter-specific manner.* Oncogene, 2001. **20**(26): p. 3332-40.

167. Ogata, T., et al., *Stimulation of peroxisome-proliferator-activated receptor alpha (PPAR alpha) attenuates cardiac fibrosis and endothelin-1 production in pressure-overloaded rat hearts.* Clin Sci (Lond), 2002. **103 Suppl 48**: p. 284S-288S.

168. Walton, P.A. and M. Pizzitelli, *Effects of peroxisomal catalase inhibition on mitochondrial function.* Front Physiol. **3**: p. 108.

169. Odajima, N., et al., *The role of catalase in pulmonary fibrosis.* Respir Res. **11**: p. 183.

170. Michaeloudes, C., et al., *TGF-beta regulates Nox4, MnSOD and catalase expression, and IL-6 release in airway smooth muscle cells.* Am J Physiol Lung Cell Mol Physiol. **300**(2): p. L295-304.

171. Baarine, M., et al., *Evidence of oxidative stress in very long chain fatty acid--treated oligodendrocytes and potentialization of ROS production using RNA interference-directed knockdown of ABCD1 and ACOX1 peroxisomal proteins.* Neuroscience, 2012. **213**: p. 1-18.

172. Patel, A.S., et al., *Epithelial cell mitochondrial dysfunction and PINK1 are induced by transforming growth factor-beta1 in pulmonary fibrosis.* PLoS One. **10**(3): p. e0121246.

173. Gabele, E., et al., *TNFalpha is required for cholestasis-induced liver fibrosis in the mouse.* Biochem Biophys Res Commun, 2009. **378**(3): p. 348-53.

174. Junn, E., et al., *Requirement of hydrogen peroxide generation in TGF-beta 1 signal transduction in human lung fibroblast cells: involvement of hydrogen peroxide and Ca2+ in TGF-beta 1-induced IL-6 expression.* J Immunol, 2000. **165**(4): p. 2190-7.

175. Rajasekaran, S., M. Vaz, and S.P. Reddy, *Fra-1/AP-1 transcription factor negatively regulates pulmonary fibrosis in vivo.* PLoS One, 2012. **7**(7): p. e41611.

176. Roy, S., et al., *Fra-2 mediates oxygen-sensitive induction of transforming growth factor beta in cardiac fibroblasts.* Cardiovasc Res, 2010. **87**(4): p. 647-55.

177. Liu, W., et al., *Antiflammin-1 attenuates bleomycin-induced pulmonary fibrosis in mice.* Respir Res, 2013. **14**: p. 101.

178. Pantelidis, P., et al., *Analysis of tumor necrosis factor-alpha, lymphotoxin-alpha, tumor necrosis factor receptor II, and interleukin-6 polymorphisms in patients with idiopathic pulmonary fibrosis.* Am J Respir Crit Care Med, 2001. **163**(6): p. 1432-6.

179. Qiu, Z., et al., *Enhanced airway inflammation and decreased subepithelial fibrosis in interleukin 6-deficient mice following chronic exposure to aerosolized antigen.* Clin Exp Allergy, 2004. **34**(8): p. 1321-8.

180. Fourtounis, J., et al., *Gene expression profiling following NRF2 and KEAP1 siRNA knockdown in human lung fibroblasts identifies CCL11/Eotaxin-1 as a novel NRF2 regulated gene.* Respir Res, 2012. **13**: p. 92.

181. Kintscher, U., et al., *PPARalpha inhibits TGF-beta-induced beta5 integrin transcription in vascular smooth muscle cells by interacting with Smad4.* Circ Res, 2002. **91**(11): p. e35-44.

8. Declaration

I declare that I have completed this dissertation single-handedly without the unauthorized help of a second party and only with the assistance acknowledged therein. I have appropriately acknowledged and referenced all text passages that are derived literally from or are based on the content published or unpublished work of others, and all information that relates to verbal communications. I have abided by the principles of good scientific conduct laid down in the charter of the Justus Liebig University of Giessen in carrying out the investigations described in the dissertation.

Date: 19.08.2015   Gani Oruqaj

Giessen, Germany

9. Acknowledgement

10. Curriculum Vitae

Der Lebenslauf wurde aus der elektronischen Version der Arbeit entfernt.

The curriculum vitae was removed from the electronic version oft he paper.

10.4. Publications

Oruqaj G, Karnati S, Vijayan V, Kotarkonda LK, Boateng E, Zhang W, Ruppert C, Günther A, Shi W, Baumgart-Vogt E. Compromised peroxisomes in idiopathic pulmonary fibrosis, a vicious cycle inducing a higher fibrotic response via TGF-β signaling. Proc Natl Acad Sci USA. 2015 Apr 21;112(16):E2048-57.

Karnati S, Graulich T, **Oruqaj G,** Pfreimer S, Seimetz M, Stamme C, Mariani TJ, Weissmann N, Mühlfeld C, Baumgart-Vogt E. Postnatal development of the bronchiolar club cells of distal airways in the mouse lung: stereological and molecular biological studies. Cell Tissue Res. 2016 Jun;364(3):543-57. doi: 10.1007/s00441-015-2354-x. Epub 2016 Jan 21.

Karnati S, Palaniswamy S, Alam MR, **Oruqaj G,** Stamme C, Baumgart-Vogt E. C22-bronchial and T7-alveolar epithelial cell lines of the immortomouse are excellent murine cell culture model systems to study pulmonary peroxisome biology and metabolism. Histochem Cell Biol. 2016 Mar;145(3):287-304. doi: 10.1007/s00418-015-1385-4. Epub 2015 Dec 21.

10.5. Posters, oral presentations

Aug. 2011, 2012, 2013	oral and poster presentations at the annual MBML retreat, Rauischholzhausen, Germany
Sep. 2011, 2012, 2013	oral and poster presentations at the annual GGL Conference, Giessen Germany
July 2012	oral presentation at the OEPM Peroxisome Meeting, Dijon, France "Role of peroxisomes in idiopathic pulmonary fibrosis"
March 2012	poster presentation at the 107th Annual Meeting, Anatomische Gesellschaft, "Peroxisomal metabolic alterations and their possible involvement in the pathogenesis of pulmonary fibrosis"
May 2013	poster presentation at the ATS Conference 2013, Philadelphia, USA, "Peroxisomes in idiopathic pulmonary fibrosis"

10.6. Awards

02/2009	University of Prishtina "Student i Dalluar" Award (Distinguished Student)
06/2009	Practical Year Stipend- Auswärtiges Amt- Deutsche Botschaft, Kosovo

10/2009-09/2010	Konrad Adenauer Stiftung Award
03/2012	Poster Award 2012, Anatomische Gesellschaft, Frankfurt, Germany
07/2012	PhD Office Travel Grant, JLU Giessen, Germany (Dijon 2012)
04/2013	MBML Student Travel Award, Giessen, Germany (ATS Conference 2013)
03/2013	GGL Laboratory Rotation DAAD Award
07/2014	64th Lindau Nobel Laureate Meetings: Young Scientist Competition

VVB